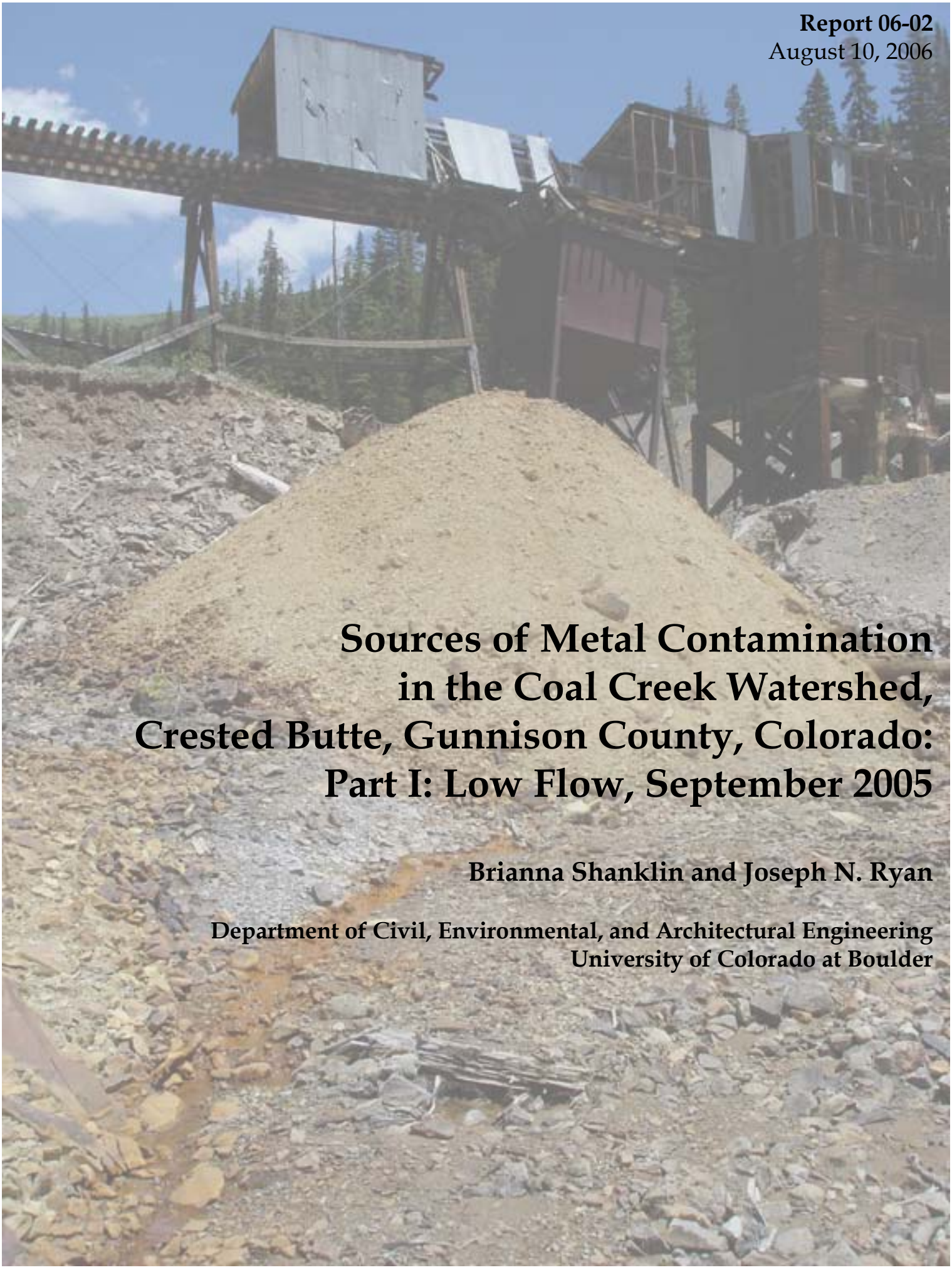

Report 06-02
August 10, 2006

Sources of Metal Contamination in the Coal Creek Watershed, Crested Butte, Gunnison County, Colorado: Part I: Low Flow, September 2005

Brianna Shanklin and Joseph N. Ryan

Department of Civil, Environmental, and Architectural Engineering
University of Colorado at Boulder

Report 06-02

Department of Civil, Environmental, and Architectural Engineering
University of Colorado at Boulder

August 10, 2006

Sources of Metal Contamination in the Coal Creek Watershed, Crested Butte, Gunnison County, Colorado: Part I. Low Flow, September 2005

Brianna Shanklin and Joseph N. Ryan

Department of Civil, Environmental, and Architectural Engineering
University of Colorado at Boulder

Contact Information:

Prof. Joseph N. Ryan
University of Colorado
428 UCB
Boulder, CO 80309-0428

phone: 303 492 0772
fax: 303 492 7317
email: joseph.ryan@colorado.edu

EXECUTIVE SUMMARY

This report details the results of a study conducted by University of Colorado researchers for the Coal Creek Watershed Coalition on the source of metals in the Coal Creek watershed during low flow. Coal Creek is the main water supply for the Town of Crested Butte in Gunnison County, Colorado. The study was funded by the University of Colorado's Outreach Committee.

Previous sampling has shown that Coal Creek is contaminated by metals and acidity from the Standard Mine on Elk Creek, a tributary of Coal Creek, and from a naturally occurring iron fen and gossan located just west of the Keystone Mine. Drainage from the Keystone Mine, which has been treated at the Mount Emmons treatment facility since 1981, also contributes metals to Coal Creek just downstream of Crested Butte's water supply intake. To confirm these results and to locate any other inputs of metals and acidity to Coal Creek, a spatially detailed investigation of contaminant sources was performed by University of Colorado researchers in September, 2005. The study was conducted at low flow because contaminant concentrations and toxicity to aquatic organisms are often highest during low flow. A companion study was completed in June, 2006, to locate metal sources at high flow; the results of the high flow investigation are not yet available.

A lithium chloride tracer-dilution test and synoptic sampling of Coal Creek allowed for the quantification of both surface and hyporheic flow and provided spatially detailed concentration and metal loading profiles for aluminum, arsenic, barium, cadmium, chromium, copper, iron, lead, manganese, nickel, and zinc along a 9.4 km reach of Coal Creek. Water draining from the iron fen and gossan near Keystone Mine was identified as the largest metal contributor in the watershed. It was a major source of aluminum, cadmium, iron, manganese, and zinc to Coal Creek. Elk Creek, which contains the Standard Mine drainage, was identified as a major source of cadmium and zinc. An unnamed tributary located 1.1 km downstream of Elk Creek was identified as a major source of chromium, iron, and nickel. Detailed results are presented in Table 14.

The Mt. Emmons Treatment Plant added calcium to Coal Creek at concentrations seven times greater than background. Large daily fluctuations in calcium concentration and hardness coinciding with times of discharge release and discontinuation are expected. These fluctuations result in daily changes in hardness-based aquatic life standards set by the Colorado Department of Public Health and Environment. Metal speciation is also affected by the hardness fluctuations. Partitioning between the dissolved and colloidal phases was investigated for aluminum, arsenic, lead, and zinc.

ACKNOWLEDGMENTS

Funding for this project was provided by the University of Colorado Outreach Committee and facilitated by Wynn Martens of the University of Colorado. Christina Progess the U.S. Environmental Protection Agency project manager for the Superfund cleanup at the Standard Mine, arranged for analysis of the metal concentrations in the water samples.

Scientific and technical assistance was provided by Steve Glazer, Tyler Martineau, and Anthony Poponi of the Coal Creek Watershed Coalition; Larry Adams and John Hess of the Town of Crested Butte; Christina Progess, Carol Beard, and Jessica Brown of the U.S. Environmental Protection Agency; John Perusek and Adolph Ortiz of Phelps-Dodge, operators of the Mt. Emmons Treatment Plant; Natalie Mladenov and JoAnn Silverstein of the University of Colorado; Suzanne Anderson of the Institute for Arctic and Alpine Research at the University of Colorado; and John Drexler and Fred Luiszer of the Laboratory for Environmental and Geological Studies at the University of Colorado.

Field and laboratory support was provided by Susan Bautts, Christie Chatterley, Lynné Diaz, Tim Dittrich, and Jeff Wong of the University of Colorado; by David Wallace; and by Anthony Poponi of the Coal Creek Watershed Coalition.

TABLE OF CONTENTS

Executive Summary iii
Acknowledgments iv
Table of Contents v
List of Tables vi
List of Figures vii

Introduction 1
Background 3
Field site 3
Abandoned mines and natural metal deposits in the Coal Creek watershed 3
Tracer-dilution method 7
Synoptic sampling method 8
Materials and Methods 9
Injection procedure 9
Synoptic sampling procedure 12
Sample processing and preservation 12
Analytical methods 14
Flow rate calculations 17
Metal-loading calculations 17
Water quality standards and hardness 19
Results 20
Coal Creek pH 20
Coal Creek total organic carbon 21
Calcium and magnesium concentration and hardness 22
Sodium chloride pulse tracer test 23
Injection tracer concentration 24
Stream and tributary tracer concentration 25
Flow rate calculations 25
Flow rates based on lithium and chloride dilution 26
Metals in Coal Creek and tributaries 31
Electron microprobe images and elemental spectra 47
Discussion 55
Suitability of lithium and chloride as tracers 55
Steady-state conditions for tracer injection 56
Hardness and the Mt. Emmons Treatment Plant effluent 57
Aquatic life and drinking water supply standard exceedances 58
Stream flow 61
Sources of metals and arsenic in the Coal Creek watershed 63
Implications of metal concentrations and loading rates for remediation 68
Colloids and metal association 70
Hardness and metal partitioning 75
Conclusions 76

References 78

LIST OF TABLES

Table 1. Sequence of events for the September, 2005, Coal Creek metal-loading tracer-dilution experiment study 11

Table 2. Minimum detection limits reported for target analytes measured using ICP-AES, ICP-MS, and IC analysis 16

Table 3. Equations used to calculate flow rates and mass loading rates (Kimball and others, 2002) for Coal Creek tracer dilution study 18

Table 4. The time of the conductivity peak in response to the pulse NaCl tracer at five sample sites. 23

Table 5. Lithium and chloride injection concentrations over the injection period 24

Table 6. Flow rates of Coal Creek sample sites, tributaries, and diversions 29

Table 7. Dissolved and total metal concentrations in blanks 32

Table 8. Tributary loading rates expressed for total and dissolved metals as a percentage of the cumulative tributary loading rate for each metal 34

Table 9. Summary of scanning electron microprobe results for mineralogical composition of colloids collected on 0.45 μm filters 54

Table 10. Chloride concentrations at the upstream end and the downstream end of the injection reach 57

Table 11. Coal Creek sample sites where the chronic and acute aquatic life toxicity standards and the drinking water supply standard were exceeded 59

Table 12. Total and dissolved metal concentrations in the Mt. Emmons Treatment Plant effluent channel during synoptic sampling on September 5and during discharge on September 6 ... 60

Table 13. The metal concentrations just upstream of the drinking water intake and at the drinking water reservoir return flow tributary 65

Table 14. Major, minor, and trace metal sources in the Coal Creek watershed 69

Table 15. Intrinsic surface complexation constants for lead and zinc adsorption on hydrous ferric oxide 74

LIST OF FIGURES

Figure 1. The Coal Creek watershed is located west of the Town of Crested Butte in northern Gunnison County, Colorado 2

Figure 2. The Coal Creek watershed including major tributaries, mines, and other geographical features 4

Figure 3. Aerial view of Coal Creek near the Keystone Mine at the base of Mt. Emmons, including the gossan located just west of the Keystone Mine, the iron fen, unnamed tributaries at stream distances of 3.294, 3.455, 3.661 km downstream of the injection site used for this study, and the Mt. Emmons Treatment Plant 6

Figure 4. Coal Creek synoptic sample sites including in-stream sites and tributaries 8

Figure 5. Lithium chloride was added to the injection solution and stirred with a paddle for 90 min until the salt was completely dissolved 10

Figure 6. Illustration of tributary drainage transported down culvert paralleling County Highway 12, through pipe underneath the road, and into Coal Creek 13

Figure 7. Coal Creek and surface tributary pH measured in the field lab within 24 h of collection 21

Figure 8. Coal Creek and tributary total organic carbon concentration 22

Figure 9. Coal Creek and tributary total calcium and magnesium concentration and hardness as mg L^{-1} $CaCO_3$ 23

Figure 10. Coal Creek and tributary total lithium concentration and flow rate calculated using lithium concentration dilution 27

Figure 11. Coal Creek and tributary dissolved chloride concentration and flow rate calculated using chloride concentration dilution 28

Figure 12. Coal Creek and tributary total and dissolved iron concentration, chronic toxicity standard, 30-day dissolved iron standard for a drinking water supply, and total iron loading rate 33

Figure 13. Coal Creek and tributary total and dissolved manganese concentration, 30-day drinking water supply dissolved manganese standard, and total and dissolved manganese loading rate 36

Figure 14. Coal Creek and tributary total and dissolved aluminum concentration, acute and chronic toxicity standards for aquatic life, and aluminum loading rate 37

Figure 15. Coal Creek and tributary total and dissolved zinc concentration, chronic and acute toxicity standards, and total and dissolved zinc loading rate 39

Figure 16. Coal Creek and tributary total and dissolved copper concentration, chronic aquatic life toxicity standard, and total and dissolved copper loading rate 40

Figure 17. Coal Creek and tributary total and dissolved cadmium concentration, chronic, acute, and acute (trout) toxicity standards, and total and dissolved cadmium loading rate 41

Figure 18. Coal Creek and tributary total and dissolved lead concentration, chronic toxicity standard for aquatic life, and total and dissolved lead loading rate 42

Figure 19. Coal Creek and tributary total and dissolved nickel concentration, chronic toxicity standard for aquatic life, and total nickel loading rate 43

Figure 20. Coal Creek and tributary total and dissolved chromium, 1-day drinking water supply standard for chromium(III) and chromium(VI), acute and chronic chromium(VI) toxicity standard, and total chromium loading rate 44

Figure 21. Coal Creek and tributary total and dissolved arsenic concentration, 30-day total recoverable arsenic maximum contaminant level (MCL) and health-based standards for a drinking water supply, and arsenic loading rate 46

Figure 22. Coal Creek and tributary total and dissolved barium concentration and loading rate 47

Figure 23. Electron microprobe images showing portions of colloids filtered from CC-0.282 (upper) and CC-9.442 (lower) water samples 49

Figure 24. Electron microprobe images showing portions of colloids filtered from the drinking water reservoir return flow 50

Figure 25. Electron microprobe images showing portions of colloids filtered from the UT-6.696 water sample 51

Figure 26. Elemental spectra for representative particles trapped on a 0.45 µm nylon filter at CC-0.128 and the drinking water reservoir return 52

Figure 27. Elemental spectra for representative particles trapped on a 0.45 µm nylon filter at CC-9.442 and the drinking water reservoir return 53

Figure 28. The loading rates for calcium along with aluminum, cadmium, copper, iron, manganese, and zinc are graphed for the 4-8 km section of the study reach to illustrate the impact of the Mt. Emmons Treatment Plant on Coal Creek metal loading rates 61

Figure 29. The colloidal fraction ($f_{colloid}$) of aluminum, arsenic, lead, and zinc in Coal Creek 73

INTRODUCTION

Over 600 km of stream reach are affected by metal-rich, acidic drainage from abandoned mining sites in Colorado (Wentz, 1974). Acid mine drainage occurs when pyrite minerals (iron sulfide, FeS_2) are leached and then oxidized. Acidic water with high iron and sulfate concentrations are the products of pyrite oxidation.

Acid mine drainage from abandoned mines as well as metal-laden drainage from a natural iron deposit are suspected to degrade water quality in the Coal Creek watershed, due west of Crested Butte, Colorado (Figure 1). The watershed has a 100-year mining legacy, with excavation and milling operations beginning in 1874 and continuing until 1974 (EPA, 2005a). The major mines in the district were the Standard Mine, the Keystone Mine, and the Forest Queen Mine. The Standard Mine was added to the National Priority List ("Superfund") in September, 2005. Drainage emanating from underground mining shafts at the Standard Mine flows into an unlined, non-engineered holding pond that overflows into Elk Creek. Elk Creek then enters Coal Creek which serves as the only drinking water supply for the Town of Crested Butte's 1500 residents. Risk of catastrophic failure of this holding pond and influx of a large quantity of metal-laden water into Crested Butte's drinking water supply is the major threat posed by the Standard Mine site. Remedial activities began at the Standard Mine in the summer of 2006.

Drainage from the Keystone Mine is treated at the Mount Emmons Treatment Plant and then released into Coal Creek just downstream of Crested Butte's drinking water intake. Ownership and managerial responsibility of this treatment plant was re-acquired by U.S. Energy Corporation in February, 2006. Despite strong opposition from several concerned citizens, U.S. Energy has announced plans to resume mining operations on Mount Emmons to exploit a "world-class" molybdenum deposit underneath the mountain (U.S. Energy, 2006).

A naturally-occurring iron-rich surface deposit, or gossan, also drains into Coal Creek. Drainage from the gossan is suspected of having a low pH and adding toxic aluminum, iron, manganese, and zinc concentrations to the watershed. A low-pH wetland, or iron fen, is located below the gossan and may also negatively impact Coal Creek water quality.

The Coal Creek Watershed Coalition (CCWC), a community group based in Crested Butte, is working to restore aquatic life habitat and protect other water uses in Coal Creek (CCWC, 2006). Recreation is the dominant monetary contributor to the local economy, having replaced mining in the late 1900's. The CCWC hopes that well-directed remedial action in the Coal Creek watershed will create a sustainable fish population and promote fishing in Coal Creek.

We are assisting the Coal Creek Watershed Coalition in an effort to identify the most toxic metal sources in the watershed. To do this, we conducted a metal-loading tracer-dilution experiment for low and high flow. This report provides the results of the low flow experiment, which was conducted in September, 2005. The tracer injection and synoptic sampling study allows calculation of metal loading rates along Coal Creek.

Metal loads pinpoint locations of greatest metal influx to Coal Creek (Kimball, 1997). Spatially-detailed characterization of Coal Creek metal loads is required for proper remedial action.

The objectives of this study were to (1) quantify and locate sources of metal input to Coal Creek, (2) investigate specific metal contributions to Coal Creek from the Standard Mine (Elk Creek) and the iron gossan, and (3) assess relationships and interactions between metal partitioning between the dissolved and colloidal phases.

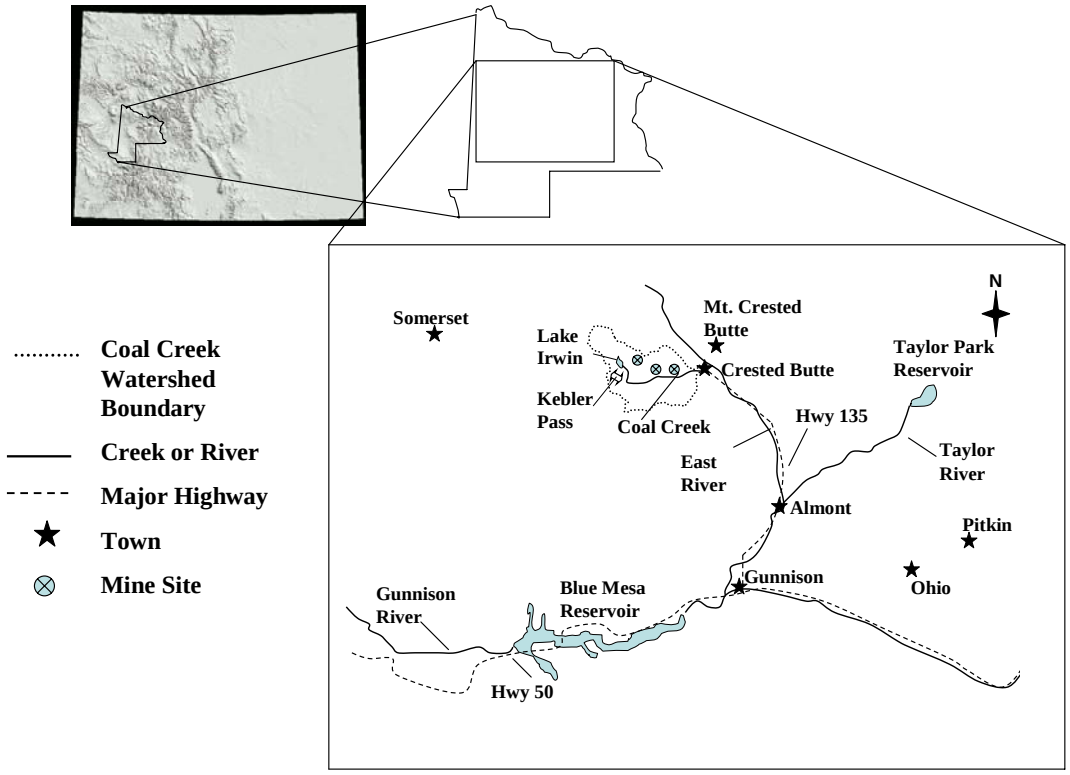

Figure 1. The Coal Creek watershed is located west of the Town of Crested Butte in northern Gunnison County, Colorado.

BACKGROUND

Field site

The Coal Creek watershed (Figures 1 and 2) drains an area of approximately 65 km^2 in the Ruby-Anthracite Range of northern Gunnison County, Colorado. Coal Creek originates near Lake Irwin in the northwestern portion of the watershed. The downstream reach of Coal Creek flows through the Town of Crested Butte on the eastern edge of the watershed before ultimately entering the Slate River, which flows south into the East River, and then into the Gunnison River. Coal Creek is paralleled by County Highway 12, the Kebler Pass Road, along most of its length.

Elevations in the watershed range from 2,900 m in Crested Butte to 4,300 m along peaks of the Ruby Range. Glacial erosion during the Pleistocene epoch shaped the Coal Creek valley. Laccoliths, or dome-shaped igneous intrusions, other resistant sedimentary rock, or crystalline or volcanic rocks characterize the higher mountains. The valley bottom is underlain by sand and gravel deposited by glacial ice or melt water (Streufert, 1999). Vegetation includes aspen, fir, and spruce forests along with treeless alpine tundra vegetation at higher elevations. Slope and aspect greatly influence microclimates. North-facing slopes receive more snowfall and have higher soil moisture contents. This greater moisture content supports more dense vegetation, especially coniferous forest. South-facing slopes tend to be drier and vegetated by sagebrush and grasses (Soule, 1976). Mean annual rainfall for the watershed is 60 cm (WRCC, 2006). The majority of precipitation falls as snow with average annual snowfall of 500 cm in Crested Butte and 1,270 cm at Kebler Pass, which is located on the western edge of the watershed.

Stream flow is dominated by snow melt. Mean annual flow is 1.46×10^7 m^3 with an average daily flow of 0.46 $m^3\ s^{-1}$ in Coal Creek just downstream of the Elk Creek confluence. Average daily flow at this location for the month of September is 0.058 $m^3\ s^{-1}$ (USGS, 2006).

Abandoned mines and natural metal deposits in the Coal Creek watershed

The watershed is rich in mineral resources. Hard rock mining began in this area, also known as the Ruby Mining District, in 1874 when the watershed belonged to the Ute Indian Reservation and continued until 1974 (EPA, 2005a). Vein deposits are contained in north-northeast-trending faults, dikes, and small stocks on the eastern faces of the Ruby Range. These veins are rich in copper, gold, lead, molybdenum, ruby silver, and zinc (Streufert, 1999). The three largest mines were the Standard Mine, the Keystone Mine, and the Forest Queen Mine, all of which lie on the southern face of Scarp Ridge, and all of which are now inactive (EPA, 2005b). The watershed is now used primarily for residential development, recreation, and water supply.

Coal Creek serves as the drinking water supply for the Town of Crested Butte. The drinking water intake diverts water from Coal Creek at a rate of 0.079 $m^3\ s^{-1}$

(Larry Adams, personal communication, 2006). Two irrigation diversions reroute flow from Coal Creek to Smith Ranch (Spann-Nettick ditch) and Town Ranch (Halazon ditch), respectively. Both diversions are located immediately west of Crested Butte. Overflow from the drinking water supply reservoir is returned to Coal Creek 60 m downstream of the Spann-Nettick diversion and 15 m upstream of the Halazon diversion (Adams, 2006).

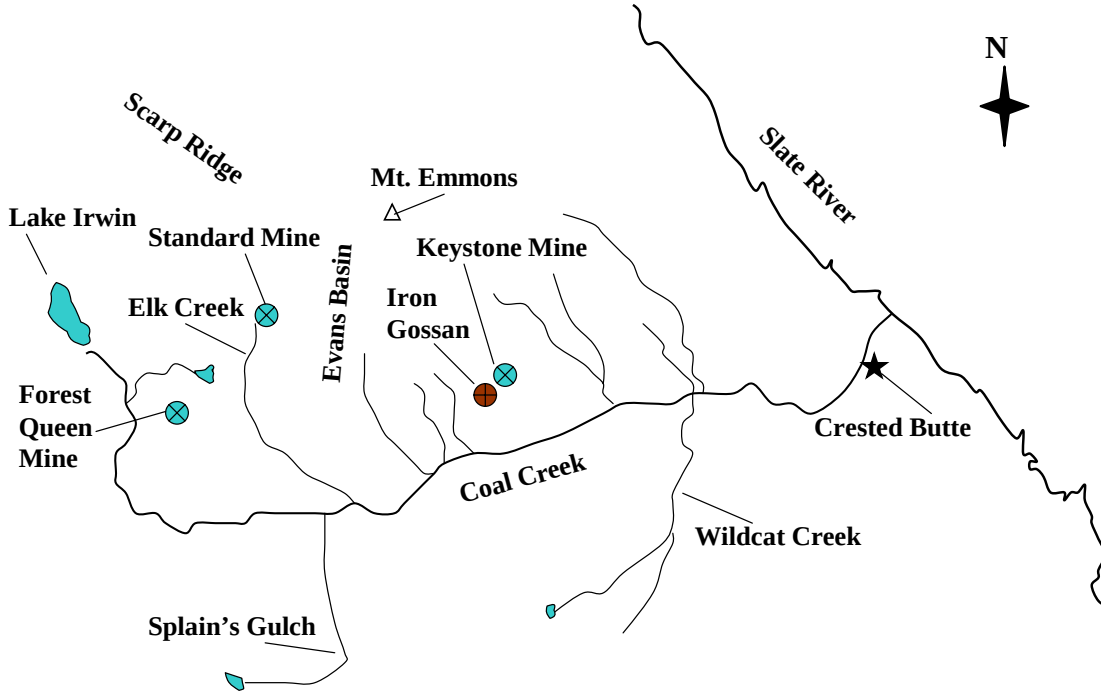

Figure 2. The Coal Creek watershed including major tributaries, mines, and other geographical features.

The Standard Mine was added to the U.S. Environmental Protection Agency (U.S.EPA) National Priority List in September, 2005. The mine sits on 4 ha of land located approximately 16 km northwest of Crested Butte. The Standard Metals Corporation owns the patented mining claims. The surrounding land is owned by the U.S. Forest Service. The mine site contains many open adits and shafts, an old mill, and railroad tracks that run 5 m above ground on rotting wooden poles. Popular hiking trails parallel the site and no access restrictions are in place. On-site wastes include 40,950 m^3 of waste rock and 22,430 m^3 of mill tailings. Acidic, metal-laden water flows out of the open adits and into Elk Creek. Flow from the Standard Mine into Elk Creek ranges from 550 to 1,100 $m^3\ d^{-1}$ during the high flow season to 5.5 to 55 $m^3\ d^{-1}$ during low flow. Suspected contaminants include arsenic, barium, cadmium, chromium, copper, lead, and zinc (EPA, 2005a). During high flow, a portion of Elk Creek flows into a non-engineered, unlined surface impoundment, or tailings pond (90 m diameter by 4.5 m deep). This impoundment is also fed by snow melt and possibly by ground water. It is constructed entirely of waste rock. Acidic mine runoff contained in the impoundment has dissolved and structurally weakened the ponds waste rock sides. Risk of

catastrophic failure and the subsequent release of a large volume of concentrated mine drainage is of particular concern. Intermittent overflow and seepage flow out of the tailings pond and back into adjacent Elk Creek, which is devoid of all aquatic life (CDPHE, 2006). Elk Creek flows into Coal Creek 3.2 km downstream of the Standard Mine site. The drinking water intake for the Town of Crested Butte is 3.4 km downstream of this confluence.

The Keystone Mine is located approximately 5.0 km northwest of Crested Butte under the south slope of Mt. Emmons (Streufert, 1999). Lead, zinc, and silver were extracted from the Keystone Mine until the mid-1970s (U.S. Energy, 2006). Acid mine drainage from the abandoned Keystone Mine contains high concentrations of lead, zinc, and cadmium. The drainage is treated at the Mt. Emmons Treatment Plant, which was built in 1981 (CCWC, 2006). The Mt. Emmons Plant also treats flow emitted from exploratory cores. These cores were drilled by the Amax Corporation as part of a feasibility study investigating the extent of molybdenum and diamond deposits. The plant cost $14 million to build and the yearly operational costs are about $1 million (U.S. Energy, 2006).

On February 28, 2006, U.S. Energy Corporation and Crested Corporation reacquired the Mt. Emmons property from the Phelps-Dodge Corporation. With the acquisition also came the responsibility of running the Mt. Emmons Treatment Plant. This 2,185 ha property contains a "world-class" molybdenum deposit. Reserves are estimated at 140 million tonnes of 0.44 percent molybdenum disulfide (MoS_2) (Streufert, 1999). The owners are actively pursuing development and mining given the highly favorable pricing environment for molybdic oxide. They are also considering the use of the Mt. Emmons Treatment Plant in future milling operations (U.S. Energy, 2006).

Silver was the main metal extracted at the Forest Queen Mine. A mill was located on-site (Hornbaker, 1984). One adit at this inactive mine drains into Coal Creek just below the old Irwin town site southeast of Lake Irwin. The flow appears to be quite low. Ongoing studies aim to determine how this drainage impacts Coal Creek (CCWC, 2006).

An iron gossan is located just west of the Keystone Mine at an elevation of 2,911 m (Figure 3). Its surface area is approximately 1.2 ha. A gossan is formed when a series of springs flow over highly mineralized and fractured bedrock rich in pyrite (FeS_2) (CCCOSC, 2006). This process forms peat terraces composed of limonite, or natural aggregate of hydrous ferric oxides lacking crystallization (Kelly, 1958). Pyrite oxidation produces acidic byproducts that lower pH. Pyritic gossans are characterized by a very dusky red to dark reddish brown or moderate brown color (Kelly, 1958). This gossan is one of eight in Colorado. An iron bog, or fen, is present down-slope of the gossan. This iron bog is a peat wetland with high nutrient content fed from upslope mineral-rich soil and ground water movement. The EPA sampled surface drainage from the iron fen in the fall of 2005. Their sampling results indicated elevated aluminum, iron, manganese, and zinc concentrations. The iron fen drainage had a pH of 3.4 (EPA, 2005a). Drainage from the fen enters Coal Creek approximately 1.9 km upstream of Crested Butte's drinking water intake from two point sources. Observations also indicate that a large

percentage of drainage from the iron fen and the gossan returns to the ground water system and enters Coal Creek as dispersed subsurface flow.

The fen supports a unique vegetative community including a round-leaved sundew, *Drosera rotundifolia*. This small, carnivorous plant has not been found anywhere else in the Central or Southern Rocky Mountains in spite of extensive searches in similar acidic fens. The U.S. Forest Service is concerned that molybdenum mining on Mt. Emmons may alter or exterminate the sundew population. Another concern is the alteration of ground water flow by mining operations, which may remove water from springs that feed the fen (USFS, 1981).

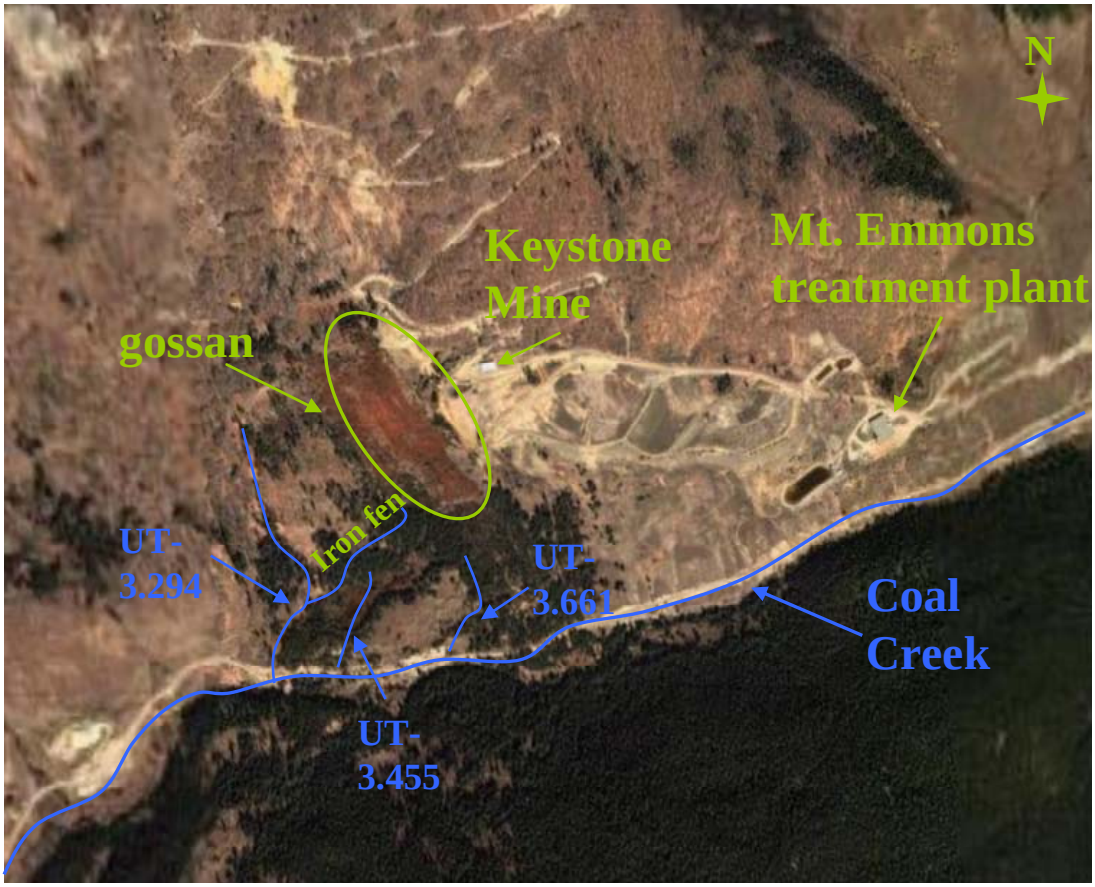

Figure 3. Aerial view of Coal Creek near the Keystone Mine at the base of Mt. Emmons, including the gossan located just west of the Keystone Mine, the iron fen, unnamed tributaries at stream distances of 3.294, 3.455, 3.661 km downstream of the injection site used for this study, and the Mt. Emmons Treatment Plant. Coal Creek flows to the northeast. The aerial photo was retrieved using Google Earth™ (http://earth.google.com).

Tracer dilution method

The tracer dilution method allows quantification of discharge by monitoring dilution of a tracer as it moves downstream. A specific concentration of tracer is injected at a constant rate to achieve steady-state conditions. This provides a known mass of tracer added to the stream. Tracer concentration is measured upstream and downstream of the injection site. Discharge is quantified based on the dilution of the tracer as it moves downstream from the injection site (Kimball, 1997). The tracer dilution method accounts for flow through the hyporheic zone, or the layer of cobbles and streambed sediment that rapidly exchanges water with the stream. Flow through the hyporheic zone is normally substantial for high-gradient, shallow mountain streams such as Coal Creek. Traditional current meter flow measurements for mountain streams are typically underestimates because flow through the hyporheic zone is not captured (Bencala and others, 1990).

The tracer dilution method also accounts for dispersed ground water inputs as well as seeps or springs discharging over a large area. These non-point sources affect quantification of flow because they contribute to the dilution of the tracer; however, the portion of flow attributable to point versus non-point sources cannot be distinguished.

The tracer-injection method requires the tracer to be inert and transported downstream in a conservative fashion, unaffected by biogeochemical reactions. The injection must continue until all parts of the stream including the hyporheic zone and all surface storage zones become saturated with tracer. Under these saturation conditions, the in-stream tracer concentration is said to be at the plateau concentration (Bencala and others, 1990). Lithium chloride (LiCl) was the tracer used for this study. Lithium is reported to act conservatively in streams with low pH (Paschke and others, 2005). The background lithium concentration of natural waters is normally significantly low. This allows for detection of a pronounced peak in lithium concentration upon tracer arrival. Chloride is commonly known as the "universal tracer" and is expected to behave conservatively in most aquatic environments (Bencala and others, 1987). All downstream reductions in tracer concentration are assumed to be a result of dilution from tributary and ground water inflow (Kimball and others, 2002). When a surface tributary is present between two sample locations, calculated inflow discharge is assigned solely to the tributary despite the possibility of ground water inputs. When no visible tributary is present, in-stream discharge increases are assumed to be a result of ground-water inflow. Again, the tracer dilution method is unable to distinguish between tributary and ground water inflow if both occur between two synoptic sample sites. The method only accounts for the total inflow between two sample sites.

This low flow tracer dilution experiment was performed along 9.4 km of Coal Creek in September 2005. Low flow studies are useful in developing base-flow metal-loading profiles. The highest metal concentrations which are most toxic to aquatic life commonly occur during the low flow season when only a small volume of water is available to dilute pollutants (Paschke and others, 2005). Low flow tracer dilution studies aid in identifying sources contributing to these toxic metal concentrations.

Synoptic sampling method

Synoptic sampling is the spatially detailed sampling of stream sites and all tributary inflows that provides a one-time description of stream and tributary chemistry. It gives a "snapshot" of stream chemistry and flow that allows quantification of in-stream loads (Kimball, 1997). The "snapshot" is not instantaneous, but represents the sampling period of several hours. A sample site spacing of hundreds of meters is recommended for practical analysis of stream chemistry (Bencala and others, 1990).

For this study, forty-seven in-stream sites and thirteen tributary sites were assigned (Figure 4). Synoptic sample sites were intended to bracket all tributary inflows. This allows for understanding and quantifying the impacts of many individual sources on the watershed as a whole. A global positioning receiver (Garmin GPS 12) global positioning receiver was used to space the in-stream sites at intervals of about 200 m and to record all sampling locations. The GPS route was marked along County Highway 12, not directly along the stream. Site coordinates are therefore slightly offset to the north of Coal Creek. The sample site spacing provided spatially detailed concentration profiles to examine metal inputs. This sampling regime is more intensive and expensive than simply measuring water-quality parameters at an outlet downstream of acid mine drainage. However, it quantifies impacts from individual sources to provide information necessary for restoration decisions (Kimball and others, 2001).

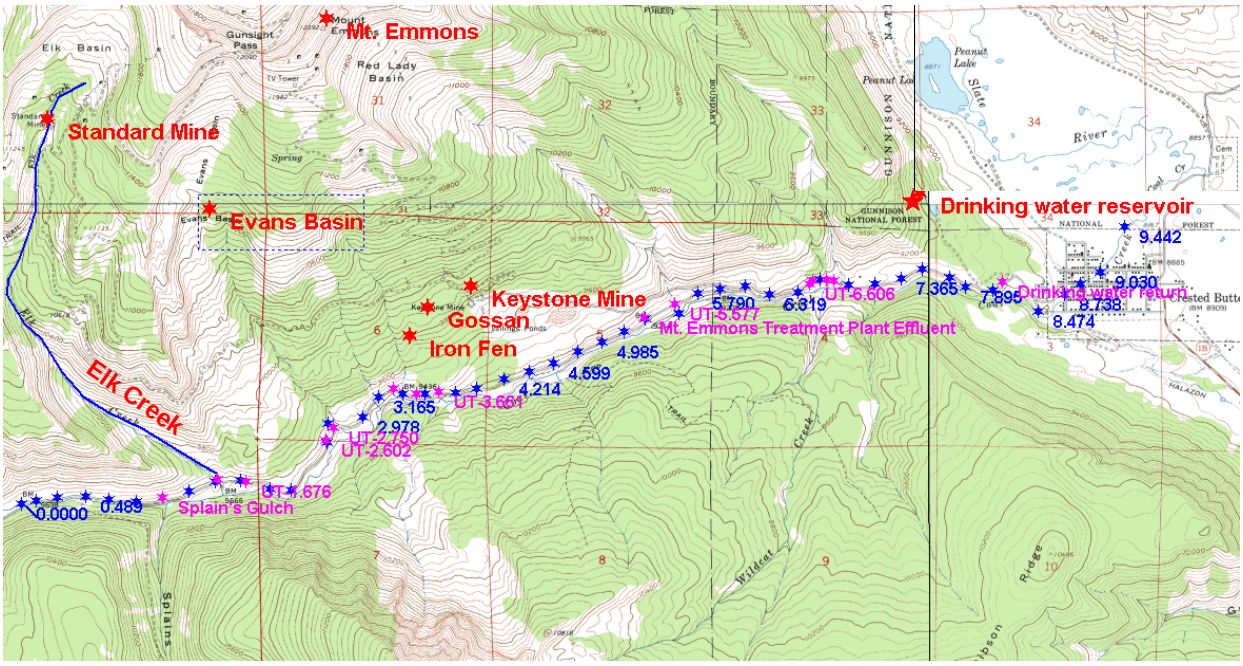

Figure 4. Coal Creek synoptic sample sites including in-stream sites (blue) and tributaries (pink). Distances from the tracer injection site (distance 0.000 at the upstream end of the study reach) are given in kilometers. The Standard Mine, Keystone Mine, iron gossan, and drinking water reservoir are also shown.

MATERIALS AND METHODS

Injection procedure

Prior to injection of the lithium chloride tracer, a sodium chloride (NaCl) pulse tracer test was conducted to determine stream velocity. The purpose of the test was to estimate the time required for the tracer to reach the downstream end of the study reach. The NaCl solution was made by mixing 22.7 kg of NaCl and 151 L of stream water in a 210 L polyethylene barrel. At 12:28 on September 3, 2005, the entire barrel containing the NaCl solution instantaneously added to Coal Creek at the injection site. Downstream transport of the tracer was documented using specific conductance meters (Orion, models 105 and 122) at five sample sites located within the first 1.3 km of the study reach. The background conductivity was measured at each of these sites. The conductivity was then monitored until it peaked and began to decline. Stream velocity was calculated by dividing the distance traveled by the time required for the conductivity to peak at each monitoring site. It was determined that a 43 h injection was required for the LiCl tracer to reach the downstream end of the study reach, the north side of the Town of Crested Butte, at a distance of 9.442 km.

The LiCl tracer solution was prepared by pumping stream water into a 405 L polyethylene tank and adding approximately 34 kg of LiCl (FMC Industrial Chemicals, LiCl anhydrous technical grade, CAS no. 7447-41-8). A downstream Li concentration 100 times greater than the upstream (background) Li concentration was desired. Calculations showed that 34 kg of LiCl added to the 405 L barrel would produce the desired in-stream spike in Li concentration. The solution was mixed with a paddle and recirculated with a pump (Fluid Metering Instruments (FMI) PM6014 pump and FMI Q410-2 pump head) for 90 min until completely dissolved (Figure 5). The injectate was sampled every 4 h for the duration of the injection. The average lithium concentration of the injection solution was later measured at 1.17×10^7 μg L^{-1}. The injection solution lithium concentration ranged from 1.13×10^7 to 1.24×10^7 μg L^{-1}. The average background lithium concentration in Coal Creek was 3.53 μg L^{-1}. The average chloride concentration was 7.59×10^4 mg L^{-1}, with a range of 2.33×10^4 to 9.64×10^4 mg L^{-1}. The average background chloride concentration in Coal Creek was 2.38 mg L^{-1}.

The stock tracer solution was replenished twice during the injection period (Table 1). On the September 4 at 09:10, 150 L of the original tracer solution remained. A new batch was prepared by pumping 208 L of stream water into a 210 L polyethylene barrel. A second barrel was used for mixing the new solution to avoid interrupting the injection process. Lithium chloride was added to the 210 L polyethylene barrel until the specific conductance of the second stock tracer solution matched the specific conductance of the original tracer solution. The specific conductance of the original solution was measured as 107.0 mS cm^{-1} with a specific conductance meter (Orion, model 105) calibrated with a 1413 μS cm^{-1} standard. A total of 16 kg of LiCl was added to the second stock tracer solution. The final specific conductance of the second stock

tracer solution was 109.5 mS cm^{-1}. The newly mixed tracer solution was pumped into the original 405 L tank at 09:40 on September 4. The specific conductance of the replenished tank was 107.5 mS cm^{-1}.

On September 4 at 17:45, 220 L of tracer solution remained in the injection tank and the specific conductance was measured at 110.5 mS cm^{-1}. A third stock tracer solution was prepared by pumping 208 L of stream water into the 210 L polyethylene barrel and adding 17 kg of LiCl so that the specific conductance reached 109.7 mS cm^{-1}. This third batch of tracer solution was then pumped into the 405 L tank and lasted for the duration of the injection.

Figure 5. Lithium chloride was added to the injection solution and stirred with a paddle for 90 min until the salt was completely dissolved.

The tracer solution was injected into Coal Creek using a pump (FMI PM6014 pump and FMI Q410-2 pump head) and flow rate controller (FMI V200 stroke rate controller). Tubing (Fisherbrand silicon tubing, 9.5 mm diameter, 3.0 mm wall) was used to transfer the tracer solution from the 405 L mixing tank through the metering pump and into the creek at the injection site. The LiCl tracer was injected over a period of 50.5 h. A constant injection rate of 250 mL min^{-1} was desired to ensure steady-state conditions. The actual measured injection rate varied from 185-280 mL min^{-1} (Table 1).

An upstream site (designated "0.000") was sampled every 4 h for the duration of the injection to provide background lithium and chloride concentrations. The upstream site was located 50 m upstream of the injection site (designated "0.051"). The most downstream site ("9.442") was located 9.4 km downstream of the injection site in the Town of Crested Butte. Samples were collected every 45 min at the downstream site on the day of synoptic sampling to identify the leading edge of the tracer plume.

Table 1. Sequence of events for the September, 2005, Coal Creek metal-loading tracer-dilution study.

Date	Clock Time	Experiment Time (h)	Activity
9/3/2005	900		Synoptic sample sites marked with GPS
	1130		First stock tracer solution prepared, 34 kg LiCl and stream water added to 405 L tank
	1300	0.0	Start of injection period, pump rate set to 250 mL min^{-1}
	1300	0.0	Upstream site sampling begins
9/4/2005	730	18.5	Pump rate decreased to 185 mL min^{-1} overnight, reset pump rate to 250 mL min^{-1}
	940	20.7	150 L of original injection solution remaining, specific conductance of solution = 107.0 mS cm-1
	940	20.7	Begin mixing second batch of stock tracer solution, 16 kg LiCl added to 210 L barrel, specific conductance = 109.5 mS cm^{-1}
	1000	21.0	Stock tracer solution replenished with second batch, new specific conductance = 107.5 mS cm^{-1}
	1110	22.2	Injection flow rate measured at 280 mL min^{-1} then reset to 255 mL min^{-1}
	1600	27.0	Flow rate measured at 250 mL min^{-1}
	1745	28.8	220 L of tracer solution remaining in 405 L tank, specific conductance = 110.5 mS cm^{-1}
	1745	28.8	Third stock tracer solution prepared by mixing 17 kg LiCl and stream water in 210 L barrel, specific conductance = 109.7 mS cm^{-1}
	1750	29.3	Third stock tracer solution added to 405 L tank, new specific conductance = 110 mS cm^{-1}
	1830	29.5	Flow rate measured at 280 mL min^{-1} then reset to 250 mL min^{-1}
	0600 - 2000	17.0 - 31.0	Injection monitored
9/5/2006	0	35.0	Flow rate measured at 250 mL min^{-1}
	620	41.3	Flow rate measured at 230 mL min^{-1} then reset to 250 mL min^{-1}
	1110	46.2	Downstream site sampling begins, continues at 45 min intervals throughout day
	1110	46.2	Flow rate measured at 260 mL min^{-1} then reset to 250 mL min^{-1}
	1300	48.0	Flow rate measured at 260 mL min^{-1} then reset to 250 mL min^{-1}
	1500	50.0	Synoptic sampling began
	1530	50.5	Tracer injection discontinued
	1530	50.5	Upstream site sampling discontinued
	2030	55.5	Synoptic sampling finished

Synoptic sampling procedure

Synoptic sampling began 50 h after the start of the injection. The sampling event lasted approximately 5.5 h. In-stream sample sites are designated with the letters "CC-" followed by a number representing the distance in kilometers from the most upstream sample site, CC-0.000. All tributary names besides Splain's Gulch, Elk Creek, the Mt. Emmons Treatment Plant effluent channel, and the drinking water return reservoir begin with the designation "UT-" to indicate their status as unnamed or unidentified tributaries. Three unnamed tributaries were not identified during GPS sample location assignment but were found during the synoptic sampling event. These tributaries were designated UT-6.606, UT-6.696, and UT-6.801.

Synoptic sampling was conducted by a six-member team. One individual remained at the injection site taking upstream and injection samples at regular time intervals and monitoring the injection pump so as to maintain a steady injection rate. A second individual stayed at the downstream end of the study reach, CC-9.442, taking samples every 45 minutes from 11:00 to 19:50 on the day of synoptic sampling. The downstream site was monitored for the entire day to allow for development of a breakthrough curve. Ideally, a rising tracer concentration followed by a plateau of the tracer concentration over time would indicate the time of tracer arrival at CC-9.442. The four remaining team members conducted synoptic sampling of Coal Creek from 15:00 to 19:50. Sampling began on the upstream section of the study reach. Team members successively proceeded, or "leap-frogged", towards the downstream end of the study reach until samples were obtained at each synoptic site.

For tributaries entering Coal Creek from culverts on the north, synoptic samples were taken from the culverts immediately south of County Highway 12 (Figure 6). Drainage entering Coal Creek from the north is typically routed along the highway, through a pipe underneath the highway, and then down-slope into Coal Creek. Field reconnaissance in June, 2006, during high flow conditions indicated that the majority of the flow from the iron fen and gossan tributaries is absorbed into the ground before entering Coal Creek. Approximately 50% of the flow from UT-3.294 and 100% of the flow from UT-3.455 and UT-3.661 re-entered the ground water system before entering Coal Creek (Figure 6). During low flow conditions, it is likely that even a larger percentage of the flow would be absorbed before entering Coal Creek.

At each sample site, stream water samples were collected in 1 L (Nalgene 1 L high density polyethylene wide mount sample bottle) and a 60 mL (Nalgene 60 mL wide mouth amber glass bottle) bottles. Samples were kept on ice in coolers for field preservation. Duplicate samples were collected at nine sites for quality assurance.

Sample processing and preservation

A portion (300 mL) of the 1 L samples was filtered through nylon membranes (Fisherbrand, 0.45 μm pore size, 47 mm diameter) using filtration vessels (Nalgene 500 mL filter holder with receiver)

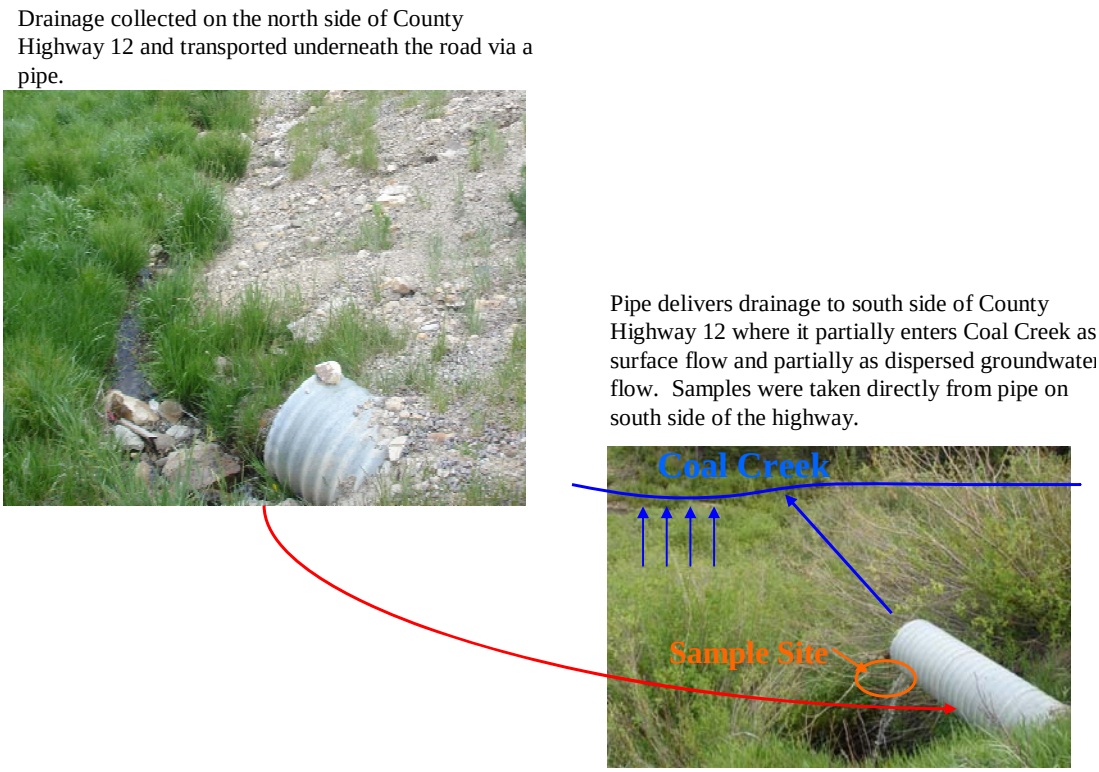

Figure 6. Illustration of tributary drainage transported down culvert paralleling County Highway 12, through pipe underneath the road, and into Coal Creek. A portion of the flow enters Coal Creek as a surface point source while a portion enters Coal Creek as dispersed subsurface flow.

upon arrival at the field laboratory. We used 0.45 µm because the lithium and metal analyses were to be performed by the EPA. The EPA and others have historically used 0.45 µm filters because of their ready availability and greater capacity for filtration before clogging (Morrison and Benoit, 2001; EPA, 2006). The historical use of the 0.45 µm filters also allows for comparison to previous studies. One disadvantage of this size filter is that the pore size is operationally defined and causes ambiguous separation of particle size classes. Many colloids in natural waters pass through 0.45 µm filters (Pham and Garnier, 1998; Morrison and Benoit, 2001). On the opposite end of the spectrum, membrane clogging can occur during filtration, reducing the effective pore size and causing the retention of an increasing mass of colloids.

Filtration vessels were rinsed three times with high-purity water (Millipore Milli-Q, greater than 18 Mohm resistivity) following each filtration. The membrane filters were handled with tweezers. Lab personnel wore gloves at all times during the filtration. A vacuum pump (Gast 0523-101Q-G582DX) with attached tubing (Fisherbrand peristaltic tubing, 6.4 mm diameter, 2.4 mm wall) was used to apply suction to the filtration vessels and increase the filtration rate. Another 300 mL of the 1 L sample was not filtered. The filtered sample composed the dissolved portion and provided dissolved constituent concentrations. The unfiltered sample provided total concentrations. The

colloidal concentration was indirectly determined as the difference between the total and dissolved concentrations.

Both the total and dissolved samples were acidified to pH < 2 with trace metal-grade nitric acid (Fisher Chemical). One mL of nitric acid was added to each 250 mL filtered and unfiltered sample using a pipette (Fisherbrand 100-1000 µL Finnpipette, U16138, and Fisherbrand Redi-Tip General Purpose 101-1000 µL pipette tips, 21-197-8F). Each 300 mL sample was further divided into a 250 mL sample and a 30 mL sample (Nalgene 250 mL and 30 mL high density polyethylene wide mouth sample bottle). The 250 mL sample was sent to the EPA laboratory for inorganic constituent analysis. The 30 mL sample along with any additional remaining sample was kept as backup at the University of Colorado at Boulder. The 60 mL samples in glass amber bottles remained unfiltered to provide total organic carbon (TOC) concentrations. TOC samples were preserved by reducing pH to less than 2 by pipetting 0.5 mL of phosphoric acid (Fisher Chemical) into the glass amber bottle.

The 250 mL total and dissolved samples were prepared, labeled, and documented in accordance with the EPA Superfund Analytical Services/Contract Laboratory Program for multi-media, multi-concentration inorganic analysis, ILMO5.3 (EPA, 2006). These total and dissolved samples were shipped overnight on ice to an EPA contract laboratory for analysis.

Analytical Methods

Sample pH was measured in the field lab within 24 h of collection (Thermo Orion 250A+ meter, 9157BN electrode). The pH meter was calibrated using pH 4 and 7 standards at room temperature. Samples were stored at room temperature before pH measurement.

Total organic carbon (TOC) concentrations were measured using a TOC analyzer (Sievers, 800 Series) 30 d after sample collection. The instrument converts organic carbon in the sample to carbon dioxide (CO_2) by oxidizing organic carbon. A gas-permeable membrane selectively allows only the CO_2 to pass through for measurement. The quantity of CO_2 produced through oxidation is directly proportional to the amount of carbonaceous material in the sample. The analyzer uses a conductometric TOC measurement technique. This technique uses conductivity meters that are not susceptible to drift or fluctuation. Calibration is only required once annually so no calibration was performed prior to these runs. Vials (Fisherbrand 15 mL glass amber vials) were labeled, filled with sample, and then loaded into the TOC autosampler. Two sample vials of high-purity water were run first to flush the system of any trace organic carbon. A vial of high-purity water was also run last sample to wash the analyzer tubing of any residual organic carbon.

Total and dissolved metal concentrations were measured by inductively coupled plasma-atomic emission spectrometry (ICP-AES) and inductively coupled plasma-mass spectrometry (ICP-MS). A total of twenty-three inorganic constituents were measured and included aluminum, antimony, arsenic, barium, beryllium, cadmium, calcium,

chromium, cobalt, copper, iron, lead, lithium, magnesium, manganese, nickel, potassium, selenium, silver, sodium, thallium, vanadium, and zinc. ICP-MS analysis was performed for constituents measured below ICP-AES detection limits. The ICP-AES and ICP-MS analyses were carried out by an EPA contract laboratory, Liberty Analytical Corporation (Cary, NC). Additional ICP-AES (ARL 3410+ and AIM 1250 sampler) analyses were performed to measure the lithium concentrations of the injectate samples at the Laboratory for Environmental and Geological Studies (LEGS), Department of Geological Sciences, University of Colorado at Boulder. These additional analyses were performed to ensure the accuracy of the measured injectate lithium concentrations.

EPA contract labs must use a computer-controlled ICP-AES with background correction, a radio frequency generator, and a supply of argon gas of welding grade or better. The EPA performs a digestion on samples analyzed with ICP-AES. The digestion consists of adding 50-100 mL of well-mixed sample, 2 mL nitric acid, and 10 mL hydrochloric acid to a heating vessel. The vessel is heated at 92-95 ^{o}C for 2 h or until sample volume is reduced by half. The sample is cooled and filtered to remove insoluble material. The sample volume is adjusted to back to pre-digestion volume with reagent water. Sample vessels are then filled and placed in the sampling carousel.

EPA contract labs must use an ICP-MS capable of scanning 5-250 atomic mass units (amu) with a minimum resolution of 1 amu peak width at 5% peak height, a conventional or extended range detector, high purity (99.99%) argon gas, a variable speed peristaltic pump, and a mass-flow controller on the nebulizer gas supply. The EPA also performs a digestion on samples analyzed with ICP-MS as described above for the ICP-AES. Following digestion, samples are ready for ICP-MS analysis.

Dissolved chloride ion concentrations were analyzed using an ion chromatograph (IC; Dionex model ICS-2000) at the Institute for Arctic and Alpine Research (INSTAAR) at the University of Colorado at Boulder. An additional filtration was performed (Onguard II Na Cartridges, Dionex PN062948) prior to IC runs to remove trace metals that might be harmful to the anion exchange column. Only dissolved chloride concentrations were measured because particulates present in unfiltered samples damage IC columns. Four standards designated as Level 1, Level 2, Level 3, and Level 4 were used. The standard concentrations were as follows. Level 4 contained 0.2 mg L^{-1} Cl, 0.05 mg L^{-1} SO_4, and 0.005 mg L^{-1} NO_3. Level 3 contained 2.0 mg L^{-1} Cl, 0.5 mg L^{-1} SO_4, and 0.05 mg L^{-1} NO_3. Level 2 contained 20.0 mg L^{-1} Cl, 5.0 mg L^{-1} SO_4, and 0.5 mg L^{-1} NO_3. Level 1 contained 200.0 mg L^{-1} Cl, 50.0 mg L^{-1} SO_4, and 5.0 mg L^{-1} NO_3. Results were corrected for machine drift using a linear regression technique based on calibration standards analyzed at the beginning and end of each run. Blanks composed of high-purity water were run intermittently throughout each run to flush the IC. The IC detects different ions based on the different rates at which they migrate through the IC column. These rates depend on the extent of interaction with ion exchange sites on the column. Ions are identified based on their retention time in the column. They are quantified by integrating sample chromatograph peak areas and comparing them to peak areas produced by the standards. The nitric acid used to preserve the samples

created large nitrate peaks on the chromatographs. The nitrate peak blocked detection of elements with similar retention times such as bromide. However, chloride detection was not impaired as chloride elutes considerably later than nitrate. Detection limits for ICP-AES, ICP-MS, and IC analyses are listed in Table 2.

Table 2. Minimum detection limits reported for target analytes measured using ICP-AES, ICP-MS, and IC analysis.

Analyte	**ICP-AES CRQL[1], µg L^{-1}**	**ICP-MS CRQL, µg L^{-1}**	**IC DL[3], µg L^{-1}**
Aluminum	200	--	
Antimony	60	2	
Arsenic	10	1	
Barium	200	10	
Beryllium	5	1	
Cadmium	5	1	
Calcium	5000	--	
Chloride			200
Chromium	10	2	
Cobalt	50	1	
Copper	25	2	
Iron	100	--	
Lead	10	1	
Lithium	5, 2[2]	--	
Magnesium	5000	--	
Manganese	15	1	
Nickel	40	1	
Potassium	5000	--	
Selenium	35	5	
Silver	10	1	
Sodium	5000	--	
Thallium	25	1	
Vanadium	50	1	
Zinc	60	2	

[1] CRQLs are contract required quantitation limits. These are minimum levels are quantitation acceptable under the contract Statement of Work (SOW; EPA, 2006).

[2] Detection limit reported by LEGS.

[3] Detection limit reported by INSTAAR.

Six suspended sediment samples were analyzed for relative elemental composition using an electron microprobe (JEOL JXA-8600) at LEGS, Department of Geological

Sciences, University of Colorado at Boulder. The microprobe is equipped with four wavelength-dispersive spectrometers and one energy-dispersive spectrometer. Analytical sensitivity ranges from 50-500 mg kg^{-1}. Samples were prepared as a flat mounts and secured with epoxy. They were then coated with a thin carbon layer using a carbon evaporator. Digital x-ray mapping images and elemental spectra (Geller dPic hardware) were obtained.

Flow rate calculations

The tracer dilution method assumes conservation of mass (Table 3, Equations 1 and 2) between upstream and downstream sample locations. Conservation of mass requires that flow or mass at a downstream sample location is equal to flow or mass at an upstream sample location plus the flow or mass entering the stream at the injection site (Kimball and others, 2002). Steady-state conditions dependent upon a constant injection tracer concentration and a constant tracer injection rate are assumed. Refer to Table 3 for all equations used for flow rate determination.

All inflow between two sites bracketing a visible tributary was assumed to be due to tributary inflow. This might not be the case in reality, because the tracer dilution method quantifies flow from point sources as well as flow from distributed ground water input or springs or seeps discharging over a large area. However, the fraction of flow input attributable to dispersed sources cannot be quantified using tracer dilution. Tributary flow rates were calculated as the difference between flow at the sample location upstream of the tributary and flow at the sample location downstream of the tributary.

The quantity Q_{lest} in Equation 6 (Table 3) was estimated. Flow downstream of tributaries containing background tracer concentrations greater than in-stream concentrations had to be estimated because tracer dilution equations break down under these conditions and no direct flow meter measurements were taken. Q_{lest} was estimated by field personnel as a percentage of in-stream flow just upstream of the tributary confluence with Coal Creek.

Metal-loading calculations

Stream flow and metal concentration at each synoptic sample site were multiplied to obtain a metal-loading rate (kg d^{-1}) for each site. These metal-loading rates produce a metal-loading profile for the length of the study reach. The load at the downstream end of a stream reach is equal to the load at the upstream end plus load contributions from all sources between the ends of the reach. The load is used to identify metal sources within the watershed. Increases in the metal load between sites indicate a metal source. Metal load decreases indicate a net loss of dissolved metal resulting from precipitation, sorption, or chemical reactions. The downstream load minus the upstream load

Table 3. Equations used to calculate flow rates and mass loading rates (Kimball and others, 2002) for Coal Creek tracer dilution study.

Calculated Variable	Equation	Variable Definition
Mass balance downstream from injection site	$M_B = Q_B C_B$ (1) $M_B = Q_A C_A + Q_{inj} C_{inj}$ (2) $Q_B = Q_A + Q_{inj}$ (3)	M_B, mass loading rate downstream of injection site C_A, tracer concentration upstream of injection site C_B, tracer concentration downstream of injection site C_{inj}, injectate tracer concentration Q_A, flow rate upstream of injection site Q_B, flow rate downstream of injection site Q_{inj}, injection flow rate
Flow rate at first site downstream of injection site with uniform background concentration	$Q_B = Q_{inj}\frac{C_{inj} - C_A}{C_B - C_A}$ (4)	All variables defined above
Flow rate at subsequent downstream sites with uniform background concentration and upstream surface inflow contribution	$Q_C = Q_B\frac{C_B - C_I}{C_C - C_I}$ (5)	C_C, tracer concentration at downstream site C_I, tracer concentration of inflow site Q_C, flow rate at downstream site
Flow rate at sites downstream of inflow with tracer concentration above background tracer concentration	$Q_D = \frac{Q_C C_C + Q_{Iest} C_{IN}}{C_D}$ (6)	C_{IN}, tracer concentration of inflow with non-uniform background concentration C_D, tracer concentration downstream of inflow of concentration C_{IN} Q_{Iest}, visually estimated inflow rate

between two sites is defined as the net load change. The cumulative load is the sum of the positive load changes for the entire study reach. The cumulative load is held constant for a negative load change between sites.

The cumulative load approximates the minimum possible metal load contributed to the stream (Kimball and others, 2002). The tributary load (%) is defined as

$$tributary\ load\,(\%) = \frac{load_i}{\sum_i load} \times 100 \quad (7)$$

where $load_i$ (kg d^{-1}) is the loading rate at a specific tributary and the sum of the loads is the cumulative total of all tributary inputs (kg d^{-1}).

Water quality standards and hardness

All surface waters in the State of Colorado must meet physical and chemical water quality requirements set by the Colorado Department of Public Health and Environment (CDPHE). Coal Creek is classified as a Class 1 – Cold Water Aquatic Life stream because the summer water temperature does not often exceed 20 ^{o}C and as a Domestic Water Supply because Coal Creek supplies Crested Butte's drinking water (CDPHE, 2005). As such, Coal Creek must meet all requirements put forth by the CDPHE for these stream types. For protection of aquatic life, CDPHE gives chronic and acute toxicity limits for metals. The chronic standard is defined as the concentration limit that protects 95% of the genera from the chronic toxic effects of metals. Acute toxicity is defined as the concentration limit that protects 95% of the genera from the lethal affects of metals. Standard exceedances should not occur more than once every three years on average (CDPHE, 2005).

Many of the CDPHE metal standards are based on hardness measured as mg L^{-1} $CaCO_3$. Hardness was calculated as the sum of the total calcium and magnesium ion concentrations:

$$Hardness = 50.05\ ([Ca] + [Mg]) \quad (8)$$

where [Ca] and [Mg] are the total concentrations of the calcium and magnesium ion in units of milliequivalents per liter (meq L^{-1}). Calcium and magnesium concentrations were measured at each synoptic sample site and allowed for hardness calculations at each site. A hardness profile for the entire length of the stream was developed. The standard and acute toxicity limits calculated as a function of hardness were compared to measured metal concentrations along Coal Creek for cadmium, chromium(III), copper, lead, manganese, nickel, and zinc. Parameters that are not hardness-based including pH and acute and chronic toxicity standards for aluminum, arsenic, chromium(VI), and iron were also compared to measured values.

The Mt. Emmons Treatment Plant adds lime during the treatment process to raise the pH of Keystone Mine drainage to between 10 and 10.5 (John Perusek, personal communication, July 15, 2005). Cadmium and manganese require this pH increase for precipitation and removal. The addition of calcium results in a significant increase in the hardness of Coal Creek downstream of the treatment plant effluent. The increase in hardness increases the CDPHE hardness-based aquatic life standards. Competition between calcium and metals for binding sites on colloids is expected to reduce the toxicity of metals to aquatic life.

RESULTS

The following chapter presents pH, total organic carbon (TOC), calcium and magnesium concentrations, hardness, metal concentrations, metal loading, and mineralogical data resulting from multiple laboratory analyses of samples collected during synoptic sampling of Coal Creek on September 5, 2005. The results represent stream chemistry at the time of the synoptic sampling. Low flow conditions existed in Coal Creek. Weather conditions were mostly sunny with a temperature of approximately 21◦C. A light rain fell for approximately 30 min during synoptic sampling. This rain event was not heavy enough to significantly influence flow or to create any runoff.

On the graphs presented in this chapter, in-stream sample sites (CC-) and unnamed tributaries (UT-) are designated by distance (km) from the upstream site (CC-0.000). The sample sites are identified by a distance downstream from the upstream site CC-0.000. The distances are presented with a precision of 1 m, or 0.001 km, to clearly establish the downstream order. The downstream order of the sites is accurate, but the precision of the downstream distances is not 0.001 km. We estimate that the precision of the downstream distances is about 50 m, or 0.050 km, because most of the locations were determined by global positioning system on County Highway 12, not at the sample site in the stream.

Two of the main natural tributaries to Coal Creek, Splain's Gulch and Elk Creek, are located at 1.080 km and 1.490 km, respectively. Two unnamed tributaries, UT-3.294 and UT-3.455, drain the iron fen. UT-3.661 contains drainage directly from the gossan (Figure 3). Crested Butte's drinking water intake at 5.390 km is followed immediately by the Mt. Emmons Treatment Plant effluent release channel at 5.405 km. The Spann Nettick ditch located at 8.029 km diverts flow out of Coal Creek between CC-7.895 and CC-8.085. Overflow from the drinking water reservoir is returned to Coal Creek through at 8.090 km. The Halazon diversion is located immediately downstream of the drinking water return flow at 8.105 km.

A large wetland exists between CC-2.072 and CC-2.734. Smaller wetlands occurred between CC-3.165 and CC-3.455 near the two iron fen drainages. Site CC-2.588 is located in the wetland reach of Coal Creek and the sample was mistakenly taken from an apparently stagnant side channel that did not exchange with the creek flow; therefore, a tracer concentration for CC-2.588 was not available. This absent data produces a discontinuity in flow and metal loading graphs at CC-2.588.

Coal Creek pH

The pH in Coal Creek varied from a minimum of 6.97 at CC-2.734 to a maximum of 7.69 at CC-9.442 (Figure 7), a range of only 0.72 pH units. The pH of Coal Creek at the Crested Butte drinking water intake (CB D.W. Intake) is 7.24. The Colorado Department of Public Health and Environment (CDPHE) set a pH window of 6.5-9.0 as the standard for cold water aquatic life. The acceptable pH range for a domestic

drinking water supply is 5.0-9.0 (CDPHE, 2005). Cold water aquatic life and domestic drinking water supply criteria for stream pH were met at all sample locations in Coal Creek. The pH of unnamed tributaries UT-3.294, UT-3.455, and UT-3.661 fell below the minimum pH standard. Unnamed tributaries UT-5.577 and UT-6.696 came within 0.1 pH units of the minimum aquatic life standard.

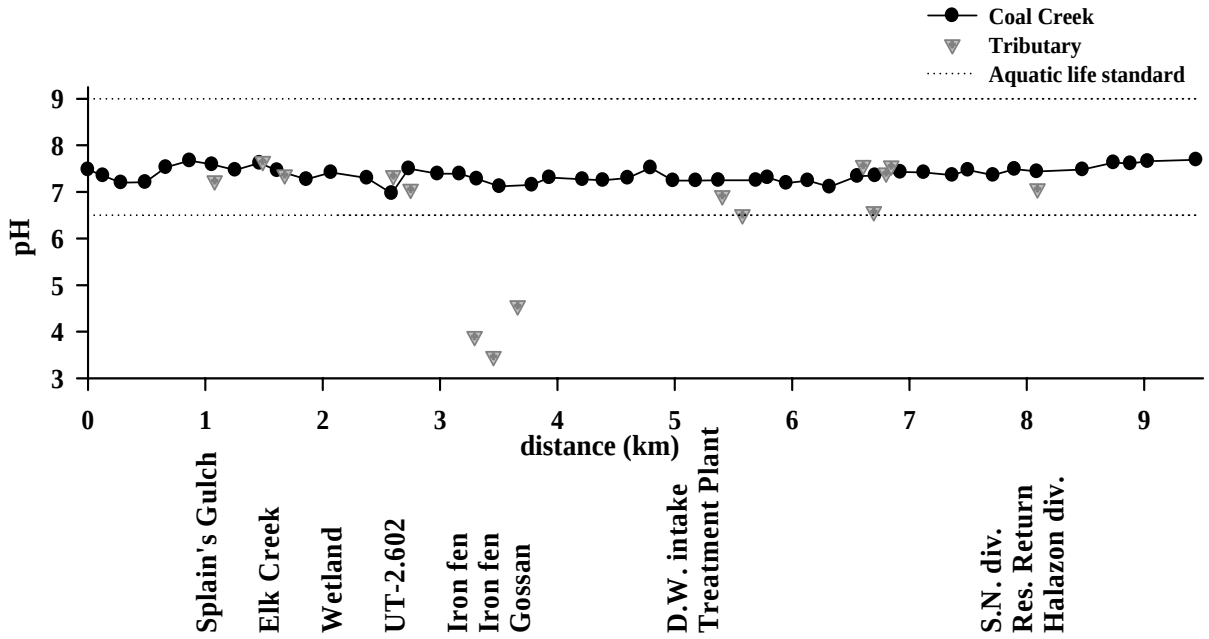

Figure 7. Coal Creek and surface tributary pH measured in the field lab within 24 h of collection. Stream and tributary pH is compared to the aquatic life standards for pH recommended by the CDPHE (CDPHE, 2005). The drinking water intake is designated "D.W. intake"; the Spann Nettick diversion as "S.N. div."; and the Halazon diversion as "Halazon div.".

Coal Creek total organic carbon

Total organic carbon concentrations were measured because TOC can influence biogeochemical processes, chemical interactions, and transport. Coal Creek total organic carbon concentrations ranged from a minimum of 1.5 mg L^{-1} at CC-6.923 to a maximum of 4.7 mg L^{-1} at CC-0.664 (Figure 8). TOC concentrations show a general decrease within this range from the upstream end of the study reach to CC-6.923. Higher TOC concentrations in the upstream reach may be attributable to lower flow and carbon inputs from the wetland. UT-3.294 contains 1.3 mg L^{-1} TOC and was the tributary with the lowest TOC concentration. UT-6.606 contains the highest tributary TOC concentration with 3.4 mg L^{-1}.

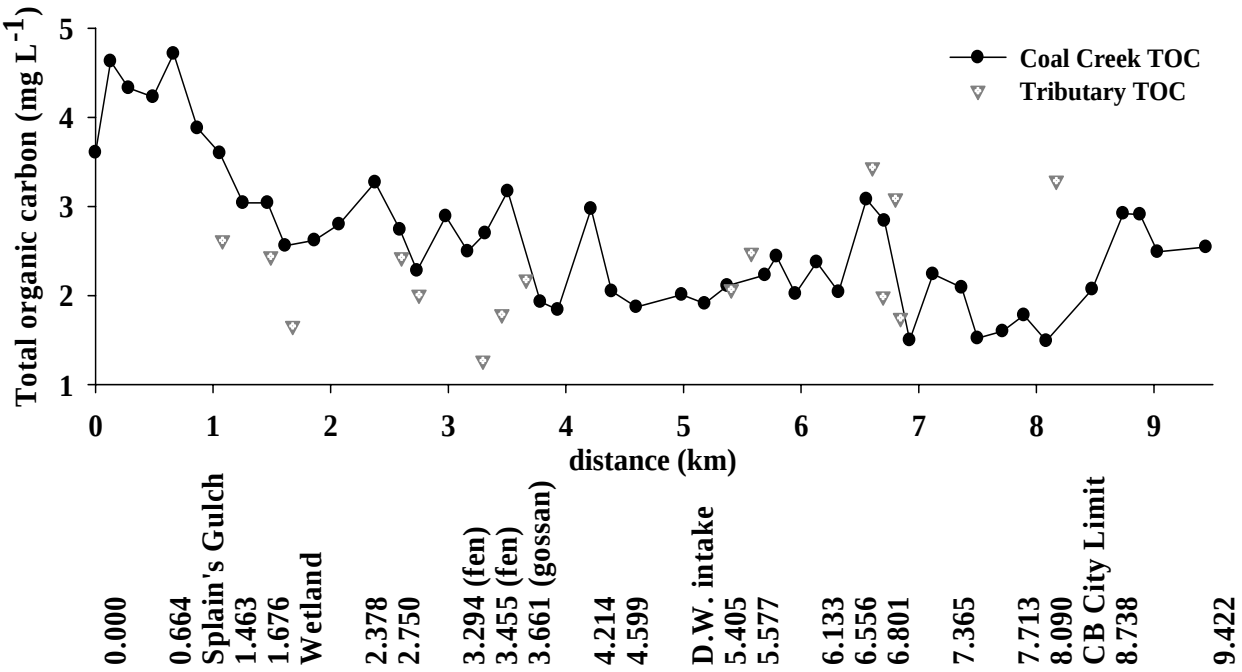

Figure 8. Coal Creek and tributary total organic carbon concentration.

Calcium and magnesium concentration and hardness

Total calcium and magnesium concentrations were used to calculate hardness in mg L^{-1} as $CaCO_3$ (Figure 9). Approximately 93% of the calcium and 94% of the magnesium was available in the dissolved form. Magnesium concentration remained nearly constant along the entire study reach. The only tributary contributing a magnesium concentration greater than the in-stream maximum was UT-3.661 with a magnesium concentration of 14.0 mg L^{-1}.

Calcium concentrations varied significantly from a minimum of 12.5 mg L^{-1} at CC-1.463 to a maximum of 154 mg L^{-1} at CC-6.556 (Figure 9). Calcium concentrations remained steady near an average of 17.8 mg L^{-1} from CC-0.000 to CC-5.372. Downstream of CC-5.372 and the Mt. Emmons Treatment Plant effluent, calcium concentrations increase until the maximum occurs at CC-6.556. A gradual decline in calcium concentration was observed following the peak at CC-6.556. Steeper concentration decreases were detected between CC-6.707 and CC-6.923 as calcium concentration drops from 148 to 120 mg L^{-1} and between CC-8.085 and CC-8.474 as concentration drops from 104 to 52.2 mg L^{-1}. The treatment plant effluent had a calcium concentration of 167 mg L^{-1}.

Hardness ranges from a minimum of 43.2 mg L^{-1} as $CaCO_3$ at CC-1.463 to a maximum of 400 mg L^{-1} as $CaCO_3$ at CC-6.556 (Figure 9). Like calcium, hardness remained stable near an average of 57.1 mg L^{-1} as $CaCO_3$ between CC-0.000 and

CC-5.372. Downstream of CC-5.372 and the Mt. Emmons Treatment Plant effluent release, hardness steadily increases until the in-stream maximum occurs at CC-6.556. Hardness gradually decreases downstream of CC-6.556. The Mt. Emmons Treatment Plant effluent had a hardness of 521 mg L^{-1} as $CaCO_3$.

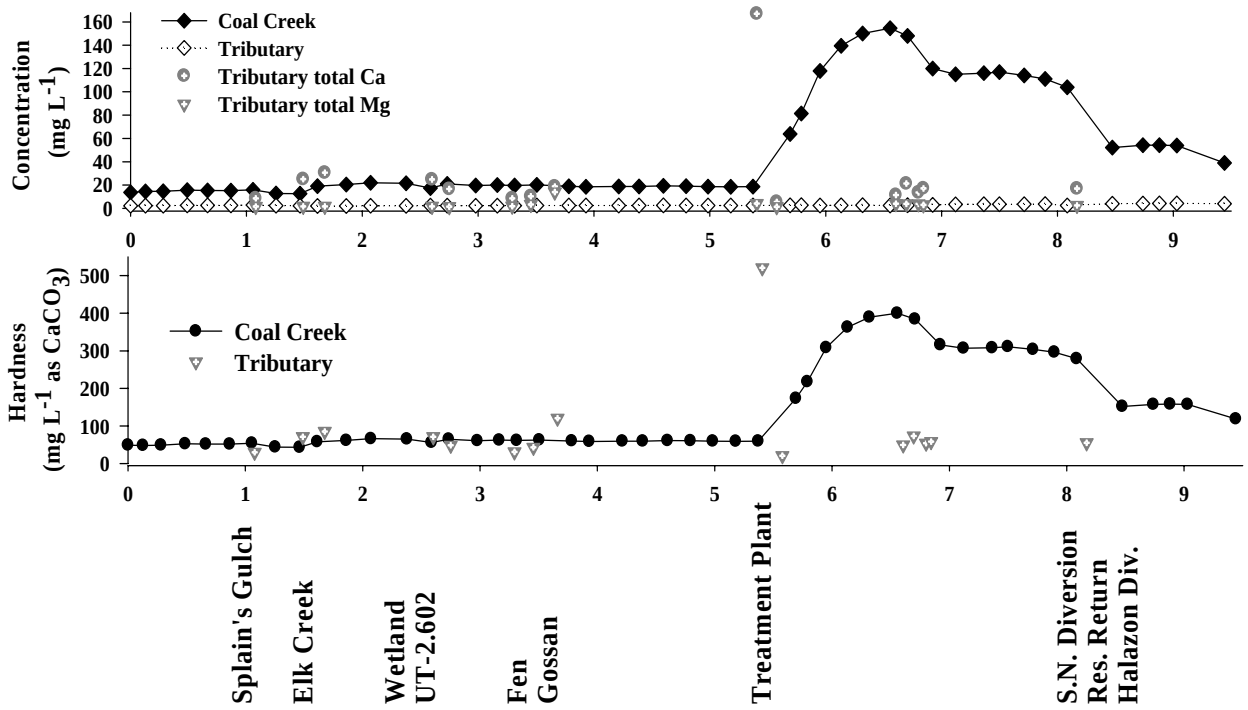

Figure 9. Coal Creek and tributary total calcium and magnesium concentration and hardness as mg L^{-1} $CaCO_3$.

Sodium chloride pulse tracer test

Arrival of the sodium chloride tracer at five sample sites was documented using a conductivity meter. The stream velocity was calculated as the distance traveled by the tracer from the injection point at a study reach distance of 0.051 km to the monitor site divided by the time between the pulse injection (12:28) and the time that conductivity peaked at the monitor site (Table 4). The calculated velocities showed a decreasing trend with downstream distance. The average velocity was 0.22 km h^{-1}. Based on this

Table 4. The time of the conductivity peak in response to the pulse NaCl tracer at five sample sites. The stream velocity was calculated at each site as described above and used to estimate the time required for the LiCl tracer to reach the most downstream sample site.

Site	Conductivity Peak Time	Velocity (km h^{-1})
CC-0.128	12:43	0.308
CC-0.489	14:03	0.289
CC-0.664	16:01	0.173
CC-0.867	17:15	0.171
CC-1.057	18:37	0.166

average velocity in this upstream reach of the study reach, an injection time of 43 h was required for the LiCl tracer to reach the most downstream sample site at 9.442 km. Background conductivity was approximately 100 μS cm^{-1} at all monitor sites.

Injection tracer concentration

Thirteen injection tank samples were taken over the course of the injection period and analyzed for lithium and chloride concentration (Table 5). These samples were taken directly from the injection tubing that transported the injection solution from the tank into Coal Creek. Lithium concentration was measured by both the Environmental Protection Agency (EPA) and the Laboratory for Environmental and Geological Sciences (LEGS) using ICP-AES.

The EPA lithium concentrations for the injection tank varied from 1.78×10^4 to 3.68×10^4 mg L^{-1} ($\sigma = 6.06 \times 10^3$ mg L^{-1}). The LEGS lithium concentrations for the injection tank varied only from 1.13×10^4 to 1.24×10^4 mg L^{-1} ($\sigma = 4.31 \times 10^2$ mg L^{-1}). Furthermore, the lithium chloride (34 kg) was added to the 405 L injection tank to produce a desired lithium concentration of 2 M, or 1.39×10^4 mg L^{-1}, and the lithium concentrations measured by LEGS was much closer to this expected lithium concentration than the EPA data. Therefore, the LEGS lithium concentrations were used for all flow calculations. The average lithium concentration of the injection solution was determined by dropping the highest and lowest lithium concentration and averaging the remaining concentrations. The average chloride concentration of the injection solution was determined in the same manner.

The injection solution was replenished twice. The lithium concentration in the LEGS data set clearly responds to addition of the newly mixed injection solution at 18:00 on September 4 (Table 5). The fresh injection

Table 5. Injection solution lithium and chloride concentrations over the injection period. Lithium concentrations were measured using ICP-AES analysis at the Laboratory for Environmental and Geological Studies (LEGS) and by the Environmental Protection Agency (EPA). Chloride concentrations were measured using IC analysis at the Institute for Arctic and Alpine Research (INSTAAR).

Sample Name	LEGS Li (mg L^{-1})	EPA Li (mg L^{-1})	INSTAAR Cl (mg L^{-1})
CC-Inj 9/3 13:07	11,300	25,300	67,000
CC-Inj 9/3 15:07	11,500	19,400	74,900
CC-Inj 9/3 17:14	11,400	27,100	73,200
CC-Inj 9/3 17:14		36,800	
CC-Inj 9/3 17:14		13,500	
CC-Inj 9/3 19:15	11,300	19,400	74,900
CC-Inj 9/4 02:00	11,300	19,900	23,300
CC-Inj 9/4 09:52	11,400	19,200	66,300
CC-Inj 9/4 14:00	11,900	23,800	96,400
CC-Inj 9/4 18:00	12,400	23,800	90,300
CC-Inj 9/5 00:00	12,200	19,800	68,300
CC-Inj 9/5 06:20	12,000	33,700	80,800
CC-Inj 9/5 11:05	12,100	17,800	80,900
CC-Inj 9/5 13:05	12,300	25,600	78,300
CC-Inj 9/5 15:05	12,200	24,800	79,800

solution raises the lithium concentration by 750 mg L^{-1} on average.

Stream and tributary tracer concentration

The average lithium concentration at the upstream site, CC-0.000, was 3.53 µg L^{-1}. The lithium concentration measured at first sampling site downstream of the injection, CC-0.128, during the synoptic sampling was 6,060 µg L^{-1}. A 1,700-fold increase in total lithium concentration between CC-0.000 and CC-0.128 resulted from the injection of the LiCl tracer between these two sites (Figure 10). Tributary lithium concentration varied from 0.95 µg L^{-1} at UT-1.676 to 128 µg L^{-1} at UT-3.661. The lithium concentration at UT-3.661 is 36 times higher than the background lithium concentration measured at CC-0.000. The treatment plant effluent had a lithium concentration of 35.8 µg L^{-1}, which is ten times more than background. All other tributaries contain no more than three times the background lithium concentration.

The dissolved chloride concentration increased by a factor of 13.5 between CC-0.000 and CC-0.128 resulting from the injection of the LiCl tracer between these two sites (Figure 11). The average dissolved chloride concentration at CC-0.000 was 2.38 mg L^{-1}, and chloride concentration increased to 32.0 mg L^{-1} at CC-0.128.

Flow rate calculations

Several estimates and assumptions were made to calculate Coal Creek flow rate. Flow rates at three diversions along the study reach are controlled and monitored. Flow diverted from Coal Creek at the Crested Butte drinking water intake (5.390 km) was estimated as 79.3 L s^{-1} (Larry Adams, personal communication, May 26, 2006). Flow estimates for the two irrigation diversions were 28.3 L s^{-1} for the Spann Nettick ditch and 14.2 L s^{-1} for the Halazon/Town Ranch ditch (Larry Adams, personal communication, May 26, 2006). These three diversions were accounted for in flow rate calculations by subtracting diversion flow from the flow rate calculated using tracer dilution at sites downstream of each diversion.

Overflow from Crested Butte's drinking water reservoir is returned to Coal Creek between CC-8.085 and CC-8.474 at a rate of 60.0 L s^{-1}. This rate was calculated by subtracting average daily drinking water usage for September (1.67×10^6 L d^{-1}, Larry Adams, personal communication, May 26, 2006) from the volume of flow diverted from Coal Creek to the drinking water reservoir (6.85×10^6 L d^{-1}).

The synoptic sites were assigned so that only one tributary was located between two in-stream synoptic sample sites. Tracer dilution equations account only for one tributary between two samples sites. Tributaries UT-6.606, UT-6.696, and UT-6.801 were not detected during site assignment, but were found later during synoptic sampling. Two unnamed tributaries, UT-6.606 and UT-6.696, entered Coal Creek between in-stream sampling sites CC-6.556 and CC-6.707. Also, both UT-6.801 and UT-6.844 entered Coal Creek between CC-6.707 and CC-6.923. For each of these tributaries, the flow rate was estimated as a percentage of the total inflow between the

sites bracketing the tributaries. These estimates were based on visual assessments made by field personnel. Both UT-6.606 and UT-6.696 were assigned half of the total inflow between sites CC-6.556 and CC-6.707. UT-6.801 was estimated to contain 90% of the total inflow between CC-6.707 and CC-6.923, while UT-6.844 was estimated to comprise the remaining 10%.

The lithium concentration in unnamed tributary UT-3.661 was several times greater than background lithium concentration. Observed flow at UT-3.661 was described as only a "trickle" by field personnel. When the standard tracer dilution equation (Equation 4) was applied at UT-3.661, the calculated flow for this tributary was 2,400 L s^{-1}. This extremely high flow rate resulted because the lithium concentration of UT-3.661 was only 8 μg L^{-1} less than the lithium concentration at CC-3.783. The standard tracer dilution equation breaks down when the in-stream tracer concentration is not at least twice as great as the tributary tracer concentration. To avoid assigning UT-3.661 an unrealistically high, flow for UT-3.661 was estimated as 1% of Coal Creek flow (Equation 6).

For the calculation of flow based on chloride dilution, an additional modification was used to account for flow from the Mt. Emmons Treatment Plant effluent channel at 5.405 km. The chloride concentration in this tributary was about 1.1 times greater than the upstream chloride concentration. The standard tracer dilution equation (Equation 4) is not valid if tributary tracer concentration is greater than the in-stream tracer concentration. Equation 6 was used to account for flow from the treatment plant. Equation 6 depends on a field estimate of tributary flow as a fraction of Coal Creek flow. Field personnel estimated flow from the treatment plant channel as 5% of Coal Creek flow. The treatment plant was not discharging at the time of sampling, but a low flow was visible. This treatment plant flow was attributed to either natural drainage or residual treatment plant effluent flow.

The chloride concentration downstream of unnamed tributary UT-5.577 was greater than the upstream chloride concentration. When Equation 4 was applied, the flow rate decreased from upstream to downstream, and the resulting flow from UT-5.577 was calculated as negative. To correct for this anomaly, UT-5.577 was assigned a small positive flow of 1.00 L s^{-1} to enable the calculation of a meaningful loading rate at UT-5.577.

Flow rates based on lithium and chloride dilution

Flow rates calculated based on lithium dilution increased from upstream to downstream sites in response to decreases in lithium concentration in Coal Creek (Figure 10). The flow rates were calculated with Equations 4, 5, and 6. The flow rate increased from 7.9 L s^{-1} at first sampling site, CC-0.128, to 2,300 L s^{-1} at the last sampling site, CC-9.442. The maximum calculated flow rate of 2,540 L s^{-1} occurs just upstream of CC-9.442. The flow rate increases with distance downstream of the injection site at all locations except between CC-6.923 and CC-7.121 and between CC-9.030 and CC-9.442. These are the sites where lithium concentrations increased slightly. Tributary flows

varied from a minimum of 2.15 L s^{-1} at unnamed tributary UT-3.661 to a maximum of 406 L s^{-1} at unnamed tributary UT-6.801.

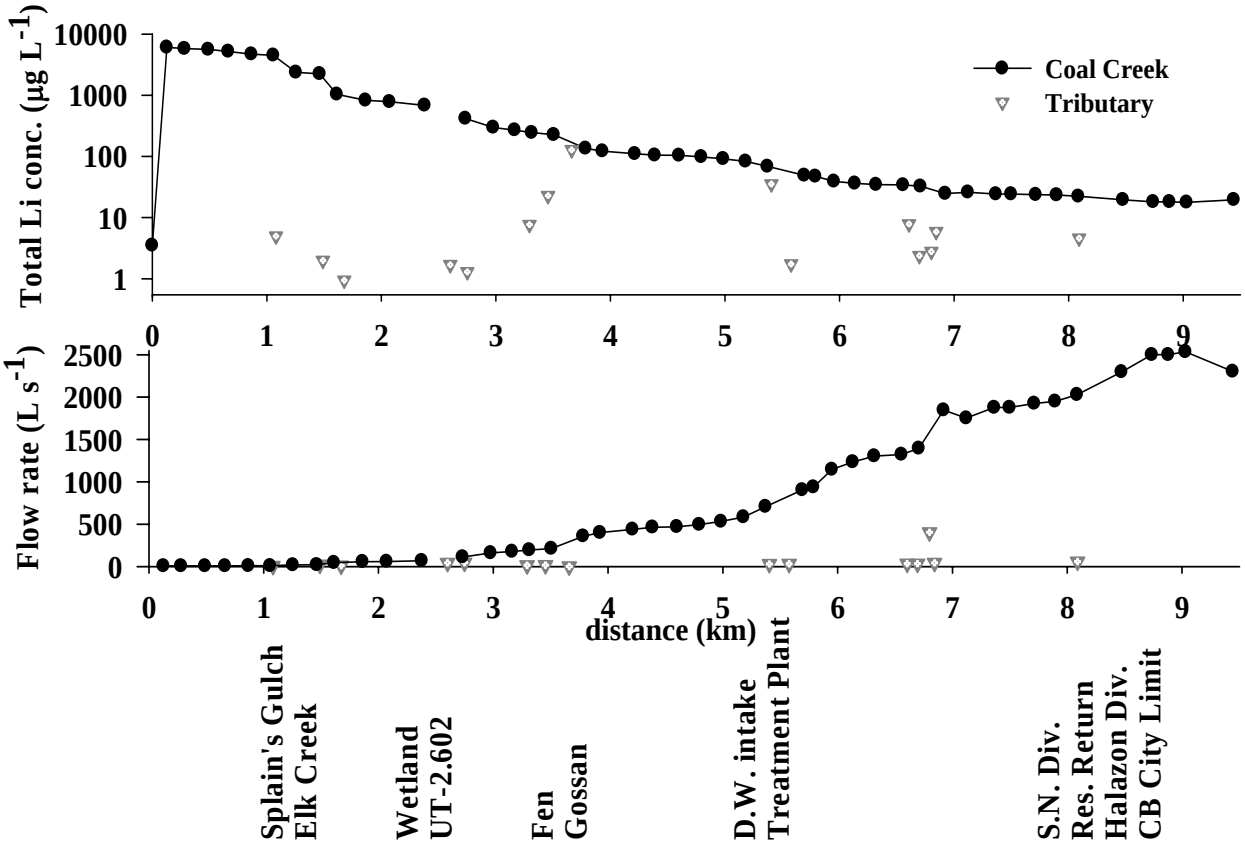

Figure 10. Coal Creek and tributary total lithium concentration and flow rate calculated using lithium concentration dilution. The flow rates determined by lithium dilution were deemed inaccurate. The flow rates used for the metal loading calculations were determined by chloride dilution (Figure 11).

Flow rates calculated based on chloride dilution steadily increased from 10.4 to 122 L s^{-1} between CC-0.000 and CC-5.180 (Figure 11). Four flow rate decreases were observed between CC-3.783 and CC-5.372. Locations where flow rate slightly decreases are locations where chloride concentration slightly increased with downstream distance. The maximum flow rate of 122 L s^{-1} occurs at CC-5.180. The flow rate decreased from 111 to 45.0 L s^{-1} between CC-5.372 and CC-5.693. Between CC-5.372 and CC-5.693, the Crested Butte drinking water intake diverts 79.3 L s^{-1} and the Mt. Emmons Treatment Plant effluent channel contributed 1.60 L s^{-1} (sample was taken after the plant discontinued effluent release for the day). Flow increased from 45.0 L s^{-1} at CC-5.693 to 85.2 L s^{-1} at CC-6.923. Slight flow fluctuations were measured between CC-6.923 and CC-7.895. The Halazon ditch diversion reduces flow in Coal Creek between CC-8.085 and CC-8.474 and flow from the drinking water reservoir is returned to Coal Creek at 8.090 km between these two sites. There is a 40.8 L s^{-1} net flow rate

increase between CC-8.085 and CC-8.474. Flow decreases slightly from CC-8.474 to CC-9.442 in response to slightly increasing chloride concentration. Site distances descriptions, and final flow rates as calculated using chloride-dilution are shown in Table 6.

The flow rates obtained using chloride dilution calculations appear to more accurately describe actual flows in Coal Creek. Just prior to the tracer study, the Coal Creek flow rate was estimated as a maximum of 142 L s^{-1} (Larry Adams, personal communication, May 26, 2006). The maximum flow rate of 2,500 L s^{-1} based on lithium dilution is unreasonable. The flow rates calculated using chloride dilution were much closer to estimated flows. Flow rates based on chloride dilution were used to calculate metal loading rates because they appear to more accurately reflect actual Coal Creek flow.

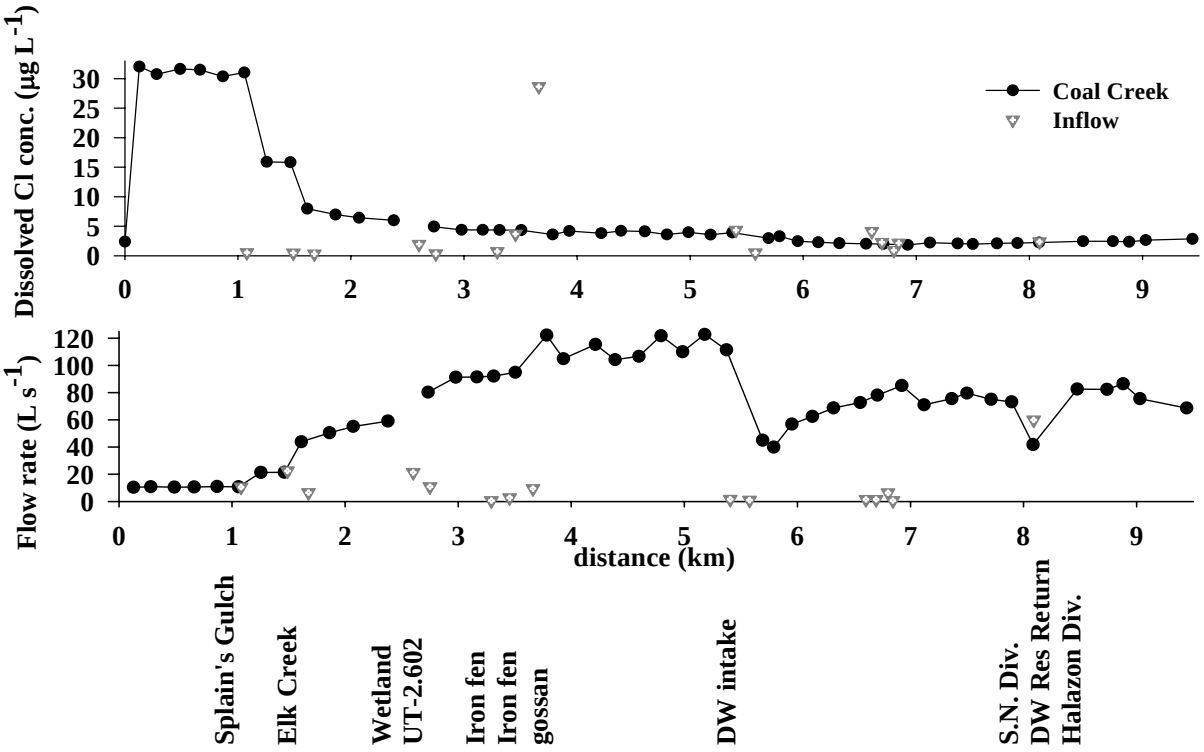

Figure 11. Coal Creek and tributary dissolved chloride concentration and flow rate calculated using chloride concentration dilution. These flow rates were used for the metal loading calculations.

Table 6. Flow rates of Coal Creek sample sites, tributaries, and diversions. Site name reflects distance (km) from the upstream sample site. Flow rates (L s^{-1}) are based on chloride dilution (Figure 11). "CC" is the abbreviation for Coal Creek and "UT" is the abbreviation for an unnamed tributary.

Site Name	Site Description/Details	In-stream Flow Rate (L s^{-1})	Tributary Flow Rate (L s^{-1})
CC-0.000	upstream site, background sampling		
CC-0.051	injection site		
CC-0.128		10.365	
CC-0.282	elevation 2967 m	10.838	
CC-0.489		10.510	
CC-0.664		10.558	
CC-0.867		10.983	
CC-1.057		10.729	
SPG-1.080	Splain's Gulch		10.587
CC-1.255		21.317	
CC-1.463	elevation 2927 m	21.400	
EC-1.490	Elk Creek (Standard Mine drainage)		22.462
CC-1.613		43.862	
UT-1.676			6.603
CC-1.862	downstream of beaver dam	50.465	
CC-2.072	wetland area	55.070	
CC-2.378	wetland area	59.045	
CC-2.588	wetland area, sampling error[1]		
UT-2.602			21.324
CC-2.734		80.369	
UT-2.750			10.911
CC-2.978	elevation 2895 m	91.280	
CC-3.165	wetland area	91.467	
UT-3.294	iron fen drainage, primary		0.678
CC-3.314	iron fen seeps	92.145	
UT-3.455	iron fen seeps		2.745
CC-3.506	iron fen seeps	94.890	
UT-3.661	iron gossan drainage, primary		9.489
CC-3.783		122.223	
CC-3.931		104.911	
CC-4.214		115.394	

Table 6. Flow rates of Coal Creek sample sites, tributaries, and diversions. Site name reflects distance (km) from the upstream sample site. Flow rates (L s^{-1}) are based on chloride dilution (Figure 11). "CC" is the abbreviation for Coal Creek and "UT" is the abbreviation for an unnamed tributary.

Site Name	Site Description/Details	In-stream Flow Rate (L s^{-1})	Tributary Flow Rate (L s^{-1})
CC-4.388	upstream of jeep trail across creek	104.209	
CC-4.599		106.625	
CC-4.794	elevation 2851 m	121.758	
CC-4.985		110.005	
CC-5.180		122.736	
CC-3.72		111.435	
5.390	Crested Butte drinking water intake	79.287	
5.405	Mt. Emmons Treatment Plant discharge		1.607
CC-5.693	upstream of Wildcat Trail bridge	44.959	
UT-5.577			1.000
CC-5.790		39.914	
CC-5.951			56.832
CC-6.133	elevation 2809 m	62.420	
CC-6.319		68.757	
CC-6.556		72.642	
UT-6.606			1.453
UT-6.696			1.453
CC-6.707		78.138	
UT-6.801			6.379
UT-6.844			0.709
CC-6.923		85.225	
CC-7.121	elevation 2782 m	71.059	
CC-7.365		75.595	
CC-7.499		79.556	
CC-7.713		75.034	
CC-7.895	elevation 2767 m	73.152	
8.029	Spann Nettick (Smith Ranch) diversion	28.317	
CC-8.085		41.801	
8.090	Crested Butte drinking water reservoir return		60.010
8.105	Halazon (Town Ranch) diversion	14.158	
CC-8.474	upstream of Crested Butte town line	82.601	
CC-8.738	corner of First Street and Sopris Avenue	82.376	
CC-8.881	corner of Second Street and Elk Avenue	86.498	

Table 6. Flow rates of Coal Creek sample sites, tributaries, and diversions. Site name reflects distance (km) from the upstream sample site. Flow rates (L s^{-1}) are based on chloride dilution (Figure 11). "CC" is the abbreviation for Coal Creek and "UT" is the abbreviation for an unnamed tributary.

Site Name	Site Description/Details	In-stream Flow Rate (L s^{-1})	Tributary Flow Rate (L s^{-1})
CC-9.030	upstream of bridge, Maroon Street	75.545	
CC-9.442	downstream of foot bridge on Butte Avenue	68.663	

[1] sample taken from stagnant pool in wetlands; very low tracer concentration.

Metals in Coal Creek and tributaries

Concentrations and loading rates for iron, manganese, aluminum, zinc, copper, cadmium, lead, nickel, chromium, arsenic, and barium will be presented in the following sections. Total and dissolved concentrations were measured for each of these metals and metalloids. All metal toxicity standards apply to dissolved metal concentrations unless otherwise stated.

Dissolved metal concentrations were greater than total metal concentrations for iron, copper, nickel, and chromium at several sites as reported by the EPA contract laboratory. Only total loading rates are graphed for these metals to exclude error associated with a possible positive interference. Obviously, the dissolved metal concentration should never be greater than the total metal concentration. An analytical error is suspected, but we have not confirmed the cause of this discrepancy. All metal concentrations were measured using both inductively coupled plasma-atomic emission spectroscopy and inductively coupled plasma-mass spectroscopy and this error occurred using both analytical techniques. Inspection of the metals analyses for blanks (high-purity water) lends some insight. The EPA measured high concentrations of dissolved iron, nickel, and chromium in the blanks, but total concentrations were either not detected or considerably lower than dissolved concentrations (Table 7). These results suggest a positive interference with dissolved measurements. A positive (or negative) spectral, physical, or chemical interference can cause concentration measurements to be greater than or less than the true concentration. A positive spectral interference occurs when overlap from the spectral line of one element creates a false high concentration measurement for a different element. Physical interferences occur when nebulization and transport processes change the viscosity and surface tension of the sample matrix. Chemical interferences include compound formation, ionization effects, and solute vaporization (EPA, 2006). Another explanation for this discrepancy may be a "memory effect." This occurs when a sample with a high metal concentration is analyzed and the sample chamber is not rinsed adequately prior to running the following sample. The cause of the dissolved/total discrepancy was undetermined. All

of the metal analyses were conducted at the EPA's contract laboratory, and establishing direct contact with laboratory personnel was not possible.

Table 7. Dissolved and total metal concentrations in blanks (mean ± one standard deviation). BDL is "below detection limit." ICP-AES is inductively coupled plasma-atomic emission spectrometry and ICP-MS is inductively coupled plasma-mass spectrometry.

	ICP-AES		ICP-MS	
Metal	Dissolved ($\mu g\ L^{-1}$)	Total ($\mu g\ L^{-1}$)	Dissolved ($\mu g\ L^{-1}$)	Total ($\mu g\ L^{-1}$)
iron	361±202	BDL		
nickel	56.1±32.9	3.85±3.37	52.0±30.6	3.07±2.97
chromium	41.3±35.3	5.5±4.9	70.5±41.0	4.5±4.5

Iron concentrations and loading rates. Coal Creek iron concentrations ranged from undetectable at several sites to a maximum of 483 $\mu g\ L^{-1}$ total iron at CC-3.165 (Figure 12). Coal Creek total iron concentration never exceeds the chronic toxicity standard for aquatic life of 1,000 $\mu g\ L^{-1}$ total recoverable iron. No acute aquatic life standard exists for iron. The 30-day dissolved iron standard for a drinking water supply is 300 $\mu g\ L^{-1}$ (CDPHE, 2005). Analytical results for dissolved iron show that this standard is exceeded at eight in-stream sites. In-stream dissolved iron concentrations are higher than in-stream total iron concentrations at several sites and unnamed tributaries. Total iron concentration is significantly higher than dissolved iron concentration in unnamed tributaries UT-2.750, UT-3.455, UT-3.661, UT-6.696, and the drinking water reservoir return, indicating a significant colloidal fraction. The greatest difference occurs at UT-6.696. UT-6.696 contains 1,960 $\mu g\ L^{-1}$ total iron and 608 $\mu g\ L^{-1}$ dissolved iron.

The total iron loading rate remains constant from CC-0.128 to CC-2.378 near an average of 0.25 kg d^{-1}. The maximum in-stream iron loading rate of 3.81 kg d^{-1} occurred at CC-3.165, just upstream of iron fen drainage (Figure 12). From CC-6.133 to CC-7.121, iron was undetectable at all sites except CC-6.707, which had a very low iron concentration. The loading rate is zero over this reach due to the undetectable iron concentrations.

The drinking water reservoir return flow at 8.090 km contributes the highest tributary loading rate of 1.92 kg d^{-1}. It comprises 42% of the tributary total iron loading rate (Table 8). UT-2.602 contributes 1.04 kg d^{-1} and 23% of the tributary iron loading rate. UT-3.661, the tributary which drains the gossan (Figure 3), contributes 0.61 kg d^{-1} and 13% of the iron loading rate (Table 8).

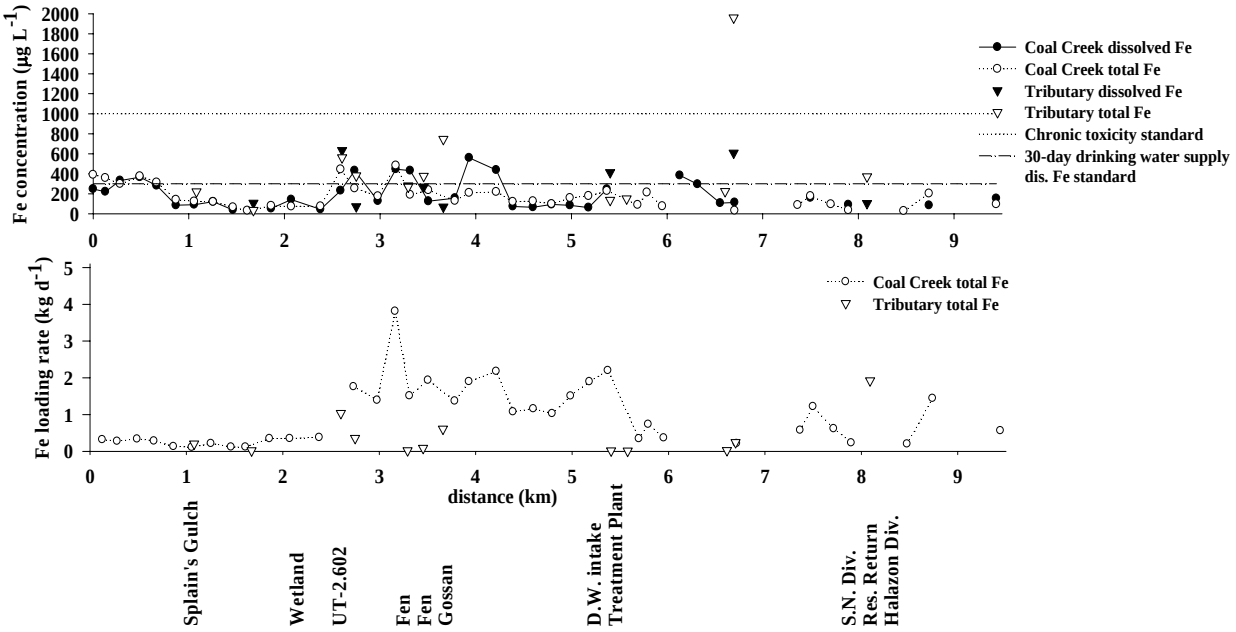

Figure 12. Coal Creek and tributary total and dissolved iron concentration, chronic toxicity standard, 30-day dissolved iron standard for a drinking water supply, and total iron loading rate. Missing data points reflect iron concentrations below the Environmental Protection Agency CRQL of 100 µg L^{-1}.

Table 8. Tributary loading rates expressed for total (above) and dissolved (below) metals as a percentage of the cumulative tributary loading rate (Equation 7) for each metal. "METP" is the Mt. Emmons Treatment Plant.

Source/ Tributary	Tot Fe (%)	Tot Mn (%)	Tot Al (%)	Tot Zn (%)	Tot Cu (%)	Tot Cd (%)	Tot Pb (%)	Tot Ni (%)	Tot Cr (%)	Tot As (%)	Tot Ba (%)
Splain's Gulch-1.080	4.4	0.2	0.5	< 0.1	5.7	< 0.1	22	11	8.7	4.6	4.5
Elk Creek-1.490	< 0.1	0.2	< 0.1	16	9.4	32	6.9	2.5	1.5	21	12
UT-1.676	0.4	0.2	< 0.1	0.8	2.9	< 0.1	< 0.1	0.8	0.6	4.0	2.1
UT-2.602	23	2.4	0.9	1.8	20	< 0.1	< 0.1	45	48	10	7.6
UT-2.750	7.9	0.5	< 0.1	2.9	8.7	< 0.1	< 0.1	16	18	2.5	3.8
UT-3.294; iron fen	0.5	2.1	3.3	3.1	0.9	3.1	0.8	0.8	0.7	0.4	0.9
UT-3.455; iron fen	1.9	9.0	13	10	2.0	12	4.1	0.9	0.3	0.3	2.0
UT-3.661; iron fen	13	62	76	49	13	39	10	18	19	2.7	12
METP effluent	0.4	1.5	2.3	1.3	2.5	2.6	0.7	0.2	0.2	0.7	0.4
UT-5.577	0.3	< 0.1	0.4	0.2	0.7	< 0.1	0.7	0.1	0.1	0.3	0.3
UT-6.606	0.6	0.1	0.5	< 0.1	0.7	< 0.1	1.8	< 0.1	< 0.1	0.3	2.8
UT-6.696	5.4	4.4	< 0.1	0.3	0.9	0.5	0.4	0.3	0.3	7.8	2.0
UT-6.801	< 0.1	< 0.1	< 0.1	0.8	2.4	< 0.1	1.6	< 0.1	< 0.1	2.8	12
UT-6.844	< 0.1	< 0.1	< 0.1	< 0.1	0.3	< 0.1	0.8	< 0.1	< 0.1	0.3	0.8
reservoir return	42	17	3.1	14	30	11	50	3.4	2.7	42	37
		Diss Mn (%)	**Diss Al (%)**	**Diss Zn (%)**	**Diss Cu (%)**	**Diss Cd (%)**	**Diss Pb (%)**			**Diss As (%)**	**Diss Ba (%)**
Splain's Gulch-1.080		< 0.1	< 0.1	0.1	4.0	< 0.1	< 0.1			< 0.1	4.5
Elk Creek-1.490		0.3	< 0.1	15	8.0	33	15			25	11
UT-1.676		0.3	< 0.1	0.1	2.6	< 0.1	< 0.1			5.4	2.7
UT-2.602		2.9	< 0.1	0.6	22	< 0.1	< 0.1			15	8.4
UT-2.750		0.3	< 0.1	1.4	8.2	< 0.1	< 0.1			3.4	3.9
UT-3.294; iron fen		2.7	3.6	3.5	0.9	3.7	3.3			< 0.1	0.9
UT-3.455; iron fen		10	14	12	2.1	15	14			< 0.1	2.1
UT-3.661; iron fen		68	78	59	8.7	46	20			2.7	12
METP effluent		2.0	2.1	1.4	2.3	3.1	2.0			< 0.1	0.5
UT-5.577		< 0.1	< 0.1	0.2	0.6	< 0.1	< 0.1			< 0.1	0.3
UT-6.606		< 0.1	< 0.1	< 0.1	0.5	< 0.1	< 0.1			0.2	2.4
UT-6.696		5.1	< 0.1	0.1	0.8	0.3	< 0.1			6.1	2.2
UT-6.801		< 0.1	< 0.1	0.3	2.5	< 0.1	< 0.1			< 0.1	13
UT-6.844		< 0.1	< 0.1	< 0.1	0.3	< 0.1	< 0.1			< 0.1	0.8
reservoir return		8.6	3.0	6.2	36	< 0.1	46			42	36

Manganese concentration and loading rate. The maximum total manganese concentration of 101 µg L^{-1} was measured at CC-2.378, directly in the center of the wetland reach (Figure 13). CC-2.588 and CC-2.734, on the downstream end of the wetland reach, also have high total manganese concentrations of 88.9 and 79.9 µg L^{-1}, respectively. Tributaries upstream of CC-2.378 do not contain high manganese concentrations. Tributary inputs do not contribute to the high manganese concentrations from CC-2.378 to CC-2.734. The source of manganese is either ground water or wetland input.

A small increase in manganese concentration occurred downstream of the Mt. Emmons Treatment Plant at 5.405 km. Concentration increased from 29.9 µg L^{-1} total manganese at CC-5.372 to 43.9 µg L^{-1} at CC-6.319. Concentrations decrease slightly with downstream distance. Manganese concentrations do not fully decrease to background concentrations along the study reach. Manganese concentrations in Coal Creek are well below the chronic and acute toxicity standards at all sites. For this reason, these standards are not included on the graph. The 30-day dissolved manganese standard for a drinking water supply is 50 µg L^{-1}. This standard is exceeded at CC-2.378 to CC-2.734, CC-3.165 to CC-3.506, CC-4.388, CC-6.133, and CC-6.319. A sharp decrease in manganese concentration occurred at CC-6.556, approximately 1.1 km downstream of the treatment plant. Most manganese is present in the dissolved form.

Of the tributaries, UT-3.661 contained the largest manganese concentration with 1,370 µg L^{-1} dissolved manganese and 1,530 µg L^{-1} total manganese. UT-6.696 also had high manganese concentrations with 669 µg L^{-1} dissolved manganese and 712 µg L^{-1} total manganese. Tributary total and dissolved manganese concentrations are similar for all tributaries except UT-3.661.

The Coal Creek manganese loading rates closely resembled Coal Creek manganese concentrations (Figure 13). The maximum loading rate of 0.62 kg d^{-1} dissolved manganese occurred at CC-2.734. The loading rate remained elevated near an average of 0.46 kg d^{-1} from CC-2.378 – CC-5.180. The loading rate decreased downstream of CC-5.372 in response to the drinking water flow diversion. A sharp loading rate decrease occurred at CC-6.556 in response to the low manganese concentration at that site.

The largest tributary dissolved manganese loading rate of 1.12 kg d^{-1} comes from UT-3.661 and comprises 67% of the manganese loading in Coal Creek. Though UT-3.294, UT-3.455, the treatment plant channel, and UT-6.696 have high manganese concentrations, flow from these tributaries is too low to produce a significant loading rate. The drinking water return channel is the only other tributary with a loading rate above the in-stream loading rate. It contributes 0.35 kg d^{-1} total manganese and 17% of the cumulative tributary manganese loading rate (Table 8).

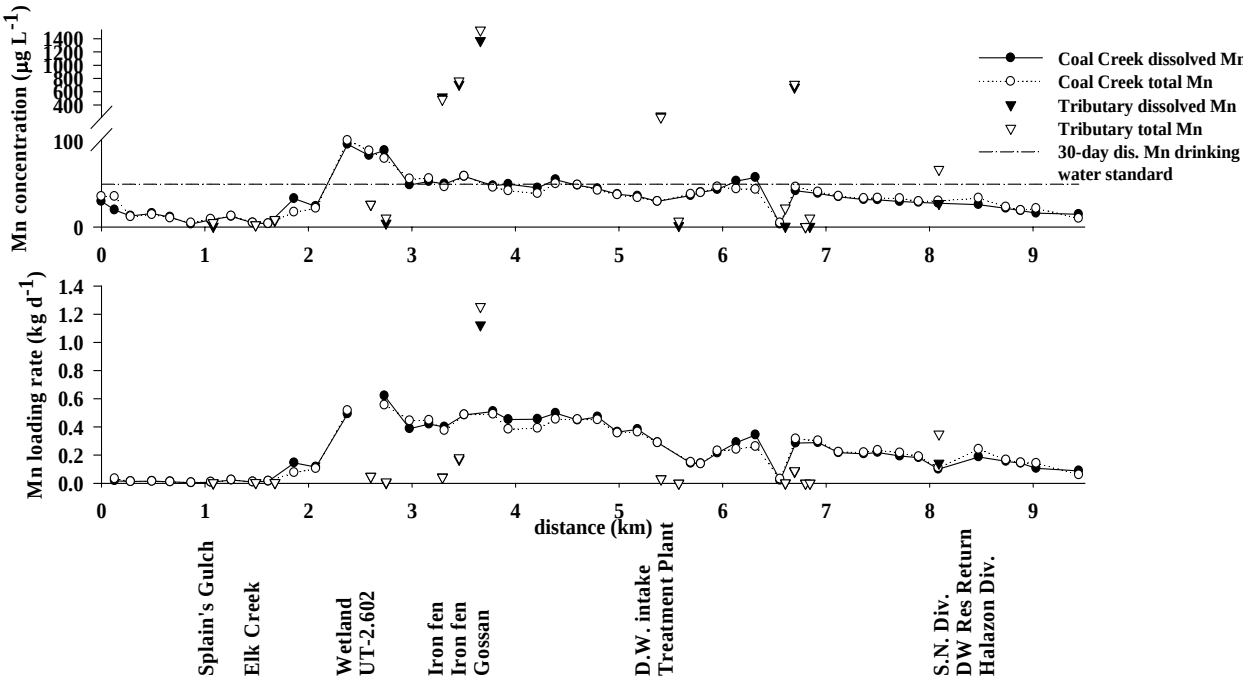

Figure 13. Coal Creek and tributary total and dissolved manganese concentration, 30-day drinking water supply dissolved manganese standard, and total and dissolved manganese loading rate.

Aluminum concentrations and loading rates. Aluminum concentrations are below the chronic toxicity standard of 87 µg L^{-1} total recoverable aluminum for sites CC-0.000 to CC-5.372 (Figure 14). Sites CC-1.255 to CC-3.314 contained no measurable aluminum. A small rise in aluminum concentration was observed between CC-5.693 and CC-7.499. CC-6.319 had the highest dissolved aluminum concentration with 221 µg L^{-1}. CC-6.556 had the highest total aluminum concentration with 294 µg L^{-1}. The CDPHE specifies that the chronic total recoverable aluminum criterion will not apply when pH is greater than or equal to 7.0 and when hardness is greater than or equal to 50 mg L^{-1} as $CaCO_3$. This is the case for all Coal Creek sites with aluminum concentrations above 87 µg L^{-1}. Aluminum concentrations above 87 µg L^{-1} are not in violation of aquatic life standards in Coal Creek. In this instance, aluminum is regulated based on the 750 µg L^{-1} total recoverable aluminum criterion (CDPHE, 2005). This acute aluminum toxicity standard is not exceeded at any in-stream site.

The unnamed tributaries UT-3.294 and UT-3.455, which drain the iron fen, and UT-3.661, which directly drains the gossan, have total and dissolved aluminum concentrations greater than 750 µg L^{-1}. UT-3.661 has the highest dissolved and total aluminum concentrations of 5,750 µg L^{-1} and 6,610 µg L^{-1}, respectively. The Mt. Emmons treatment plant discharge also has total and dissolved aluminum concentrations greater than 750 µg L^{-1}. During synoptic sampling, the treatment plant discontinued the daily effluent release. A second sample was taken from the

Mt. Emmons Treatment Plant effluent channel on September 6, 2005, at 10:49 when effluent was being released. This sample was taken to detect any differences in constituents when effluent was being released and when it was not. This sample is not graphed in Figures 10 and 11 because it was not collected during the synoptic sampling. On September 6, this tributary contained 728 µg L^{-1} dissolved aluminum and 1,020 µg L^{-1} total aluminum.

The aluminum loading rate peaks at the same locations as the aluminum concentration (Figure 14). The dissolved loading rate reaches a maximum of 1.31 kg d^{-1} at CC-6.319. The total loading rate reaches a maximum of 1.85 kg d^{-1} at CC-6.556, approximately 1.1 km downstream of the treatment plant. A smaller spike of 1.30 kg d^{-1} total aluminum occurs at CC-9.030, within the Crested Butte city limit upstream of the bridge on Maroon Street. UT-3.661 contributes the greatest aluminum loading rate of the tributaries with 5.01 kg d^{-1} total aluminum. This is 76% of the tributary total aluminum loading rate. UT-3.455 contributes 0.86 kg d^{-1} total aluminum, which is 13% of the total aluminum loading rate. Though UT-3.294 and the treatment plant channel contained high aluminum concentrations, the loading rate is not substantial because of the low flow rates at these sites. UT-3.294 contributed 3.3% of the total aluminum loading rate and the treatment plant effluent added only 2.3% (Table 8).

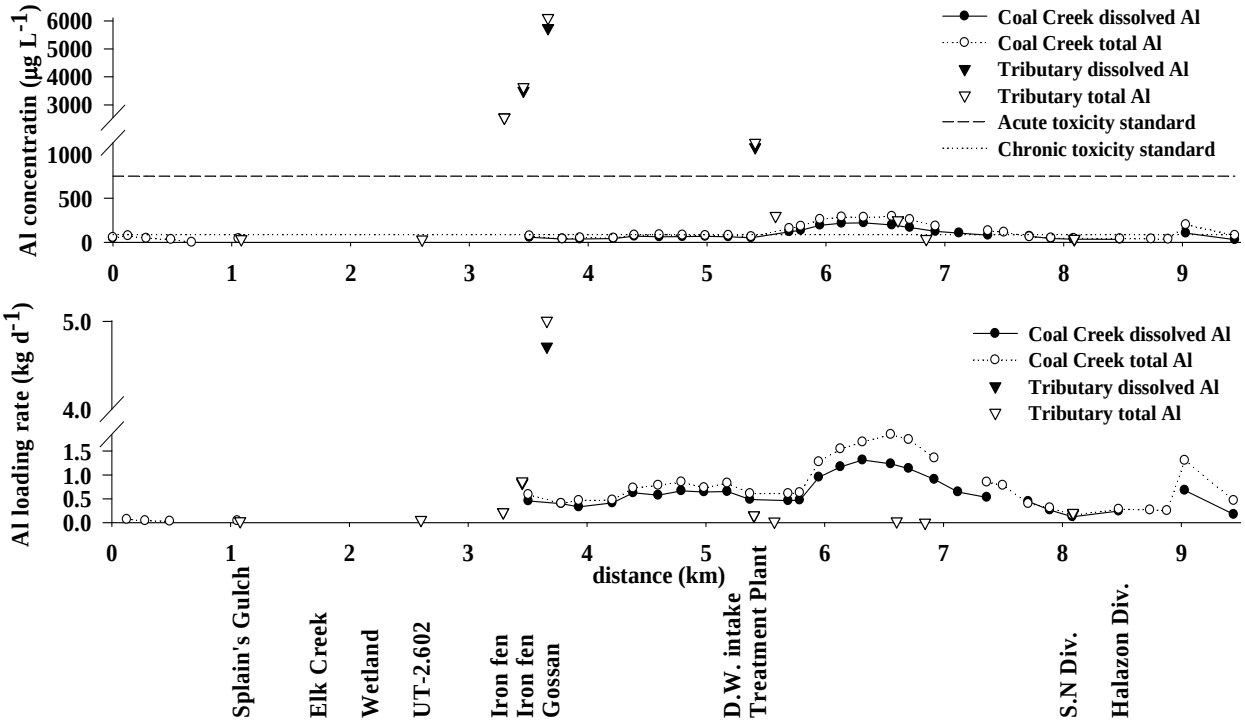

Figure 14. Coal Creek and tributary total and dissolved aluminum concentration, acute and chronic toxicity standards for aquatic life, and total and dissolved aluminum loading rate.

Zinc concentrations and loading rates. The maximum in-stream zinc concentration occurs at CC-6.319 (Figure 15). CC-6.319 total and dissolved zinc concentrations are 187 µg L^{-1} and 199 µg L^{-1}, respectively. Acute toxicity standards are exceeded at CC-1.613 to CC-2.072, CC-3.506, and CC-4.388 to CC-5.372. Coal Creek zinc concentrations exceed CDPHE chronic toxicity standards at sites CC-1.613 to CC-2.378 (just downstream of Elk Creek), CC-3.506 (downstream of iron fen drainage), and CC-4.388 to CC-5.372 (just downstream of the iron gossan drainage). Though there are high in-stream zinc concentrations from CC-5.693 to CC-8.085 (immediately downstream of the Mt. Emmons effluent channel at 5.405 km), toxicity standards were not exceeded during the sampling event. The Mt. Emmons Treatment Plant released effluent throughout the day, causing a large influx of calcium to Coal Creek. The increased calcium concentration produced an increase in hardness downstream of the effluent channel. Because zinc toxicity standards are hardness-based, values for the toxicity standards increased downstream of the treatment plant effluent channel.

Several tributaries exceeded the chronic and acute toxicity standards. These include Elk Creek, UT-3.294, UT-3.455, UT-3.661, and the treatment plant effluent channel. The concentration of zinc is highest in UT-3.661. UT-3.294, UT-3.455, and UT-3.661 contain drainage from the iron fen. These three tributaries contribute the highest zinc concentrations to Coal Creek.

Total and dissolved zinc concentrations have very similar values along the entire study reach. At ten in-stream sites and four tributaries, dissolved zinc concentrations were slightly greater than total zinc concentrations.

A spike in the total zinc loading rate from 0.0041 to 0.49 kg d^{-1} is observed directly downstream of the Elk Creek confluence. Elk Creek contributed a zinc loading rate of 0.51 kg d^{-1}. This rate comprised 16% of zinc contributions to Coal Creek (Table 8). UT-3.661, entering Coal Creek between CC-3.506 and CC-3.783, contributes the largest dissolved zinc loading rate of 1.99 kg d^{-1} and 49% of zinc contributions. Zinc influx from UT-3.661 produced a spike in Coal Creek zinc loading rate from 0.77 kg d^{-1} at CC-3.506 to 1.31 kg d^{-1} at CC-4.388. The maximum in-stream zinc load in Coal Creek was 1.42 kg d^{-1} at CC-4.794, midway between the iron fen drainages and the drinking water intake. The zinc loading rate abruptly decreased between CC-5.372 and CC-5.693 in response to loss of flow to the drinking water diversion. The Spann Nettick diversion produced a similar, but less pronounced, zinc loading rate decrease between CC-7.895 and CC-8.085. A loading rate is not graphed at point CC-2.588 because a sampling error occurred and a flow rate at this site could not be determined. The zinc concentration at CC-2.588 is less than that of the surrounding sites. This supports the suspicion that the sample at CC-2.588 was taken from a stagnant pool in the wetlands.

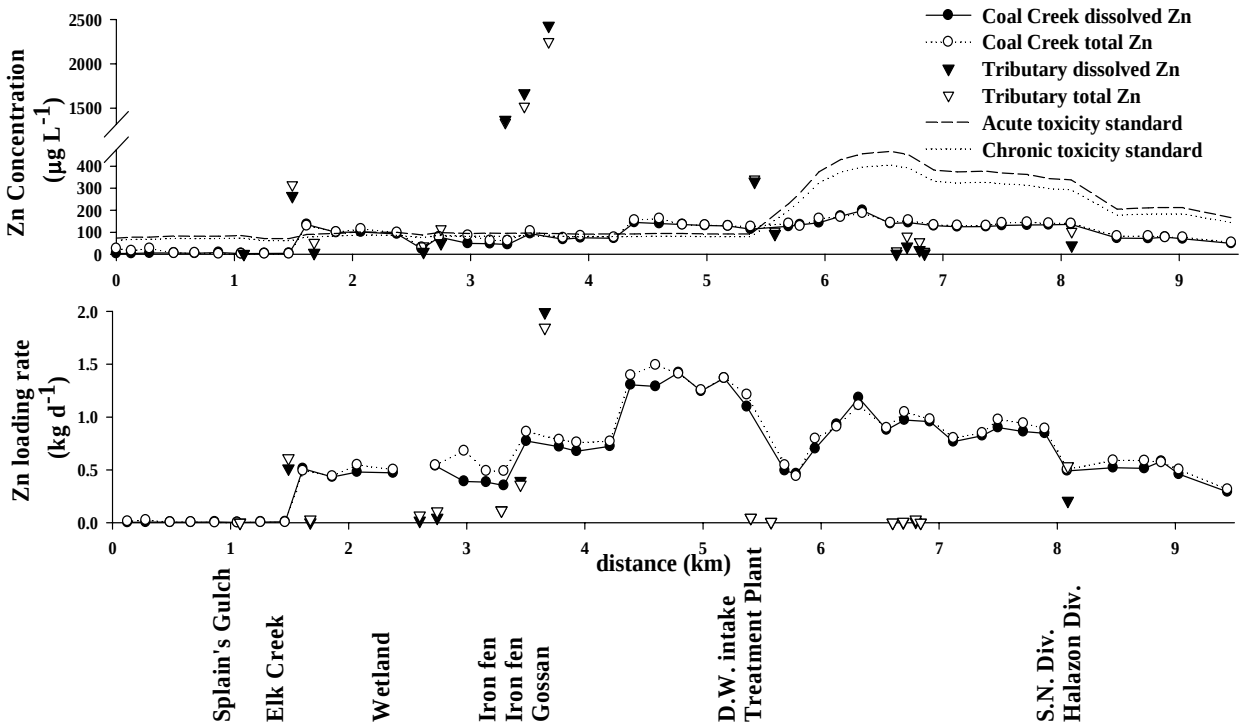

Figure 15. Coal Creek and tributary total and dissolved zinc concentration, chronic and acute toxicity standards, and total and dissolved zinc loading rate.

Copper concentration and loading rate. Copper concentration showed a small increasing trend from the upstream to the downstream end of the study reach (Figure 16). The maximum total copper concentration of 3.65 µg L^{-1} was measured at CC-9.030, within the Crested Butte city limit just upstream of the bridge on Maroon Street. No in-stream sites exceeded the chronic toxicity standard for aquatic life. The acute toxicity standard is much greater than in-stream concentrations and is not shown in Figure 16. The highest tributary total copper concentrations were measured at UT-3.661 (gossan drainage) and the treatment plant effluent channel.

The copper loading rate also showed a small increasing trend from the upstream to the downstream end of the study reach (Figure 16). The maximum total copper loading rate of 0.024 kg d^{-1} occurred at CC-9.030. The loading rate decrease as a result of the drinking water and Spann Nettick diversions. All tributary loading rates are less than adjacent in-stream loading rates except at UT-2.602 and the drinking water reservoir return channel. UT-2.602 contributed 20% of total tributary inputs and the drinking water reservoir return flow contributed 30% (Table 8).

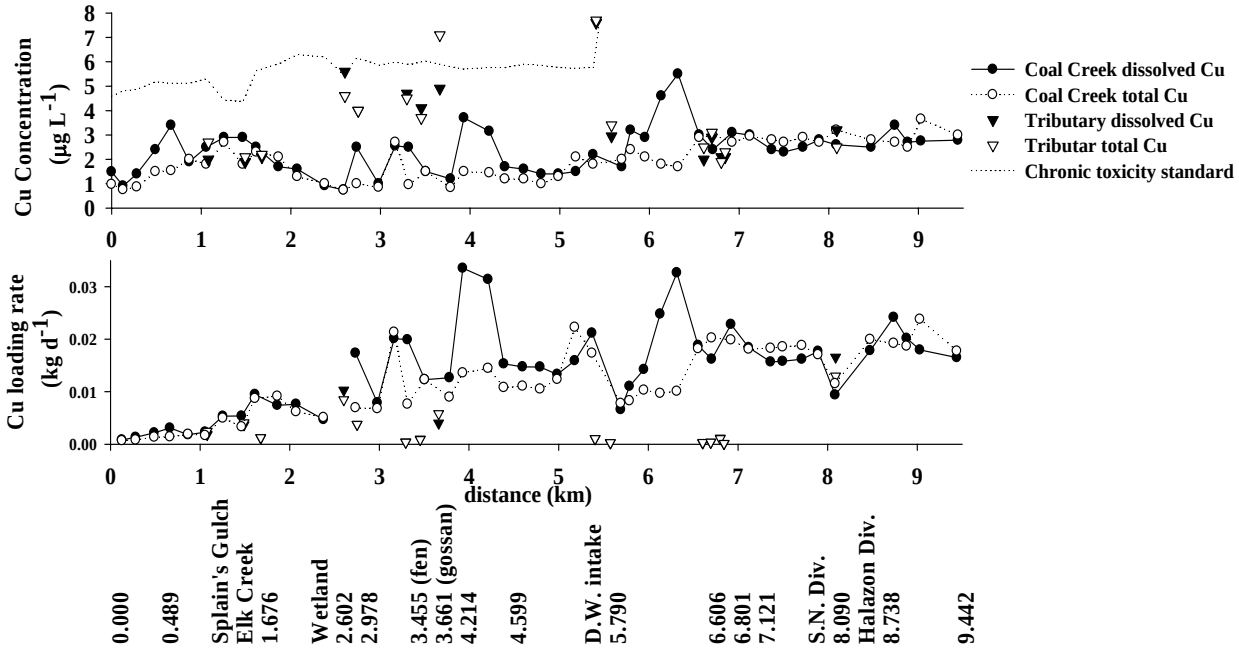

Figure 16. Coal Creek and tributary total and dissolved copper concentration, chronic aquatic life toxicity standard, and total and dissolved copper loading rate.

Cadmium concentrations and loading rates. Cadmium concentrations remained stable near an average of 0.46 µg L^{-1} from CC-1.463 0.4 km downstream of Splain's Gulch to CC-5.372, immediately upstream of the Mt. Emmons Treatment Plant effluent (Figure 17). Cadmium was not detected in samples from CC-0.000 to CC-1.255 or in Splain's Gulch. CC-6.319 contained the maximum in-stream dissolved cadmium concentration of 1.6 µg L^{-1}. A small rise in cadmium concentration was observed between CC-5.693 and CC-8.085. The average concentration between these sites was 1.09 µg L^{-1}. Effluent from the Mt. Emmons Treatment Plant channel is the likely source of this slight rise in cadmium concentration. Downstream of the drinking water reservoir return at 8.090 km, cadmium is diluted to concentrations close to those of CC-1.463 to CC-5.372.

The chronic toxicity standard for aquatic life for cadmium is exceeded at CC-1.613 to CC-2.378, CC-2.734, CC-2.978, CC-3.314 to CC-5.693, CC-5.951, CC-6.133, CC-6.707 to CC-7.121, and CC-7.713 to CC-8.085. The cadmium toxicity standards are hardness-based; therefore, these standards increased significantly downstream of the Mt. Emmons Treatment Plant due to the high calcium content of the effluent. If the chronic toxicity standard upstream of the treatment plant were extended to downstream sites to represent times when effluent is not released, it is possible that several more sites between CC-5.693 and CC-8.085 would exceed the chronic standard. The acute and trout acute standards are not exceeded at any in-stream sites. The 1-day

total recoverable cadmium standard for a drinking water supply is 5 µg L^{-1}. This standard is not shown because all in-stream sites are well below this concentration.

UT-3.294, UT-3.455, and UT-3.661, the iron fen and gossan drainages, contributed the highest cadmium concentrations. In-stream concentration does not increase downstream of the iron fen drainages. Elk Creek and the Mt. Emmons Treatment Plant channel also contributed concentrations above in-stream levels.

The maximum dissolved cadmium loading rate of 9.50×10^{-3} kg d^{-1} occurred at CC-6.319. The loading rate increased from CC-1.463, upstream of Elk Creek, to CC-6.319. The drinking water supply diversion caused a drop in total loading rate, as did the Spann Nettick diversion.

UT-3.661 and Elk Creek contribute the greatest tributary cadmium loading rate (Figure 17). The total cadmium loading rate is 4.92×10^{-3} kg d^{-1} at UT-3.661 and 4.08×10^{-3} kg d^{-1} at Elk Creek. UT-3.661 contributed 39% of the total tributary cadmium loading rate while Elk Creek added 32%. UT-3.455 added 12% of the total cadmium loading rate while the drinking water return added 11%. Though the total cadmium loading rate from the treatment plant channel is only 3.26×10^{-4} kg d^{-1} and 2.6% of the cumulative tributary loading rate, the in-stream loading rate is greatest downstream of the treatment plant (Table 8).

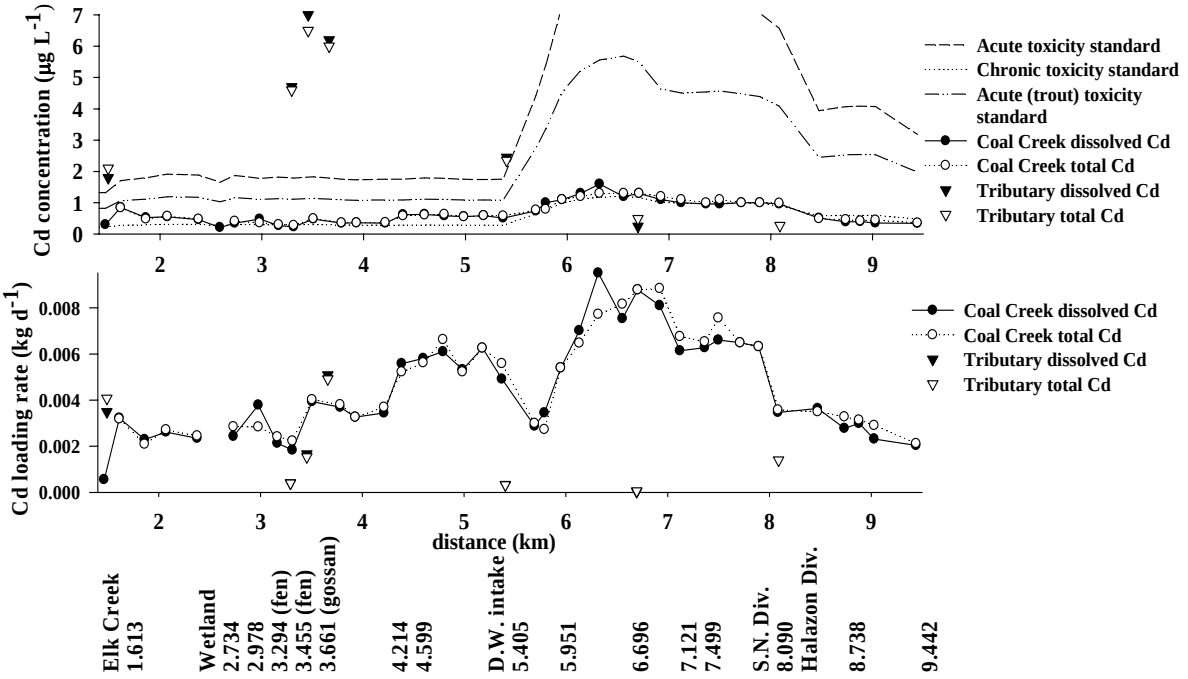

Figure 17. Coal Creek and tributary total and dissolved cadmium concentration, chronic, acute, and acute (trout) toxicity standards, and total and dissolved cadmium loading rate.

Lead concentrations and loading rates. Lead concentrations are low in Coal Creek. The average total lead concentration from the upstream background site to CC-3.506 was 0.23 µg L^{-1}, with the exception of site CC-1.862, which had a total lead concentration of 1.13 µg L^{-1} (Figure 18). The maximum in-stream lead concentration occurs at CC-3.931 and is 1.50 µg L^{-1} total lead. The chronic and acute toxicity standards for dissolved lead were not exceeded at any Coal Creek sites. The 1-day dissolved lead drinking water supply standard of 50 µg L^{-1} was also not exceeded at any site. The acute toxicity and drinking water standards are much greater than in-stream concentrations and are not shown in Figure 18. Total and dissolved lead concentrations were not detected at all but six sites between CC-3.783 and CC-9.030. Total and dissolved lead concentrations are similar, indicating that most lead exists in the dissolved form and that the colloidal fraction is small.

Splain's Gulch was the tributary with the highest total lead concentration. UT-3.455, UT-3.661, UT-6.844, and UT-6.606 also contained significant total lead concentrations.

CC-3.931 has the greatest total lead loading rate of 0.014 kg d^{-1}. CC-6.844 and CC-6.707 also had total lead loading rates greater than the average loading rate of 1.1×10^{-3} kg d^{-1}. The drinking water return at 8.090 km contains the largest tributary total lead loading rate, 50% of the cumulative tributary loading rate. Splain's Gulch adds 22% of the tributary total lead loading rate and UT-3.661 adds 10% (Table 8).

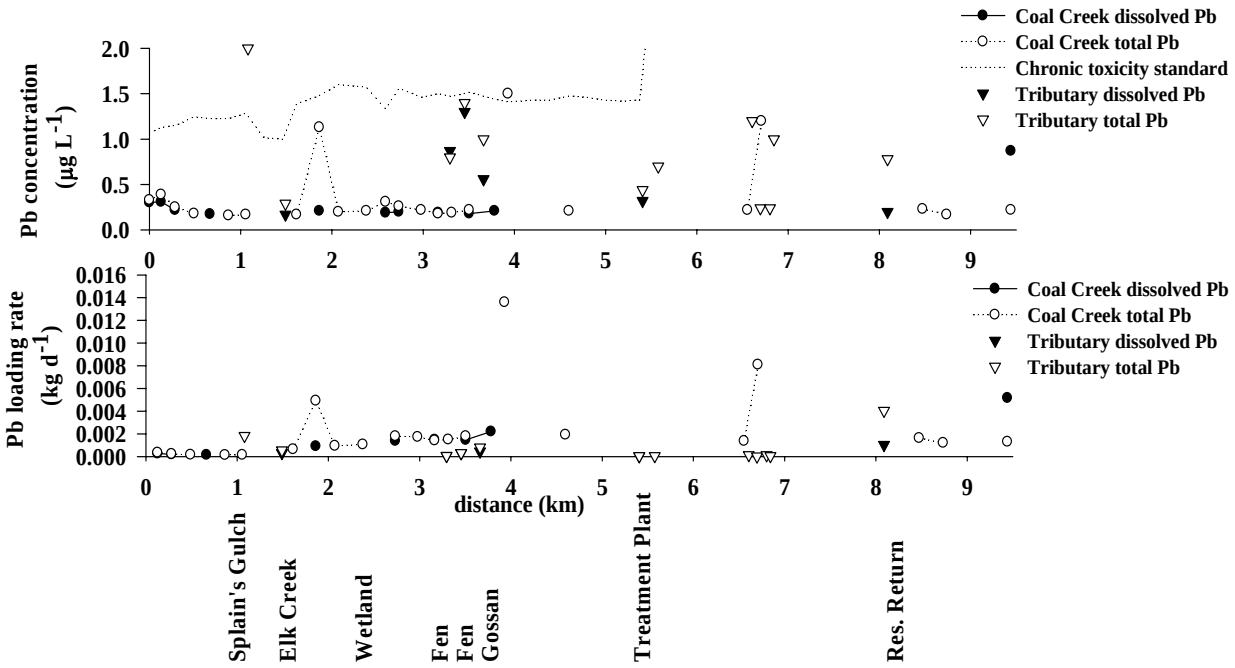

Figure 18. Coal Creek and tributary total and dissolved lead concentration, chronic toxicity standard for aquatic life, and total and dissolved lead loading rate. Missing data points are sites with lead concentrations less than the Contract Required Quantitation Limit.

Nickel concentration and loading rate. The total nickel concentration exceeded the chronic aquatic life toxicity standard for dissolved nickel only at CC-3.165 (Figure 19). The acute toxicity standard is not exceeded at any in-stream locations and is therefore not shown. The total nickel concentration fluctuates along the length of the study reach. Higher concentrations are measured at CC-1.255, CC-5.790, and CC-9.030.

The four tributaries with the greatest total nickel concentrations are Splain's Gulch, UT-2.602, UT-2.750, and UT-3.661 (gossan drainage). The elevated nickel concentrations at CC-1.255 and CC-3.165 may result from high nickel input from Splain's Gulch, UT-2.602 and UT-2.750.

The maximum total nickel loading rate of 0.38 kg d^{-1} occurred at CC-3.165 (Figure 19). Elevated loading rates are located from CC-3.931 to CC-4.214, CC-4.985 to CC-5.372, and CC-9.030. The loading rate at CC-5.372 is 0.19 kg d^{-1} and the loading rate at CC-9.030 is 0.19 kg d^{-1}. The highest tributary loading rate of 0.12 kg d^{-1} comes from UT-2.602 and is 45% of cumulative tributary loading rate. UT-3.661 contributes 18% of the tributary loading rate with 0.048 kg d^{-1} (Table 8).

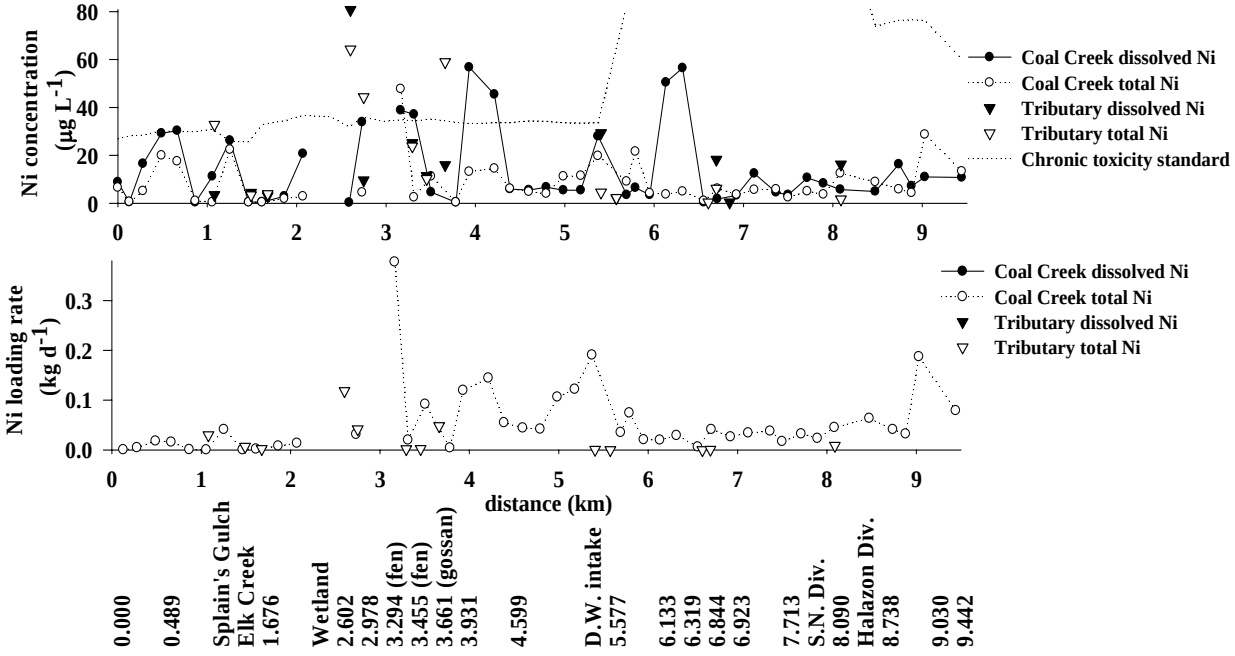

Figure 19. Coal Creek and tributary total and dissolved nickel concentration, chronic toxicity standard for aquatic life, and total nickel loading rate.

Chromium concentration and loading rate. Dissolved chromium concentrations in Coal Creek fluctuated substantially (Figure 20). The highest total chromium concentrations were measured at CC-0.664, CC-3.165, CC-5.790, and CC-9.030. If the majority of chromium is in the dissolved state and all of the chromium is in the +VI oxidation state, the total chromium concentrations show that the chronic and acute toxicity standards for dissolved chromium(VI) are exceeded at numerous sampling sites. The 1-day drinking water supply standard for hexavalent total chromium is exceeded at CC-0.664, 0.6 km downstream from the injection, and CC-3.165, immediately upstream of the iron fen. The highest tributary total chromium concentration of 123 µg L^{-1} was measured at UT-2.602. UT-2.750, UT-3.294, UT-3.661, and Splain's Gulch also contained relatively high total chromium concentrations.

The total chromium loading rate was less than 0.10 kg d^{-1} over most of the tracer test reach, but spikes in loading rates were observed (Figure 20). The highest loading rates occurred at CC-3.165, CC-5.372, and CC-9.030. The maximum in-stream loading rate at CC-3.165 was just downstream of the larger tributary loads at UT-2.602 and UT-2.750, though these tributary loads are not as large as the load at CC-3.165. The other spikes in in-stream loading rate are unrelated to tributary input. These increases in chromium loading rate may have been a result of ground water inputs.

UT-2.602 had the largest tributary total chromium loading rate, 48% of the total tributary chromium loading rate (Table 8). UT-3.661 contributed 19% and UT-2.750 contributes 18%.

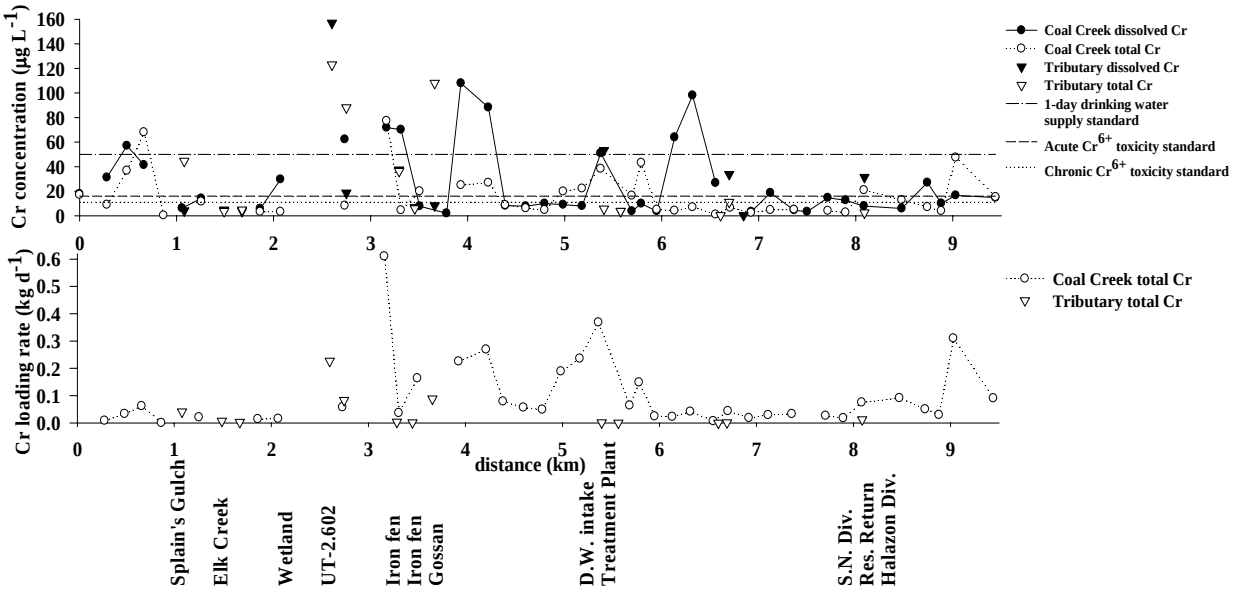

Figure 20. Coal Creek and tributary total and dissolved chromium, 1-day drinking water supply standard for chromium(III) and chromium(VI), acute and chronic chromium(VI) toxicity standard, and total chromium loading rate.

Arsenic concentration and loading rate. Arsenic concentrations decreased from upstream to downstream. The maximum arsenic concentrations of 15.9 μg L^{-1} dissolved arsenic and 21.4 μg L^{-1} total arsenic occurred at CC-0.128 (Figure 21). The colloidal fraction is greatest at CC-0.128. It is 5.9 μg L^{-1}.

The arsenic aquatic life standards are not hardness-dependent. The acute standard is 340 μg L^{-1} and the chronic standard is 150 μg L^{-1} (CDPHE, 2005). In-stream and tributary concentrations are well below the standards at all sample sites. The 30-day total recoverable arsenic standard for a drinking water supply is 10 μg L^{-1}. This standard is a maximum contaminant level established under the federal Safe Drinking Water Act (CDPHE, 2005). The maximum contaminant level was exceeded only over the first 1.1 km of the tracer test reach. The standard for fish ingestion is 7.5 μg L^{-1}. This standard was exceeded over the initial 1.2 km of the study reach. Tributary arsenic concentrations are below in-stream concentrations except for at UT-6.696 and the drinking water reservoir return.

The maximum arsenic loading rate of 0.035 kg d^{-1} dissolved arsenic occurs at CC-5.180, 0.210 km upstream of the drinking water intake (Figure 21). Three distinct segments of the loading rate curve were apparent. The loading rate averaged 0.013 kg d^{-1} dissolved arsenic over the first 2.378 km of the tracer test reach. The loading rate spiked in response to increased flow rates beginning at CC-2.734. The average arsenic loading rates from CC-2.734 to CC-5.372 were 0.028 kg d^{-1} dissolved arsenic. Following CC-5.372, the loading rate decreased in response to the drinking water flow diversion and decreasing arsenic concentration. The average loading rate from CC-5.693 to CC-9.442 is 0.0058 kg d^{-1} dissolved arsenic.

Tributary loading rates were lower than in-stream loading rates except at the drinking water reservoir return channel which contributed 42% of the tributary total arsenic loading rate (Table 8). Elk Creek added 21% and UT-2.602 added 10%.

Barium concentration and loading rate. Coal Creek barium concentration averaged 34.7 μg L^{-1} dissolved barium and 37.8 μg L^{-1} total barium from over the first 1.463 km of the tracer test reach (Figure 22). A concentration drop occurred at CC-1.613 due to dilution from Elk Creek. The barium concentration averaged 24.4 μg L^{-1} dissolved barium and 25.1 μg L^{-1} total barium between CC-1.613 and CC-5.693. Barium concentration increased downstream of CC-5.790 until the total concentration peaked at 58.9 μg L^{-1} at CC-44. No aquatic life standards for barium are in effect. The 1-day drinking water standard is 1000 μg L^{-1} total recoverable barium while the 30-day drinking water standard is 490 μg L^{-1} (CDPHE, 2005). In-stream and tributary concentrations were below these standards at all sites.

The four closely grouped tributaries from 6.606 to 6.844 km downstream of the injection, UT-6.606, UT-6.696, UT-6.801, and UT-6.844, had some of the highest barium concentrations. The maximum in-stream concentration occurred approximately 2.156 km downstream of these tributaries.

The barium loading rate showed a generally increasing trend, except where the loading rate dropped in response to the drinking water and Spann Nettick diversions (Figure 22). The maximum total barium loading rate of 0.42 kg d^{-1} occurred at CC-8.881.

All tributary loading rates were less than in-stream loading rates. The drinking water return channel contributed 37% of the cumulative tributary barium loading rate (Table 8). UT-3.661 and UT-6.801 added 12% each.

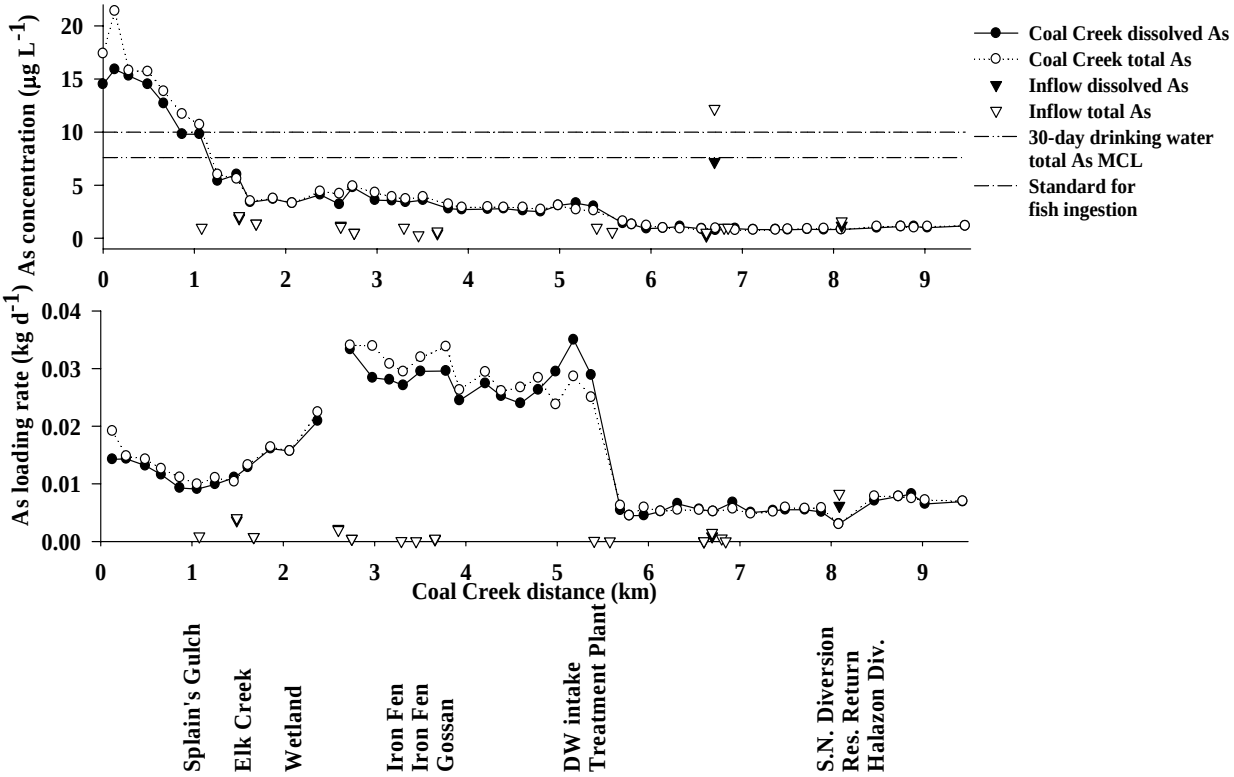

Figure 21. Coal Creek and tributary total and dissolved arsenic concentration, 30-day total recoverable arsenic maximum contaminant level (MCL) and health-based standards for a drinking water supply, and arsenic loading rate.

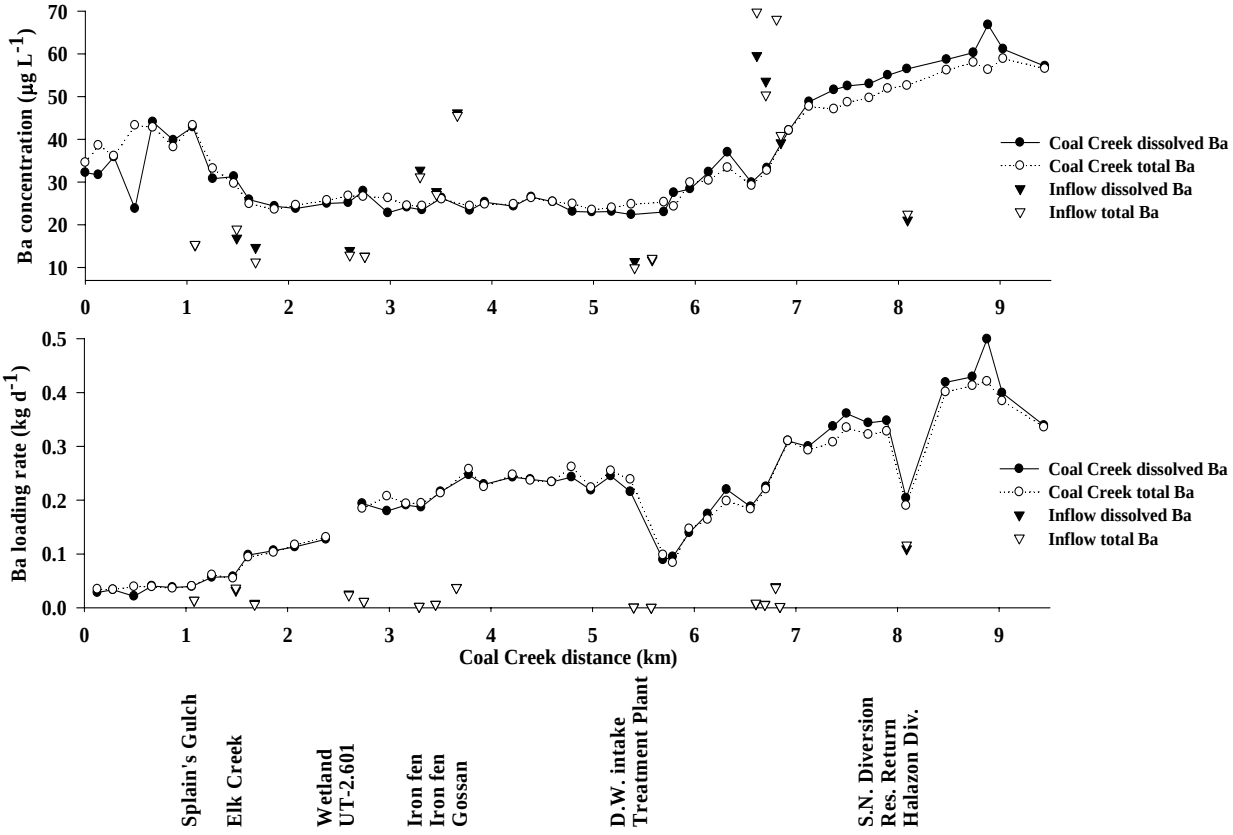

Figure 22. Coal Creek and tributary total and dissolved barium concentration and loading rate.

Electron microprobe images and elemental spectra

Scanning electron microscopy (SEM) was used to assess morphology and elemental composition at four in-stream and two tributary synoptic sample sites; CC-0.128, CC-0.282, CC-6.556, CC-9.442, UT-6.696, and the drinking water return. Sample water (500 mL) was filtered through 0.45-µm nylon mesh filters in order to trap colloidal material. Though others are wary of using arbitrary filter mesh sizes to define dissolved constituents, historically, 0.45-µm filters have been used to separate dissolved constituents from particulates (Kennedy and others, 1974; Danielsson, 1982; Ryan and Gschwend, 1990; Pham and Garnier, 1998; Morrison and Benoit, 2001). Furthermore, the EPA required 0.45 µm filtration for the inductively-coupled plasma (ICP) analyses. Morphology of the samples alone does not adequately distinguish a mineral. However, the elemental composition (mol%) of a mineral coupled with morphological characteristics can be used to identify mineralogy (Mudroch and others, 1977).

Electron microprobe images for CC-0.128, CC-9.442, the drinking water reservoir return channel at 8.090 km, and UT-6.696 are presented in Figures 23-25. The figures show some of the minerals present at each of these sites. An unidentified clay mineral,

iron and manganese oxyhydroxides, and microcline were found at CC-0.128 (Figure 23). The oxyhydroxides are filamentous. Albite, clay, iron oxyhydroxide, microcline, plagioclase, and quartz were some of the minerals present at CC-9.442 (Figure 23). Manganese oxyhydroxide was present in the drinking water reservoir return flow (Figure 24). The iron oxyhydroxide at UT-6.696 appeared to be bacterially controlled as indicated by the filamentous morphology (Figure 25). Particle sizes can be determined by comparing individual particles with the scale shown at the bottom of each micrograph.

The relative abundance of various elements was determined following the guidelines set forth by Mudroch and others (1977) for several minerals using electron microprobe spectra. Elemental spectra for microcline (CC-0.128), illite (drinking water return channel), manganese oxyhydroxide (drinking water return channel), and iron oxyhydroxide (CC-9.442) minerals are shown in Figures 26 and 27. Oxygen and hydrogen do not appear in the oxyhydroxide spectra. This method has a poor sensitivity for light elements with atomic numbers less than 15 (Mudroch and others, 1997).

Table 9 presents a list of representative minerals found at each of the six samples sites that were investigated. The mineralogical composition was inferred based on electron microprobe images and elemental ratios apparent in the spectra (Mudroch and others, 1977). Though these minerals are considered representative of each respective sample, other minerals may also be present at these sites, but may not have shown up in these analyses. The relative predominance of these minerals as a fraction of the entire sample was not determined.

In-stream sites were not dominated by any one mineral. An array of minerals was present at each site. CC- 0.128 had no iron oxyhydroxide as expected for in-stream sites upstream of mining inputs. Conversely, iron oxyhydroxide was found at CC-0.282 although it is upstream of mine drainage. CC-6.696 did not contain the iron oxyhydroxides indicative of acid mine drainage impact, though this site is downstream of Elk Creek, the iron fen, the gossan, and the Keystone Mine. No pattern relating to the upstream versus the downstream mineralogical composition could be established. Both tributaries analyzed with the electron microprobe contained large amounts of either manganese or iron oxyhydroxides.

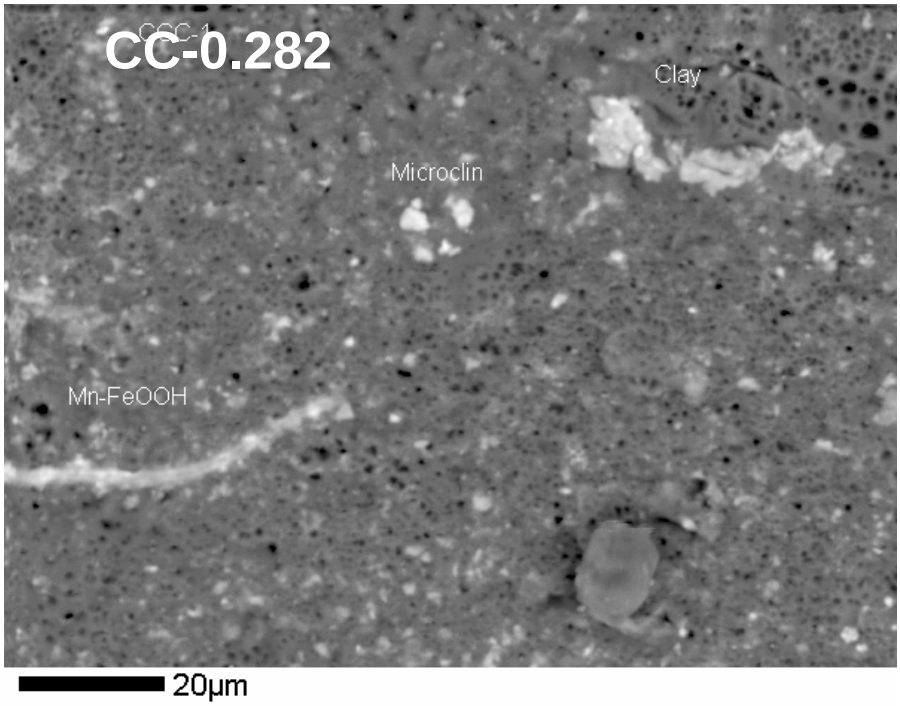

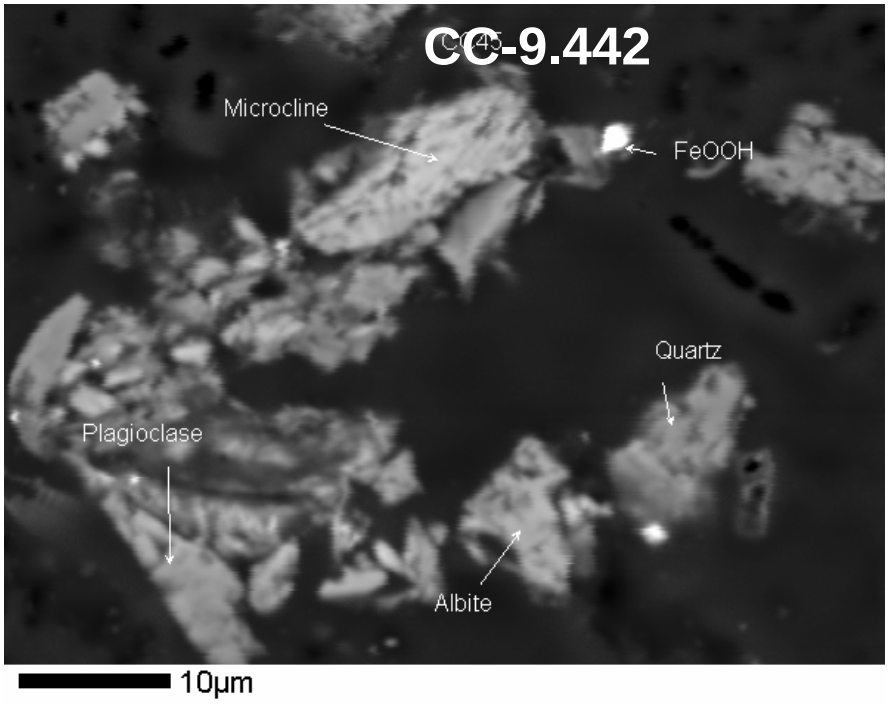

Figure 23. Electron microprobe images showing portions of colloids filtered from CC-0.282 (upper) and CC-9.442 (lower) water samples. The colloids were trapped on a 0.45 µm nylon membrane filter. Minerals were tentatively identified with the aid of elemental analysis. The magnification is 2,000× for the CC-0.282 micrograph and 950.0× for the CC-9.442 micrograph.

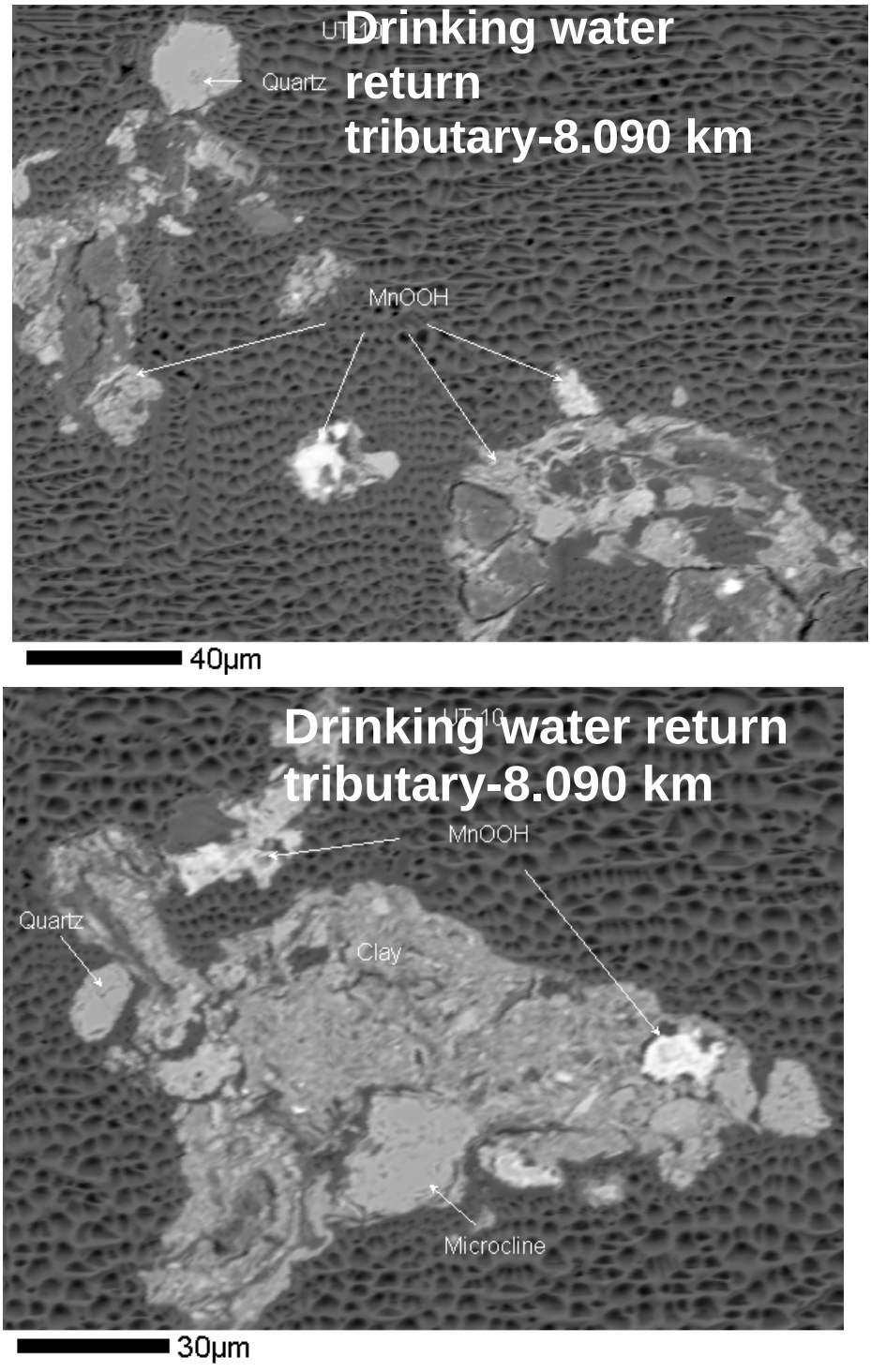

Figure 24. Electron microprobe images showing portions of colloids filtered from the drinking water reservoir return flow. Minerals were tentatively identified with the aid of elemental analysis. The magnification is 575.0× in the top micrograph and 733.3× in the bottom micrograph.

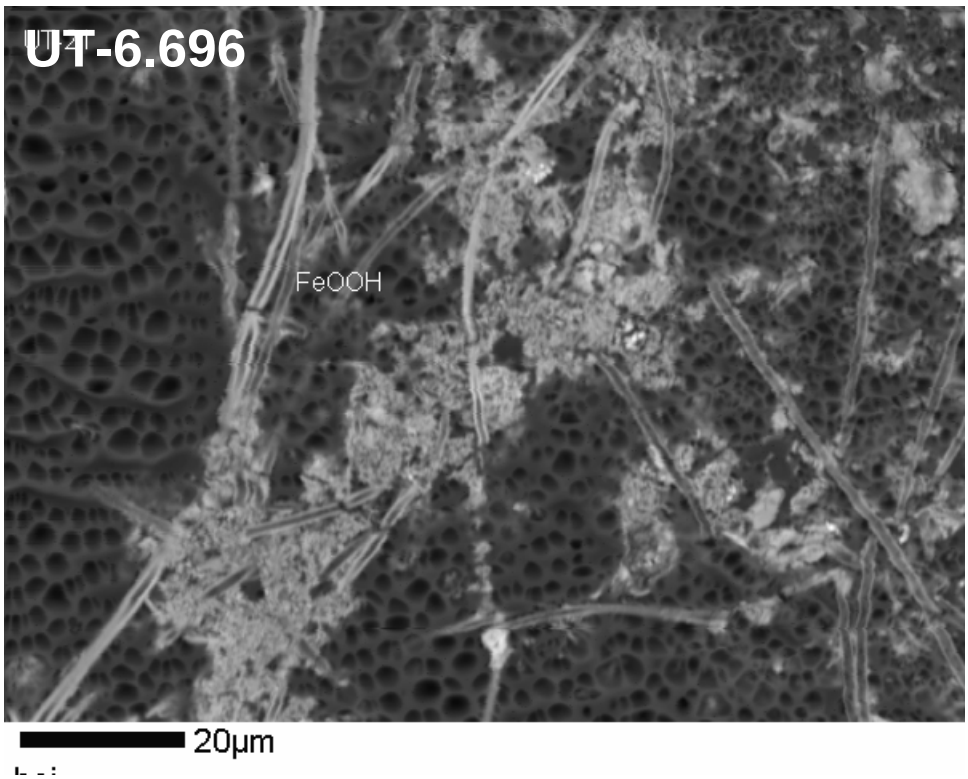

Figure 25. Electron microprobe images showing portions of colloids filtered from the UT-6.696 water sample. Minerals were tentatively identified with the aid of elemental analysis. The magnification is 1,100×.

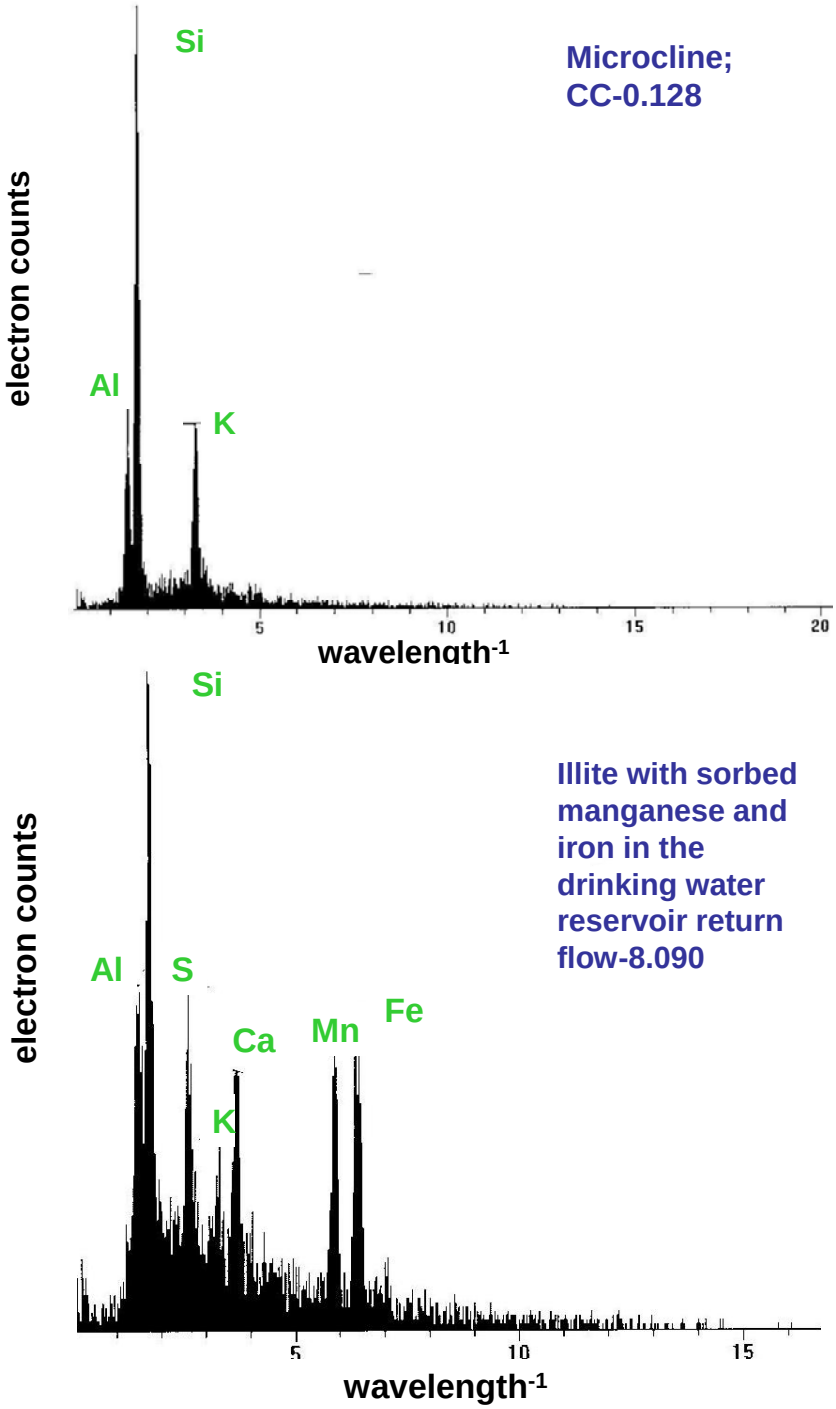

Figure 26. Elemental spectra for representative particles trapped on a 0.45 µm nylon filter at CC-0.128 (upper spectrum) and the drinking water reservoir return channel (lower spectrum). The upper spectrum was identified as microcline (potassium feldspar; $KAlSi_3O_8$) following the guidelines of Mudroch et al. (1977). The lower spectrum was identified as illite with adsorbed manganese and iron.

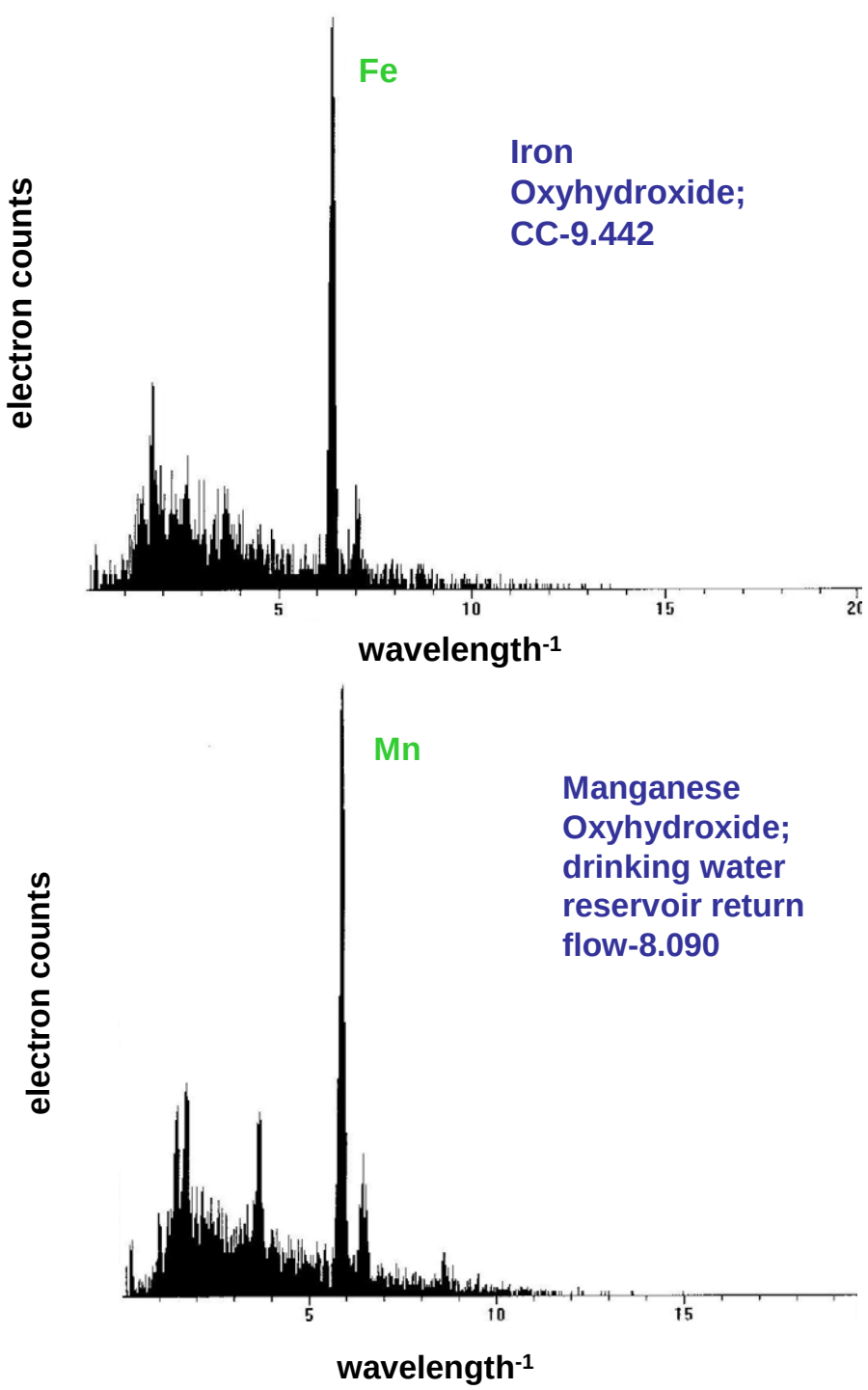

Figure 27. Elemental spectra for representative particles trapped on a 0.45 µm nylon filter at CC-9.442 (upper spectrum) and the drinking water reservoir return (lower spectrum). The upper spectrum is an iron oxyhydroxide. The lower spectrum is a manganese oxyhydroxide of unknown composition.

Table 9. Summary of scanning electron microprobe results for mineralogical composition of colloids collected on 0.45 μm filters. Mineralogy was inferred based on particle morphology and elemental analysis.

Sample Site	Minerals Identified
CC-0.128	Microcline, Pyroxene
CC-0.282	Albite, Calcite, Iron Oxyhydroxide, Iron-Manganese Oxyhydroxide, Magnesium Silicate, Microcline, Plagioclase
CC-6.556	Albite, Microcline, Pyroxene, Quartz
CC-9.442	Albite, Calcite, Iron Oxyhydroxide, Microcline, Plagioclase, Quartz
Drinking water reservoir return	Manganese Oxyhydroxide, Albite, Clay, Iron Oxyhydroxide, Microcline, Pyroxene, Sphene, Quartz
UT-6.696	Iron Oxyhydroxide, Calcite, Pyroxene, Quartz

DISCUSSION

Suitability of lithium and chloride as tracers

An appropriate tracer must have several characteristics to qualify it for use in a tracer injection study. The tracer must be (1) conservative, or non-reactive and not prone to sorb to solid material, (2) insensitive to variations in pH and metal chemistry that occur naturally within the study reach, (3) at concentrations several times greater than background concentrations, (4) cost-effective, and (5) it must not pose a risk to human health or aquatic life (Bencala and others, 1986, Bencala and others, 1990).

Flow rates calculated using lithium dilution were gross overestimates with values as excessively high as 2,500 L s^{-1} (Figure 10). This flow rate is approximately 80 times greater than the flow rate estimated by Coal Creek Watershed Coalition members (Tyler Martineau, personal communication, September 1, 2005) just prior to the tracer study and inconsistent with historical flow records as well as with the substantial volume of flow diverted from Coal Creek. We concluded that lithium did not behave conservatively in Coal Creek and that lithium dilution data was not useful in correctly estimating Coal Creek flows. Though lithium chloride was an effective tracer in Lefthand Creek (Wood and others, 2004), previous tracer studies in the Redwell Basin, a watershed adjacent to the Coal Creek watershed, show that lithium does not behave conservatively at pH greater than 6 (Briant Kimball, personal communication, November, 16, 2005). Even a tracer that sorbs moderately may not be suitable under low flow conditions in a shallow stream frequently surrounded by wetlands like Coal Creek.

Shallow streams allow more contact between sorbing solutes in the water column and the streambed (Bencala, 1990). With an average pH of 7.38, moderate TOC concentrations, shallow depths, and surrounding wetlands, it is likely that lithium bonded to organic matter in the water column and the hyporheic zone. Based on lithium concentrations, the calculated flow doubles as Coal Creek passes a wetland (CC-2.072 to CC-2.734) (Figure 10), but it was clear in the field that flow did not actually double over this reach. Significant transient storage means a longer solute residence time through the wetland reaches. Longer residence times in zones with an abundance of sediment surfaces (wetlands) provide greater opportunity for reactions otherwise limited by availability of reactive surfaces or kinetic restraints (Broshears and others, 1993). The tracer dilution equation breaks down when processes other than dilution affect the tracer concentration.

Lithium was originally thought to be a suitable tracer because background lithium concentrations were quite low in natural waters (Kimball and others, 2002). A lithium salt tracer injection easily raises stream lithium concentration by at least an order of magnitude in streams with low background lithium concentrations. This fulfills the requirement that in-stream tracer concentration be substantially higher than inflow tracer concentration. The difference between in-stream and inflow tracer concentration

must be greater than the analytical uncertainty associated with the concentration data (Bencala, 1987).

Lithium chloride is among the more expensive tracers; however, the cost was not inhibitory as only 67 kg was required to raise concentrations to adequate levels during low flow. Furthermore, aquatic ecosystems are not negatively impacted by the introduction of lithium chloride at the concentrations used for this study.

Previous studies show that chloride behaves conservatively as only physical processes such as dilution, dispersion, and transient storage influence the attenuation of chloride concentration. Biogeochemical reactions have minimal impact on chloride attenuation (Bencala, 1985; Bencala and others, 1986; Bencala and others, 1987; Bencala and others, 1990). Chloride is commonly referred to as the "universal tracer" because of its conservative behavior; however, it is also more likely to be present in moderate concentrations in natural waters (Bencala, 1990). Atmospheric deposition and weathering are sources of chloride in natural systems (Kimball and others, 2002).

Steady-state conditions for tracer injection

The tracer dilution method is dependent upon a steady-state in-stream tracer concentration. Because the tracer injection flow rate fluctuated slightly and a tracer arrival curve at the most downstream site, CC-9.442, was not available, we cannot prove that the system was at steady-state. However, velocity estimates and available chloride concentration data for CC-9.442 support the arrival of the tracer at CC-9.442 and the establishment of steady-state in-stream conditions.

Based on the pulse sodium chloride injection, the average velocity along the first 1.3 km of the study reach was 0.221 km h^{-1} (Table 4). If this velocity remained steady for the length of the study reach, then a LiCl injection period of 43 h would be required for the tracer to reach CC-9.442. This was a conservative estimate because the velocity was observed to increase as flow rate increased with downstream distance (with the exception of flow through the wetlands). The tracer was injected for 50.5 h, 7.5 h longer than required, to ensure that the tracer reached the CC-9.442 at the downstream end of the study reach.

Velocity estimates were also made based on the distance traveled by the calcium-laden effluent entering Coal Creek from the Mt. Emmons Treatment Plant. The treatment plant discontinued daily discharge at 16:00. Calcium concentrations are maximum at CC-6.319, CC-6.556, and CC-6.707, indicating the location of the trailing edge of the effluent "plug" in Coal Creek (Figure 9). These sites were sampled at 18:30, 17:50, and 18:12, respectively. Stream velocity between the treatment plant and these sites was calculated as the distance between the treatment plant and the site divided by the sample time minus 16:00. The average velocity along this reach was 0.528 km h^{-1}. This velocity is greater than that calculated for the first 1.3 km of the study reach, indicating that the observation that stream velocity increases with downstream distance was valid.

In Coal Creek, the background chloride concentration is 2.38 mg L^{-1} (Figure 11). This background chloride concentration limited the analytical resolution of Coal Creek concentration data. The in-stream chloride concentration dropped to within 1.0 mg L^{-1} of the background chloride concentration by CC-5.693 and to within 0.5 mg L^{-1} of background concentrations at the most downstream site, CC-9.442 (Table 10). Several tributaries also contained chloride concentrations similar to in-stream chloride concentrations. The coefficient of variance (*CV*; %) for chloride concentrations resulting from ion chromatograph (IC) analysis as defined by the equation

$$CV = \frac{\sqrt{\sum (x_i - x_{avg})^2}}{N - 1} \quad (9)$$

where x_i is the chloride concentration of each sample in the data set, x_{avg} is the mean chloride concentration of the data set, and N is the number of data points was calculated for ten sets of duplicate IC measurements. The average *CV* was 5.25%. Because the in-stream chloride concentration was within 5.25% of the background concentration at several sites downstream of CC-5.951, analytical uncertainty is expected to influence calculated flow rates at some sites in this reach. However, Table 10 shows that the average chloride concentration at CC-9.442 stabilized at 0.40 mg L^{-1} greater than the background chloride concentration. This margin of difference is greater than any differences caused by variance and shows that the chloride tracer reached the downstream end of the study reach.

Table 10. Chloride concentrations at the upstream end, CC-0.000, and the downstream end, CC-9.442, of the injection reach.

Sample Date and Time	CC-0.000 (mg L^{-1})	CC-9.442 (mg L^{-1})
9/3/2005 12:10	2.36	
9/3/2005 14:12	2.11	
9/3/2005 14:12	2.45	
9/32005 16:08	2.57	
9/3/2005 18:07	2.26	
9/4/2005 02:00	2.59	
9/4/2005 10:05	3.14	
9/4/2005 14:02	1.95	
9/4/2005 18:00	2.24	
9/5/2005 11:06	2.50	
9/5/2005 13:02	2.34	
9/5/2005 11:10		2.44
9/5/2005 12:00		2.53
9/5/2005 12:45		3.01
9/5/2005 13:30		2.66
9/5/2005 14:15		2.55
9/5/2005 14:15		2.87
9/5/2005 15:00		2.96
9/5/2005 15:45		2.85
9/5/2005 16:30		2.67
9/5/2005 16:30		2.97
9/5/2005 17:15		2.69
9/5/2005 18:00		2.61
9/5/2005 18:45		2.40
9/5/2005 18:45		2.71
9/5/2005 19:30		3.56
9/5/2005 19:50		3.25
Average	**2.40**	**2.80**

Hardness and the Mt. Emmons Treatment Plant effluent

Hardness behaves similarly to calcium and reflects the dependence of hardness on calcium concentration. The sharp spike in calcium concentration downstream of the Mt. Emmons Treatment Plant effluent produces a similar sharp spike in hardness. The

Mt. Emmons Treatment Plant adds lime during the treatment process to achieve a pH above 10 (John Perusek, personal communication, July 15, 2005). The pH is increased to precipitate and remove cadmium and manganese in the plant's flotation process. The calcium used during the treatment process enters Coal Creek when the effluent is released.

The sites with high calcium and hardness concentrations graphically depict the downstream movement of the treatment plant effluent "plug" (Figure 9). The treatment plant discontinues effluent release by 16:00 each day. The release is not steady; it varies from 0.00 to 78.9 L s^{-1} over each day (John Perusek, personal communication, July 15, 2005). All synoptic samples from CC-5.693 to CC-9.442 were taken between 17:42 and 19:45 on September 5, 2005. Calcium and hardness concentrations peak at CC-6.556, approximately 1.2 km downstream of the treatment plant-5.405. This lag distance between the treatment plant and the peak represents the distance traveled by the effluent "plug" between 16:00, when the treatment plant discontinued discharge of the effluent, and 17:50, when CC-6.556 was sampled. The sharp drop in calcium concentration and hardness between CC-6.707 and CC-6.923 may represent a change in the treatment plant effluent discharge rate, but detailed records of the effluent discharge rate were not available. The decline in calcium concentration and hardness between CC-8.085 and CC-8.474 is a result of dilution from the drinking water reservoir return flow.

Large daily fluctuations in calcium concentration and hardness in Coal Creek are expected. When the treatment plant is discharging effluent, downstream calcium concentration will be approximately 12 times greater than upstream calcium concentration at low flow conditions. Consequently, hardness and hardness-based aquatic life toxicity standards will also show daily fluctuations. Hardness-based acute and chronic toxicity standards are not to be exceeded more than once every three years on average and should be computed using the lowest daily calcium and magnesium concentrations (CDPHE, 2005). When hardness drops, toxic metal uptake by aquatic organisms increases because less calcium and magnesium is present to compete with the toxic metals for binding sites on gills and in the digestive tract. For comparison purposes, hardness-based standards upstream of Mt. Emmons discharge can be extrapolated to sites downstream to represent conditions when elevated calcium is not present in Coal Creek.

Aquatic life and drinking water supply standard exceedances

Metal concentrations in Coal Creek exceeded CDPHE acute and chronic standards for aquatic life and drinking water supply standards at several sample sites along the study reach (Table 11). Cadmium, chromium, nickel, and zinc exceeded the chronic toxicity standard. Cadmium, chromium, and zinc exceeded the acute toxicity standard. Arsenic exceeded the drinking water supply and fish ingestion standard for along the initial 1.2 km of the study reach. Chromium, iron, and manganese also exceeded the drinking water standard at several sample sites.

Table 11. Coal Creek sample sites where the chronic and acute aquatic life toxicity standards and the drinking water supply standard were exceeded. **Bold** indicates sites where daily decreases in calcium concentrations corresponding to times when the treatment plant is not discharging could decrease aquatic life standards enough to cause exceedances.

Metal	Chronic Standard Exceeded	Acute Standard Exceeded	Drinking Water Standard Exceeded
Aluminum	None	None	-- [1]
Arsenic	None	None	CC-0.000 - CC-1.057
Barium	--	--	None
Cadmium	CC-1.613-2.378, CC-2.734-2.978, CC-3.314-5.693, CC-5.951-6.133, CC-6.707-7.121, CC-7.713-8.085, **CC-5.790, CC-6.319-6.556, CC-7.365-7.499, CC-8.474-9.442**	**CC-5.951 - CC-7.121**	None
Chromium	CC-0.000, CC-0.489-0.664, CC-1.255, CC-3.165, CC-3.506, CC-3.931-4.214, CC-4.985-5.790, CC-8.085-8.474, CC-9.030-9.442	CC-0.000, CC-0.489-0.664, CC-1.255, CC-3.165, CC-3.506, CC-3.931-4.214, CC-4.985-5.790, CC-8.085, CC-9.030	CC-0.664, CC-3.165
Copper	None	None	None
Iron	--	None	CC-0.282-0.489, CC-2.588, CC-3.165-3.314 CC-3.931-4.214, CC-6.133
Lead	None	None	None
Manganese	None	None	CC-2.378-2.734, CC-3.165-3.506, CC-4.388, CC-6.133-6.319
Nickel	CC-3.165	None	None
Zinc	CC-1.613-2.378, CC-3.506, CC-4.388-5.372, **CC-5.693-8.085**	CC-1.613-2.072, CC-3.506, CC-4.388-5.372 **CC-5.693-8.085**	None

[1] -- Standard does not exist

The calcium input from the Mt. Emmons Treatment Plant produced in-stream increases in the hardness-based aquatic life standards when the plant was discharging. When the plant discontinues discharge, the calcium concentrations in Coal Creek are expected to decrease, producing subsequent decreases in the hardness-based aquatic life standards. Some metals with concentrations below aquatic life standards when the plant is discharging are likely to exceed standards when the plant is not discharging. To predict when this occurred, the hardness-based standards upstream of the treatment plant were assumed to extend downstream. The metal concentrations added to Coal Creek when the plant was discharging and when it was not were also considered. Bold sample sites in Table 11 designate that aquatic life standards were not exceeded during treatment plant discharge, but are predicted to be exceeded when the plant is not discharging.

Because the treatment plant was not discharging at the time of synoptic sampling on September 5, the site was sampled a second time on the morning of September 6, 2005, when effluent was being released. Flow during the synoptic sampling was only 1.61 L s^{-1}. The exact flow rate on September 6 is unknown. Metals in the synoptic sample taken on September 5 are attributable to residual treatment plant flow. Relatively high concentrations of aluminum, cadmium, copper, iron, manganese, and zinc were present in the Mt. Emmons Treatment Plant effluent channel at 5.405 km on one or both of the sample days (Table 12). Aluminum, cadmium, copper, manganese, and zinc had lower concentrations on September 6, presumably as a result of dilution from the treatment plant effluent. Total aluminum concentration was 10% lower and dissolved aluminum was 33% lower on September 6. Total cadmium, copper, manganese, and zinc concentrations decreased by 62%, 21%, 63%, and 79%, respectively. The iron concentration increased from undetectable concentrations on September 5 to 136 µg L^{-1} total iron on September 6. Aluminum, cadmium, copper, and zinc inputs raised Coal

Table 12. Total and dissolved aluminum, copper, iron, manganese, and zinc concentrations in the Mt. Emmons Treatment Plant effluent channel at 5.405 km during synoptic sampling on September 5 (after discharge from the plant ceased) and during discharge on September 6. BDL is an abbreviation for "below detection limit".

metal	treatment plant effluent after discharge	treatment plant effluent during discharge	decrease (%)
Al (µg L^{-1})			
Total	1130	1020	10
Dissolved	1080	728	33
Cd (µg L^{-1})			
Total	3.4	1.3	62
Dissolved	3.4	1.5	56
Cu (µg L^{-1})			
Total	8.6	6.8	21
Dissolved	8	7.2	10
Fe (µg L^{-1})			
Total	BDL	136	--
Dissolved	BDL	-- [1]	--
Mn (µg L^{-1})			
Total	318	117	63
Dissolved	--	120	--
Zn (µg L^{-1})			
Total	562	120	79
Dissolved	567	93.2	84

[1] -- Valid concentration not obtained

Creek loading rates for these metals downstream of the treatment plant-5.405, despite a decrease in flow due to the drinking water intake diversion (Figure 28). The spatial distribution of the elevated in-stream calcium and aluminum, cadmium, copper, and zinc concentrations corresponds to the transport of treatment plant effluent along Coal Creek. For example, aluminum peaks approximately 1 km downstream of the treatment plant, with elevated aluminum concentrations 0.25 – 2.1 km downstream (Figure 15 and 29).

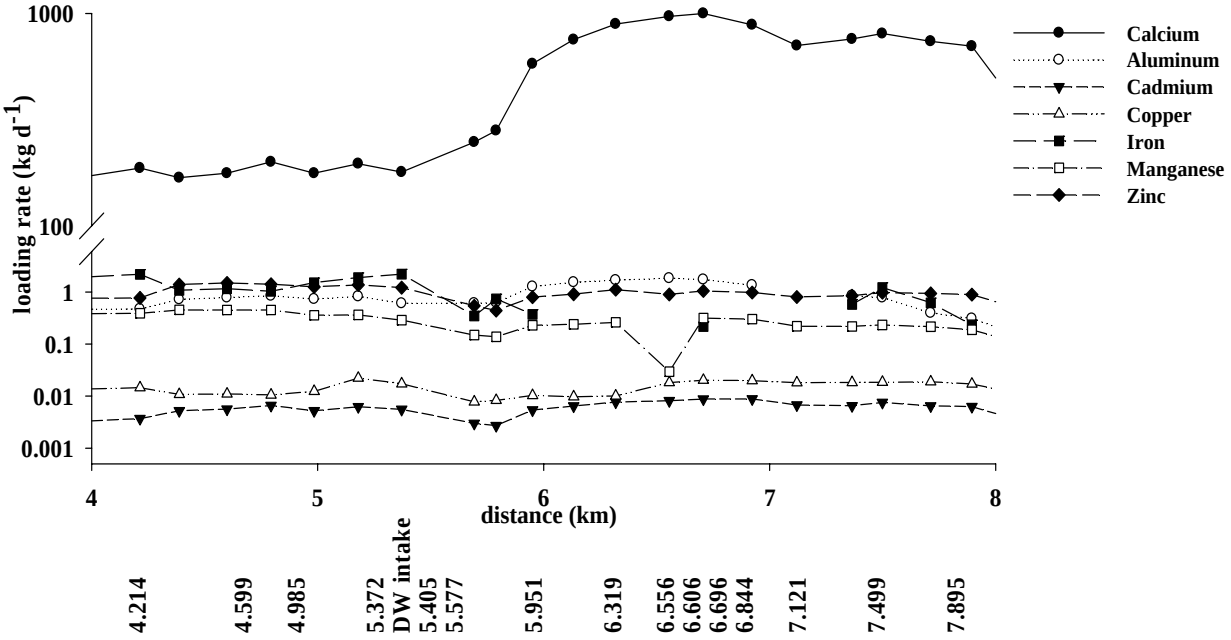

Figure 28. The loading rates for calcium along with aluminum, cadmium, copper, iron, manganese, and zinc are graphed for the 4-8 km section of the study reach to illustrate the impact of the Mt. Emmons Treatment Plant on Coal Creek metal loading rates.

Stream Flow

From 1941 to 1946, the U.S. Geological Survey maintained a stream gauge on Coal Creek just downstream of the Elk Creek confluence. The location of the gauge was equivalent to the location of CC-1.862 used in this study. The USGS measured an average September flow rate of 58.2 L s^{-1} and an average September 5 flow rate of 66.8 L s^{-1} during those years. The flow rate at CC-1.862 calculated using the chloride dilution data was 50.5 L s^{-1} on September 5, 2005. Possible climactic changes since the 1940s, the relatively short time span over which USGS measured flow rate, and the time gap between USGS data and the data pertaining to this study do not allow for a direct comparison. However, USGS flows are within 17 L s^{-1} of the flow rates calculated using chloride dilution. This establishes confidence that tracer dilution flow rates are

reasonable and representative of true flow, at least for the upstream end of the study reach through CC-1.862.

Also, diversion flow rates were known, with the greatest flow of 79 L s^{-1} removed by the drinking water intake at 5.405 km. The Coal Creek flow rate was only 1.4 times greater than drinking water diversion flow rate as calculated using chloride dilution, but 8.9 times greater when calculated using lithium dilution (Figures 10 and 11). Visually estimated flows were much closer to the chloride-calculated flow rates.

Without stream gauge measurements for the day of the tracer study, exact hyporheic flow cannot be determined. Previous studies indicate that up to 40% of stream discharge may occur as underflow through the hyporheic zone in mountainous gravel-bed streams (Zellweger and others, 1989). A study of flow in Peru Creek in Summit County, Colorado, showed that the area of the hyporheic zone may increase by a factor of 2 through wetland reaches like those in Coal Creek (Jeffrey Wong, personal communication, July 12, 2006).

Three diversions of flow from Coal Creek and one flow return affected the flow rate during low flow conditions. The Crested Butte drinking water intake is the most upstream flow diversion. The large flow reduction between CC-5.372 and CC-5.693 illustrates the significant impact the drinking water intake effects on Coal Creek (Figure 11). The intake removed 79 L s^{-1}, 71% of the Coal Creek flow rate just upstream of the intake. The Spann Nettick agricultural diversion removed 28 L s^{-1} from Coal Creek between CC-7.895 and CC-8.085. The drinking water return flow re-enters Coal Creek at fluctuating rates between CC-8.085 and CC-8.474 and offset flow losses to the Halazon agricultural diversion during the tracer test. There was a net flow increase between CC-8.085 and CC-8.474. Tracer dilution equations do not account for flow losses to diversions. Manual adjustments as described in section 4.7 were required in order to account for these losses. The tracer dilution equation (Equation 5) is a mass balance equation which assumes a decrease in in-stream tracer concentration resulting from surface or dispersed ground water inflows. Because no decrease in tracer concentration results when flow is removed from a stream, this equation cannot be used in reverse to calculate diversion flow rates.

The accuracy of this estimated flow rate of the drinking water reservoir return was supported with a secondary flow rate calculation for the drinking water reservoir. Because the Mt. Emmons treatment plant created a spike in downstream calcium concentrations, it was found that calcium could be viewed as a tracer at the two sites bracketing the drinking water reservoir. When the standard tracer dilution equation was applied using calcium as the tracer, a flow rate of 61.5 L s^{-1} was obtained. This is only a 2.5% difference from the estimated flow rate, confirming that the flow rate used to calculate metal loading rates for the drinking water reservoir return was an accurate estimate.

Sources of metals and arsenic in the Coal Creek watershed

All of the sampled tributaries as well as dispersed ground water flow may serve as contributors of toxic metal concentrations and loading rates to Coal Creek. The following discussion will address the sources of each of the ten metals and arsenic analyzed for this study.

The following metal sources are only representative of the sources of metals under low flow conditions. It is expected that high flow conditions will effectively dilute metal concentrations. Dilution would result in fewer aquatic life and drinking water standard exceedances. However, we must also consider that higher flows will increase flow rates from mine adits as well as the iron fen and the gossan. Such an increase may negate dilution effects as the effective metal concentration would remain the same as the metal inputs increased along with overall flow rates. In this instance, the metal loading rates would also greatly increase compared to low flow loading rates.

Tributaries entering Coal Creek from culverts along County Highway 12 (the Kebler Pass Road) were sampled directly out of the pipes immediately south of the highway (Figure 6). A more appropriate sampling location would have been immediately upstream from the tributaries entry point into Coal Creek, but in most cases, the small flows coming from the culverts could not be traced down to Coal Creek – the flow typically disappeared into the subsurface. Some error may be associated with taking samples from the pipes under County Highway 12.

Elk Creek was suspected of contributing elevated arsenic, barium, cadmium, chromium, copper, lead, and zinc loading rates to Coal Creek (EPA, 2005b). The iron fen was also suspected of contributing elevated metal concentrations to Coal Creek, particularly for aluminum, iron, manganese, and zinc (EPA, 2005b). Drainage from the iron fen enters Coal Creek from the north through the unnamed tributaries UT-3.294, UT-3.455, and UT-3.661. Though unnamed tributary UT-3.294 contains the majority of the iron fen drainage, it also received flow input from uncontaminated drainage from the north. UT-3.661 drains directly from the gossan area where barren limonite, or a natural aggregate of hydrous ferric oxide, is exposed at the ground surface.

Flow from the fen tributaries travels approximately 40 m downhill to Coal Creek. Field reconnaissance in June, 2006, during high flow conditions showed that the majority of the flow from these culverts is absorbed into the ground before entering Coal Creek. Approximately 50% of the flow from UT-3.294 and 100% of the flow from UT-3.455 and UT-3.661 re-entered the ground water system before entering Coal Creek. During low flow conditions, it is likely that even a larger percentage of the flow would be absorbed before entering Coal Creek. This may allow for removal of some contaminants through transport through the subsurface.

When assessing the impact of loading rates from the drinking water reservoir return flow, it was important to determine whether metal concentrations in this tributary were similar to Coal Creek metal concentrations just upstream of the drinking water intake at CC-5.372. The coefficient of variance (Equation 8) between metal concentrations at these two sites was calculated and found to be significantly different in the drinking

water return flow as compared to that of Coal Creek at CC-5.372 (Table 13). The average coefficient of variance of all eleven metals was 42.6%. This high degree of variation makes it necessary to treat the drinking water return flow as having its own chemical signature separate from that of Coal Creek at CC-5.372. This flow must be exposed to additional manganese and iron sources as the concentrations of these metals are higher in the drinking water return flow. The other metals are either diluted or attenuated out of solution as concentrations are lower in the drinking water return flow. It is also important to note that the flow rate used in all metal loading calculations for the drinking water reservoir return was estimated as the difference between the estimated rate of diversion at the drinking water intake and the average monthly drinking water usage rate (Larry Adams, personal communication, May 26, 2006). Error associated with these estimates may affect calculated loading rates from the drinking water reservoir return flow. Future monitoring of metal concentrations and flow rates at this site are recommended to confirm any metal sources arising from this tributary.

Iron sources. The iron loading rate increases by a factor of 4.6 at the downstream of end of UT-2.602. Unnamed tributary UT-2.602 contributed 23% of the cumulative tributary iron loading rate. The majority of aquatic life concentration exceedances for iron occurred within 2.0 km downstream of UT-2.602 (Table 11). Clearly, UT-2.602 was a source of increased downstream iron loading rate; however, the Coal Creek iron loading rate downstream of the tributary was greater than the loading rate input by the tributary. Additional iron inputs may come from iron liberation downstream of the wetlands, a lack of surfaces for iron sorption, or ground water iron input. The greatest iron loading rate of 42% of the cumulative tributary input occurred at the drinking water return tributary. However, the in-stream loading rate did not increase immediately downstream. It did spike 0.6 km downstream of the drinking water return flow, yet it is unclear whether this is related to inputs from the drinking water reservoir or from an unidentified source.

Though the dissolved iron data were inconclusive, daily variations of the dissolved iron concentrations may be occurring. Previous studies have found that dissolved iron concentrations are greatest at midday as a result of the photoreduction of dissolved ferric iron and iron oxyhydroxides (McKnight and others, 1992; Tate and others, 1995). Photoreduction of these species produces an increase in the dissolved ferrous iron concentrations with increasing solar radiation.

Despite possible daily fluctuations in dissolved iron concentration, it is hypothesized that almost all of the iron in Coal Creek is in the colloidal phase. In natural waters, iron precipitates to form amorphous and crystalline forms of iron oxyhydroxides around pH 6.5. The average pH of Coal Creek is 7.3; therefore, iron should be mostly in a colloidal form.

Manganese sources. Unnamed tributary UT-3.661 contributed 62% of the cumulative tributary manganese loading rate and 1.25 kg d^{-1}. The Coal Creek metal loading rate

remains elevated and constant for more than 1.0 km downstream of this tributary despite increasing flows and no other significant manganese sources. This may signify the existence of dispersed ground water manganese inputs in this reach. The two highest manganese loading rates occurred in the wetland reach, indicating that significant manganese inputs enter Coal Creek in this reach, perhaps through dispersed ground water flow.

Table 13. The metal concentrations at CC-5.372, just upstream of the drinking water intake, and at the drinking water reservoir return flow tributary. BDL is an abbreviation for "below detection limit" and NA means a valid metal concentration was not available.

metal	metal concentration upstream of drinking water intake ($\mu g\ L^{-1}$)	metal concentration in reservoir return flow ($\mu g\ L^{-1}$)	coefficient of variance (%)
Al Dissolved	50.4	35.5	24.5
Total	63	40	31.6
As Dissolved	3	1.2	60.6
Total	2.6	1.6	33.7
Ba Dissolved	22.4	21.1	4.2
Total	24.8	22.5	6.9
Cd Dissolved	0.51	BDL	-- [1]
Total	0.58	0.27	51.6
Cr Dissolved	NA	NA	--
Total	38.3	2.4	124.7
Cu Dissolved	1.8	3.2	39.6
Total	2.2	2.5	9.0
Fe Dissolved	NA	NA	--
Total	229	371	33.5
Pb Dissolved	BDL	0.2	--
Total	BDL	0.78	--
Mn Dissolved	30	27.4	6.4
Total	29.9	67.3	54.4
Ni Dissolved	NA	NA	--
Total	19.8	1.7	119.1
Zn Dissolved	114	40.1	67.8
Total	126	103	14.2
		Average CV	**42.6**

[1] -- The coefficient of variance could not be calculated.

Aluminum sources. Unnamed tributary UT-3.661, containing drainage from the gossan, also contributed the highest cumulative tributary aluminum loading rate of 76% at 5.01 kg d^{-1}. Because the iron fen tributary contributions do not substantially increase

aluminum loading in Coal Creek, we surmise that the metals are attenuated in the soil and ground water between the County Highway 12 and Coal Creek. Aluminum concentrations never exceeded aquatic life standards (Table 10). Recall that a large percentage of the drainage from the iron fen tributaries reentered the ground water system before entering Coal Creek. Flow rates increase downstream of the iron fen, indicating that iron fen drainage does enter Coal Creek as dispersed ground water flow. However, tributary samples were taken from culverts immediately south of County Highway 12 and may not be representative water entering the stream. Transport through the soil allows opportunity for metal removal through sorption. Aluminum is readily adsorbed by oxides, clay minerals, and organic matter in the soils. Travel through the soil and ground water system provides adequate time and opportunity for these metals to sorb to soil material and be effectively removed from the water column before entering Coal Creek.

Though the aluminum loading rate of the treatment plant effluent is low (Table 8), the aluminum loading rate increases downstream of the site and mimics the shape of the treatment plant effluent "plug." The loading rate increases with downstream of the plant following the same pattern, though less pronounced, as the calcium concentration increases (Figure 26). This indicates that the treatment plant may qualify as a minor or trace aluminum source when discharging.

Zinc sources. Unnamed tributary UT-3.661, which drains the iron gossan, had the greatest zinc loading rates of 1.84 kg d^{-1} and 49% of the cumulative tributary loading rate (Table 8). The Coal Creek zinc loading rates showed only small increases downstream of the iron fen and gossan. Aquatic life standards were exceeded downstream of UT-3.661.

The Elk Creek contribution of zinc was greatest loading rate (0.61 kg d^{-1}) recorded for any metal in the watershed. Elk Creek added 16% of the cumulative tributary zinc loading rate. Coal Creek zinc loading increased by a factor of 120 downstream of Elk Creek. Zinc concentrations exceeded the chronic toxicity standard downstream of Elk Creek.

Copper sources. Unnamed tributary UT-2.602 added 20% of the tributary cumulative total copper loading rate (Table 8) and produced downstream increases in the Coal Creek copper loading rate. UT-3.661 added 13% of the cumulative tributary copper loading rate and also affected downstream increases in the Coal Creek copper loading rate. The drinking water reservoir return flow at 8.090 km added 30% of the cumulative copper loading rate. The copper concentration of the return flow was about the same as that of Coal Creek (Table 12). The loading rate is the highest of all tributaries because of the larger flow entering Coal Creek from the reservoir.

Cadmium sources. Both Elk Creek and unnamed tributary UT-3.661 (the gossan drainage) contributed high cadmium loading rates to Coal Creek. Elk Creek added 32% of the cumulative tributary total cadmium loading rate, while UT-3.661 added 39%.

Aquatic life standards were exceeded downstream of both Elk Creek and UT-3.661 (Table 10). UT-3.455 (iron fen drainage) contributed 12% of the cumulative tributary loading rate.

Lead sources. The drinking water reservoir return flow contributed 50% of the cumulative lead loading rate. The lead concentration of the return flow was approximately 3 times greater than typical in-stream lead concentrations. Splain's Gulch contributed 22% of the cumulative tributary total lead loading rate. Splain's Gulch also had the highest lead concentration of any of the tributaries. Minor lead sources were UT-3.661 and Elk Creek.

Nickel sources. Unnamed tributary UT-2.602 contributed the highest cumulative tributary nickel loading rate of 45%. UT-2.750 and UT-3.661 (the gossan drainage) contributed significant cumulative tributary loading rates of 16 and 18%, respectively. The in-stream loading rate spikes just downstream of UT-2.602 and UT-2.750 and concentrations exceed the chronic toxicity standard for aquatic life (Table 10). Splain's Gulch contributed 11% of the cumulative tributary loading rate (Table 8).

Chromium sources. The sources of chromium are very similar to the sources of nickel. Unnamed tributary UT-2.602 contributed the highest cumulative tributary chromium loading rate of 48%. UT-3.661, UT-2.750, and Splain's Gulch contributed loading rates of 19%, 18%, and 8.7%, respectively. Water quality standards are exceeded downstream of Splain's Gulch, UT-2.602 and UT-2.750, and the gossan drainage.

Arsenic sources. Arsenic concentrations and loading rates differ from the pattern of the other metals. The metals described above tend to show increasing concentrations and loading rates with downstream distance. Arsenic concentrations decreased from the upstream to downstream reaches of Coal Creek, but the loading rate increased up to the drinking water intake. This indicated that additional arsenic sources enter Coal Creek. The increasing arsenic loading rate was not a result of arsenic input from any of the sampled tributaries. It is possible that arsenic is released from wetlands or ground water during low flow. Downstream of the intake, the loading rate decreases as a result of decreasing arsenic concentration and higher flow rates. Of the identified tributaries, Elk Creek contributed 21% of the cumulative tributary loading rate. Though concentrations were no higher than in-stream concentrations, the drinking water reservoir return flow contributed 42% of the cumulative tributary loading rate. UT-2.750 and UT-2.696 added 10% and 7.8% of the loading rate, respectively.

Barium sources. Barium input from UT-6.606, UT-6.696, UT-6.801, and UT-6.844 most likely increases barium concentrations downstream of these tributaries, however the flow from these sites was so low that loading rates were not substantial. Of these four tributaries, UT-6.801 added the highest percentage of the cumulative tributary loading rate with 12%. Increases in barium concentration and loading rates upstream of the

iron fen cannot be attributed to any of the sampled inflows. In-stream barium concentration is greater than the concentration of tributary input in this reach. Similarly to arsenic, barium must enter Coal Creek through dispersed ground water flow or an unidentified tributary upstream of the study reach.

Implications of metal concentrations and loading rates for remediation

The major metal sources for ten metals and arsenic under low flow conditions have been identified (Table 14). The gossan drainage (UT-3.661) was a major source of aluminum, cadmium, iron, manganese, and zinc in Coal Creek. Unnamed tributary UT-2.602 was a major source of chromium, iron, and nickel. Elk Creek was a major source of cadmium and zinc as well as a trace source of arsenic, barium, copper, and lead.

The metals entering Coal Creek from Elk Creek and the Standard Mine drainage may be eliminated by the EPA's remediation of the Standard Mine site. Remedial activities at the Standard Mine site include dewatering of the surface impoundment, channelization of surface flow, and removal of mining debris (EPA, 2005b). These activities began during the summer of 2006. Repository construction and removal of waste rock piles and tailings will take place in 2007. If the remediation is a success, Coal Creek cadmium and zinc concentrations and loading rates downstream of the Elk Creek confluence should significantly decrease and water quality standards should not be exceeded. The clean-up should also remove any trace amounts of arsenic, barium, copper, or lead entering Coal Creek through Elk Creek.

The Coal Creek wetland immediately downstream of the Elk Creek confluence may be effectively removing metals from solution. The methods employed in this study may underestimate the actual metal loading rates entering Coal Creek if metals are quickly attenuated by plant, sediments, or microbes in the wetland (Hernandez, 1995). It is likely that wetland sediments contain toxic metal concentrations. Wetland remediation or dredging may be needed in addition to the remedial activities planned for the Standard Mine.

Drainage from the iron fen and gossan creates the greatest number of water quality criteria exceedances and concentration and metal loading rate increases. Coal Creek is impaired more severely by drainage from the fen and gossan than by drainage from Elk Creek and the Standard Mine. Because the fen and gossan are natural deposits (Figure 3) that support a diverse array of vegetation and wildlife including the endangered *Drosera rotundifolia,* clean-up efforts may prove controversial.

Unnamed tributary UT-2.602 was not identified as a major metal source prior to this study. This tributary drains a portion of Evans Basin, which is located on the north side of Coal Creek between Elk Creek and the Keystone Mine (Figure 2). Flow at UT-2.602 was only 21.3 L s^{-1} during the tracer test. The high metal loading rates at this site are predominantly a result of high metal concentrations. The source of these metals is unclear and future reconnaissance and research of this site is recommended.

Table 14. Major, minor, and trace metal sources in the Coal Creek watershed. The major sources were defined as any source that caused water quality standards to be exceeded and/or contributed a cumulative tributary metal loading rate greater than or equal to 33%. Minor sources were those that added 12-32% of the cumulative tributary metal loading rate. Trace sources were those that added 5-11%. For arsenic and barium, input from an unidentified upstream tributary or dispersed ground water flow overshadowed contributions from any of the other tributaries. The tributaries with the highest cumulative loading rates were considered trace sources.

Metal	Major sources	Minor sources	Trace sources
Aluminum	UT-3.661 (gossan)		
Arsenic	Unidentified upstream tributary and ground water		Elk Creek DW res return UT-2.750 UT-6.696
Barium	Unidentified upstream tributary and ground water		Elk Creek DW Res Return UT-2.750 UT-6.801
Cadmium	UT-3.661 (gossan) Elk Creek	UT-3.455 (fen)	DW Res Return
Chromium	UT-2.602	UT-3.661 (gossan) UT-3.294	Splain's Gulch
Copper		UT-2.602 DW Res Return wetland ground water	Elk Creek UT-2.750 Splain's Gulch
Iron	UT-2.602 UT-3.661 (gossan) DW res. return	wetland groundwater	UT-2.750 UT-6.696
Lead	DW res. return	Splain's Gulch	UT-3.661 (gossan) Elk Creek
Manganese	wetland groundwater UT-3.661 (gossan)	DW Res return	UT-3.455 (fen)
Nickel	UT-2.602	UT-3.661 (gossan) UT-3.294	Splain's Gulch
Zinc	UT-3.661 (gossan) Elk Creek	DW res. return	UT-3.445 (fen)

Return flow to Coal Creek from the drinking water reservoir contained unexpectedly high percentages of the cumulative tributary loading rate for arsenic, barium, copper, iron, lead, manganese, and zinc. Metal concentrations at this site were generally not the highest tributary concentration; however, the flow rate as calculated as the difference between the average drinking water intake rate and the drinking water usage rate (60.01 L s^{-1}) was the greatest of all the tributaries (Larry Adams, personal communication, May 26, 2006). The process resulting in the addition of these metals to the flow between the drinking water intake and the reservoir return is not known.

Also, iron and manganese inputs enter the water somewhere between the drinking water intake and the reservoir return, while the other metals are diluted along this route (Table 13). It is recommended that the source of the additional iron and manganese be located.

Colloids and metal association

Colloids are critical components in streams affected by acid mine drainage (AMD) because their extensive surface areas strongly influence metal partitioning. Colloids dictate the mobility and bioavailability of metals in the environment. The fate of metals in acid mine drainage-affected streams is dependent upon interactions with colloid surfaces through adsorption, complexation, nucleation or dissolution, and surface-controlled redox chemistry as well as stream chemistry (Zanker and others, 2002; Zanker and others, 2003; Sullivan and Drever, 2001; Macalady and others, 1990; Macalady and others, 1991; Schemel and others, 2000; McKnight and others, 1992). Iron oxyhydroxides are the dominant mineral in mine drainage, while aluminosilicates and aluminosilicates with iron oxyhydroxysulfates may also be present in smaller quantities. These colloids dominate because of the oxidation of iron(II) and the subsequent hydrolysis of Fe^{3+} and Al^{3+} in acid mine drainage solutions. As mine drainage is diluted by stream waters, a greater quantity of aluminosilicates with associated iron and sulfur, manganese oxyhydroxides, and quartz minerals comprise the colloidal fraction.

In Coal Creek, a diverse array of colloidal minerals was present (Figures 23-27; Table 9). No pattern related to the presence of iron oxyhydroxides upstream and downstream of mine drainage could be established. Both tributaries analyzed with the electron microprobe, though not mine drainage sites, were predominantly composed of iron oxyhydroxides or manganese oxyhydroxides. Colloidal analyses showed that while one or two minerals may be dominant in tributaries, the mineralogy becomes more diverse upon entry to Coal Creek.

The large surface area of iron oxyhydroxide colloids promotes sorption of toxic metals like lead, copper, zinc, and cadmium. The sedimentation of iron oxyhydroxide colloids is detrimental to aquatic life by filling permeable openings in the streambed that are normally habitat for benthic invertebrates (Clements, 1994). Upon entry to waters of near-neutral pH downstream of mines, such as Coal Creek, trace metals such as aluminum, arsenic, iron, lead, and copper that were adsorbed to the colloids in more

acidic reaches may be immobilized due to colloid coagulation and sedimentation (Galan and others, 2003; Zanker and others, 2003; Sullivan and Drever, 2001; Schemel and others, 2000; McKnight and others, 1992; Kimball and others, 1995). For example, the solubility of aluminum hydroxide ($Al(OH_3)(s)$) is strongly pH-dependent. Aluminum is predicted to precipitate above a pH of 5, and precipitation often results in the coating of the streambed with aluminum hydroxide, a white precipitate. Such white precipitate was observed in drainage from the gossan tributary to Coal Creek.

Colloids have a net negative charge in most natural waters as a result of organic matter coatings. However, in streams affected by acid mine drainage, a plethora of fresh iron oxyhydroxide surfaces are likely to be present. Dissolved organic carbon (DOC) concentrations are also expected to be low, resulting in the possibility of positively-charged colloidal surfaces. The capacity of a colloid to sorb metals may be enhanced by modification of iron oxyhydroxide surfaces through sorption or co-precipitation of anions. For example, cadmium sorption has been enhanced by incorporation of silica on iron oxyhydroxide surfaces. Also, the sorption of DOC may increase copper and aluminum oxide sorption onto iron oxyhydroxides (Macalady and others 1991; McKnight and others, 1992).

For this study, water samples were filtered through 0.45 μm membranes because the EPA was providing the metal analysis and because the metal concentrations must be compared with historical data. This filtration method offers several distinct advantages in that it removes suspended sediment and large organic matter than would settle during transport and storage, it removes bacteria and microorganisms that could cause biological transformations within the sample matrix, and it is the most widely used filtration method which allows for easy comparison of results from different studies; however, this method has also been widely criticized (Danielsson, 1982; Morrison and Benoit, 2001). The filter size is operationally defined and may cause separation of various particle size classes. Also, filtration artifacts such as contamination, colloid and solute adsorption onto the membrane, and coagulation and clogging on the membrane filter can produce significant errors in trace metal measurements. Where iron is normally associated with the large-size colloidal fraction (>0.45 μm), cadmium, manganese, and zinc are generally found in several different colloidal size classes (Kennedy and others, 1974; Pham and Garnier, 1998). With respect to trace metals found in various size classes, filtration through an arbitrarily chosen mesh size such as 0.45 μm would allow some colloids to pass while others are retained. This can significantly skew measurements of the particulate and colloidal fraction.

The observed distribution coefficient (K_d^{obs}, L kg^{-1}) describes metal distribution between the dissolved and colloidal phase. Because precipitation and adsorption are considered to be the most important processes affecting interphase interactions, it is important to consider K_d^{obs} when assessing the partitioning of metals between the colloidal and dissolved phase. K_d^{obs} is an empirical metric that is dependent upon a diverse array of parameters which influence chemical and physical attenuation (EPA, 1999). K_d^{obs} is described by the equation

$$K_d^{obs} = \frac{C_s}{C_w} \quad (10)$$

where C_s (mg kg^{-1}) is the colloidal metal concentration and C_w (mg L^{-1}) is the dissolved metal concentration. Colloidal mass was not measured, so the concentration of metals associated with the colloids could not be calculated, and an alternative computation was used to describe partitioning. The colloidal fraction ($f_{colloid}$) was calculated as

$$f_{colloid} = \frac{C_{total} - C_{dissolved}}{C_{total}} \quad (11)$$

where C_{total} is the total (unfiltered) metal concentration and $C_{dissolved}$ is the dissolved (filtered) metal concentration. The difference between C_{total} and $C_{dissolved}$ is the concentration of metal in the colloidal (0.45 μm-filtered) phase (mg L^{-1}). The colloidal fraction was calculated as an average over the length of the study reach for the eleven metals included in the study (Figure 29). The standard error is significant because the colloidal fraction varied significantly from site to site. Only aluminum, arsenic, lead, and zinc had positive $f_{colloid}$ values because dissolved concentrations exceeded total concentrations on average for the other seven metals.

It is expected that some fraction of the colloids passed through the 0.45 μm filters. This expectation was supported by the electron microprobe images (Figures 23-25) that show pore sizes in excess of 0.45 μm. This artifact would contribute to dissolved concentrations very close to total concentrations. Analytical error associated with the closeness of total and dissolved concentrations resulted in negative values (physically impossible) for the colloidal fraction for the remaining seven metals. Other possible reasons for the discrepancy between total and dissolved colloidal concentrations have been previously discussed.

Lead dominates the colloidal fraction with a mean $f_{colloid}$ value of 0.83 (Figure 29). Aluminum has a mean $f_{colloid}$ value of 0.36, demonstrating the second highest capacity to bind with minerals that make up the colloidal phase, although some of the aluminum measured as colloidal is likely part of the colloidal minerals rather than adsorbed on the colloids. Arsenic and zinc are also present in the colloidal phase to a lesser degree than both lead and aluminum. Though dissolved iron concentrations were unavailable, it is expected that iron is predominantly available in the colloidal phase and that its $f_{colloid}$ value is higher than that of lead.

The speciation behavior of these metals is dependent on pH. The neutral pH of Coal Creek supports metal sorption to colloidal material (Smith and others, 1990). Substantial colloidal fractions were anticipated. The $f_{colloid}$ value for zinc and arsenic were low at approximately 0.1. Recent studies show that zinc is initially sorbed more strongly to organic matter and then to hydrous iron oxides (Kimball and others, 2002). This means that a significant portion of sorbed zinc may be contained in organic biofilms coating the stream bottom or in iron hydroxides or oxyhydroxides that settle from the water column. These zinc removal pathways may explain the low occurrence of zinc in the colloidal phase.

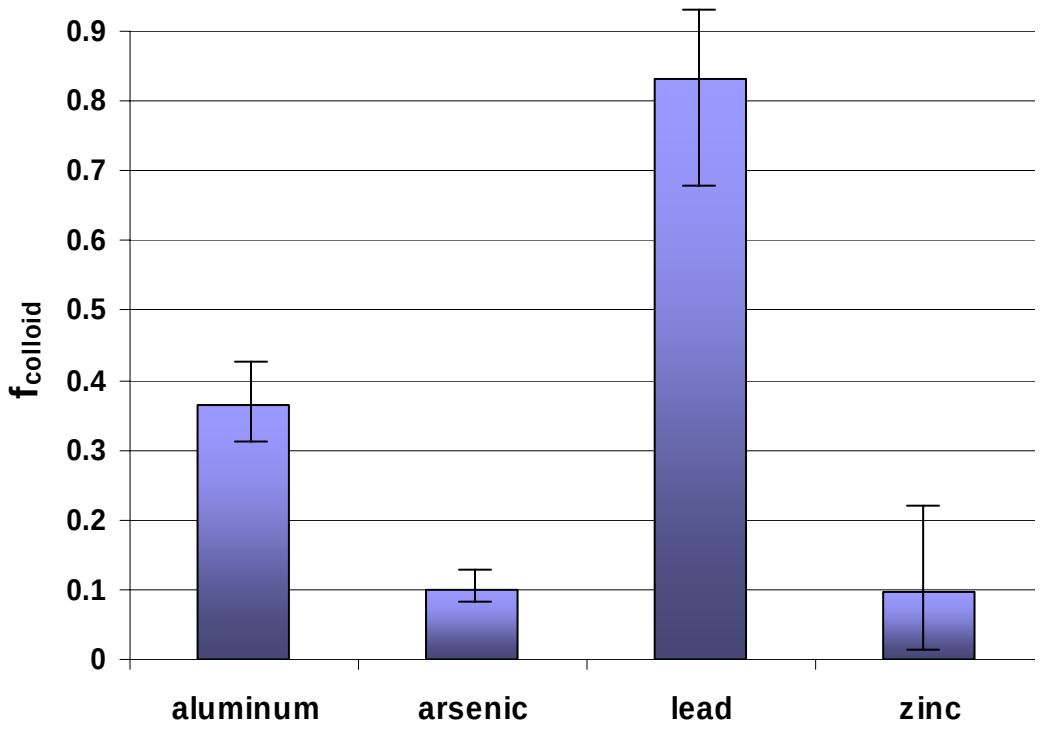

Figure 29. The colloidal fraction ($f_{colloid}$) of aluminum, arsenic, lead, and zinc in Coal Creek.

Although arsenic has been known to partition to iron oxyhydroxides more readily than lead and zinc, only a small fraction of arsenic existed in the colloidal phase in Coal Creek. Galan and others (2003) found that trace metals accumulated in iron oxyhydroxides in the order

Fe > As > Pb > Cr > Ni > Cu > Mn > Cd > Zn

Though the lead colloidal fraction was much greater than the zinc colloidal fraction in Coal Creek, the arsenic colloidal fraction was much smaller than that of lead and did not follow suit with previous experimental findings (Figure 29). Arsenic may preferentially associate with larger iron oxyhydroxides that settle from solution.

A previous study on the Lefthand Creek watershed in Boulder County, Colorado, reported colloid aluminum fractions as high as 0.9 in streams affected by acid mine drainage (Wood and others, 2004). Thermodynamic predictions indicate that colloidal aluminum concentrations should be high at neutral pH in any system where aluminum exists in equilibrium with gibbsite or any other aluminosilicate. The smaller than expected colloidal aluminum fraction in Coal Creek may be a result of aluminosilicate colloids passing through the 0.45 µm membrane filter. Other environmental factors such as complexation by dissolved phase natural organic ligands may be responsible for the significant dissolved aluminum concentrations (Kimball and others, 1995).

The high colloidal lead fraction correlates well with expected partitioning behavior for this metal. Lead is expected to dominate the colloidal phase because it

readily adsorbs to colloids (Abd-Elfattah and Wada, 1981; Brown and Hem, 1984; EPA, 1999; Macalady and others, 1990; Dzombak and Morel, 1990; Wood and others, 2004; Bautts, 2006). One study found that lead absorbs to minerals in the following order:

iron oxides < halloysite < imogolite, allophane < humus, kaolinite < montmorillonite (Abd-Elfattah and Wada, 1981). Iron oxyhydroxides were one of the major chemical components found in the selected samples analyzed for colloidal elemental composition (Figures 23, 25-27). The presence of iron oxide minerals in Coal Creek would support lead adsorption into the colloidal phase, particularly at neutral pH.

The partitioning behavior of lead and zinc was compared to published surface complexation constants, K_{int}, for these metals (Table 15; Dzombak and Morel, 1990). No comparable K_{int} values were available for aluminum or arsenic. A higher surface complexation constant signifies a greater affinity for the metal to bind to a hydrous ferric oxide. The intrinsic surface complexation constant for aluminum and arsenic is expected to be between those for zinc and lead. The low colloidal zinc fraction is consistent with the surface complexation constant and observed zinc partitioning at other acid mine drainage sites during low flow (Kimball and others, 1995). A larger colloidal zinc fraction is expected under high-flow conditions due to the resuspension of colloids that aggregate and settle when flow is low. This hypothesis was not tested in Coal Creek.

Table 15. Intrinsic surface complexation constants for lead and zinc adsorption on hydrous ferric oxide (Dzombak and Morel, 1990).

Metal	Intrinsic surface complexation constant (K_{int})
lead	$10^{4.65}$
zinc	$10^{0.99}$

Iron and manganese oxyhydroxides, silica, and aluminum were the major chemical components found in the tributary samples selected for elemental analysis (Figures 23-27). Manganese oxyhydroxide was the dominant mineral at the drinking water return tributary (Figures 24 and 26). Colloidal manganese concentrations were higher at this tributary than at any other tributary and much higher than in-stream colloidal manganese. The presence of manganese oxyhydroxide in the colloidal fraction coupled with the large colloidal fraction concentrations indicate that significant removal of manganese from the water column to colloidal particulates is occurring in the drinking water reservoir return flow.

This same phenomenon occurred with respect to iron at UT-6.696. The colloidal iron concentration at UT-6.696 is greater than at any other in-stream or tributary site. The total iron concentration at UT-6.696 is approximately 6 times higher than in-stream average. However, UT-6.696 only contributes 5.4% of the total tributary iron load. Flow at UT-6.696 was small and partially accounts for the small iron load despite the high iron concentration. Iron precipitation from the dissolved phase to ferric oxyhydroxide complexes most certainly accounts for further removal of iron from solution.

Hardness and metal partitioning

Downstream of treatment plant effluent channel, Coal Creek hardness peaks at a concentration seven times greater than upstream hardness as a result of calcium input (Figure 8). Hardness, measured as the sum of calcium and magnesium concentration (Equation 2), competes with other divalent cations (metals) for binding sites on iron hydroxide complexes and organic matter (Macalady and others, 1990; Nelson and others, 1986; Allen and others, 1993). Metal concentrations in the colloidal phase are expected to decrease in response to increased competition with calcium downstream of the treatment plant. Weaker-binding metals such as zinc and cadmium are expected to be more affected than stronger-binding metals like lead. For instance, adsorption of cadmium to iron oxyhydroxides may be greatly reduced may the presence of zinc and calcium, resulting in enhanced mobility and bioavailability of cadmium. Both zinc and calcium have greater affinities than cadmium for binding with iron oxyhydroxides. This hypothesis could not be tested with the data available for this study due to large standard deviation associated with the colloidal fraction upstream and downstream of the treatment plant.

CONCLUSIONS

The purpose of this research was to use tracer dilution and synoptic sampling to identify sources of metals in Coal Creek. The impact of acid mine drainage from the Standard Mine (Elk Creek) and the iron fen and gossan on the Coal Creek watershed was investigated. Concentrations and metal loading rates for ten metals and arsenic were reported for a 9.4 km stretch of Coal Creek (Figures 12-22) and the major, minor, and trace sources of each of these metals were identified. Metal concentrations, loading rates, and metal sources are characteristic of low flow conditions. Low flow conditions are typically the most toxic and dangerous to aquatic life as less water is available for dilution. Colloidal material was analyzed at select sites to provide a general assessment of the mineralogical composition of Coal Creek and its tributaries. Relationships between the dissolved and colloidal phase metal fractions were compared to established partitioning behavior for aluminum, arsenic, lead, and zinc.

Cadmium, chromium, and zinc exceed chronic and acute aquatic life toxicity standards at several locations along the study reach (Table 11). Drinking water supply standards were exceeded by arsenic, iron, and manganese (Table 11), though these exceedances were not at the location of the drinking water intake.

The Mt. Emmons Treatment Plant contributed large calcium concentrations to Coal Creek when discharging. The influx of calcium caused hardness-based aquatic life toxicity standards to increase downstream of the plant during the time of synoptic sampling. Large daily fluctuation in the calcium concentrations and hardness-based aquatic life toxicity standards downstream of the treatment plant are expected. Cadmium and zinc are expected to exceed aquatic life standards at additional locations downstream of the treatment plant when it is not discharging (Table 10).

The gossan was found to be the major threat to Coal Creek water quality (Table 13). The gossan contributed elevated aluminum, cadmium, iron, manganese, and zinc concentrations and loading rates. UT-2.602 was the second greatest threat to water quality. This tributary was not previously suspected of adding metals to Coal Creek, however, it contributed elevated levels of chromium, iron, and nickel to the stream. It is recommended that potential metal sources emanating from this tributary be further investigated. Elk Creek was found to be a major contributor of cadmium and zinc to Coal Creek, producing aquatic life standard exceedances and elevated loading rates for these two metals. An unidentified upstream surface tributary or dispersed ground water flow added arsenic and barium to Coal Creek.

The colloidal fraction was examined for aluminum, arsenic, lead, and zinc (Figure 29). Lead dominated the colloidal phase followed by aluminum. Arsenic and zinc had significantly smaller colloidal fractions. A diverse array of colloidal minerals were present in Coal Creek, including the iron oxyhydroxides and aluminosilicates characteristic of acid rock drainage solutions. However, these minerals did not dominate the colloidal fraction and their presence or absence in colloid samples could not be related to their location upstream or downstream of acid rock drainage sources.

Increases in hardness were produced downstream of the Mt. Emmons treatment plant as a result of high calcium concentrations in the treatment plant effluent. The source of this calcium is lime used during the treatment process to raise pH and precipitate metals. This increase in calcium concentration caused hardness-based aquatic life standards to increase. Colloidal metal fractions are expected to decrease downstream of the plant as a result of increased competition with calcium cations. A higher fraction of these metals would consequently be available in the dissolved phase, where they pose a threat to aquatic life and ecosystem health. However, no correlations between the colloidal fraction and the increase in hardness could be established with available data to investigate this hypothesis.

REFERENCES

Abd-Elfattah, A. and Wada, K., 1981. Adsorption of lead, copper, zinc, cobalt, and cadmium by soils that differ in cation exchange material. *Journal of Soil Science* **32**: 71-283.

Allen, H.E., Perdue, E.M., and Brown, D.S., 1993. *Metals in Groundwater: Adsorption to Heterogeneous Surfaces*. Lewis Publishers, Boca Raton, Florida. pp. 1-36.

Bautts, S.M., 2006. An investigation of metal concentrations in waste rock piles, stream water, benthic macroinvertebrates, and stream bed sediments to assess long-term impacts of intermittent precipitation events in the Lefthand Creek watershed, northwestern Boulder County, CO. M.S. Thesis, University of Colorado, Boulder, Colorado. 150 pp.

Bencala, K.E., 1985. Performance of sodium as a transport tracer - experimental and simulation analysis. Selected Papers in the Hydrologic Sciences, U.S. Geological Survey Water Supply Paper 2270, 83-89.

Bencala, K.E., McKnight, D.M., Zellweger, G.W., and Goad, J., 1986. The stability of rhodamine WT dye in trial studies of solute transport in an acidic and metal-rich stream. Selected Papers in the Hydrologic Sciences, U.S. Geological Survey Water Supply Paper 2310, 87-95.

Bencala, K.E., McKnight, D.M., and Zellweger, G. W., 1987. Evaluation of natural tracers in an acidic and metal-rich stream. *Water Resources Research* **23**(**5**): 827-836.

Bencala, K.E, McKnight, D.M., and Zellweger, G.W., 1990. Characterization of transport in an acidic and metal-rich mountain stream based on a lithium tracer injection and simulations of transient storage. *Water Resources Research* **26**(**5**): 989-1000.

Broshears, R.E., Bencala, K.E., Kimball, B.A., and McKnight, D.M., 1993. Tracer-dilution experiments and solute transport simulations for a mountains stream, St. Kevin Gulch, Colorado. U.S. Geological Survey, Water-Resources Investigations Report 92-4081, 18 pp.

Brown, D.W., and Hem, J.D., 1984. Development of a model to predict the adsorption of lead from solution on a natural streambed sediment. U.S. Geological Survey Water-Supply Paper 2187, 35 pp.

CCCOSC, 2006. The Geneva Creek iron fen, Clear Creek Open Space Commission. Retrieved June 1, 2006 from http://www.co.clearcreek.co.us/OSWebsite/GenevaCreek.htm.

CCWC, 2006. Crested Butte, A National Historic District, Coal Creek Watershed Coalition. Retrieved May 26, 2006, from http://www.crestedbutte.govoffice2.com/index.asp?cType =B_B ASIC&SEC=%7BE820970E-625C-4CAA-ADF1-F95CB758956C%7D.

CDPHE, 2005. Regulation No. 31: The Basic Standards and Methodologies for Surface Water, 5 CCR 1002-31. Colorado Department of Public Health and Environment Water Quality Control Commission, Denver, Colorado.

CDPHE, 2006. List of Superfund sites in Colorado: Standard Mine. 2006, Colorado Department of Public Health and Environment, Hazardous Materials and Waste Management Division. Retrieved April 9, 2006 from http://www.cdphe.state.co.us/hm/rpstandard.htm.

Clements, W.H., 1994. Benthic invertebrate community responses to heavy metals in the Upper Arkansas River Basin, Colorado. *Journal of the North American Benthological Society* **13**: 30-44.

Danielsson, L.G., 1982. On the use of filters for distinguishing between dissolved and particulate fractions in natural waters. *Water Research* **16**:179-182.

Dzombak, D.A., and Morel, F.M.M., 1990. *Surface Complexation Modeling: Hydrous Ferric Oxide*. John Wiley & Sons, New York, New York. pp. 392.

EPA, 1999. Understanding variation in partition coefficient, K_d, values. U.S. Environmental Protection Agency Report No. 402-R-99-004A, 609 pp.

EPA, 2005a. Hazard ranking system documentation record: Standard Mine, CO0002378230, U.S. Environmental Protection Agency. Retrieved April 16, 2006 from http://www.epa.gov/region8/superfund/co/standard/.

EPA, 2005b. National Priorities List: Standard Mine, Gunnison National Forest, Colorado. Retrieved April 16, 2006 from http://www.epa.gov/superfund/sites/npl/nar1740.htm.

EPA, 2006. Multi-media, multi-concentration inorganic analyses ILM05.3. Retrieved May 18, 2006 from http://epa.gov/superfund/programs/clp/ilm5.htm.

Galan, E., Gomez-Ariza, J.L., Gonzalex, J.C., Fernandez-Caliani, Morales, E., and Giraldez, I., 2003. Heavy metal partitioning in river sediments severely polluted by acid mine drainage in the Iberian Pyrite Belt. *Applied Geochemistry* **18**: 409-421.

Hernandez, K.S., 1995. Acid mine drainage in the Rockford Tunnel wetland, Idaho Springs, Colorado: metal speciation and distribution. M.S. Thesis, University of Colorado, Boulder. pp. 153.

Hornbaker, A. L., 1984. Metal mining activity map of Colorado and directory, 1984. Map Series 24, Colorado Geological Survey, Department of Natural Resources, Denver, Colorado.

Kelly, W.C., 1958. Topical study of lead-zinc gossans. Bulletin 46, New Mexico Bureau of Mines and Mineral Resources, Socorro, New Mexico. 80 pp.

Kennedy, V.C., Zellweger, G.W., and Jones, B.F., 1974. Filter pore size effects on the analysis of Al, Fe, Mn, and Ti water. *Water Resources Research* **10**:785-790.

Kimball, B.A., 1997. Use of tracer injections and synoptic sampling to measure metal loading from acid mine drainage. U.S. Geological Survey Fact Sheet-245-96, U.S. Department of the Interior, West Valley City, Utah.

Kimball, B.A., Callender, E., and Axtmann, E.V., 1995. Effects of colloids on metal transport in a river receiving acid mine drainage, upper Arkansas River, Colorado, U.S.A. *Applied Geochemistry* **10**: 285-306.

Kimball, B.A., Runkel, R.L., and Gerner, L.J., 2001. Quantification of mine-drainage inflows to Little Cottonwood Creek, Utah, using a tracer-injection and synoptic-sampling study. *Environmental Geology* **40**: 1390-1404.

Kimball, B.A., Runkel, R.L., Walton-Day, K., and Bencala, K.E., 2002. Assessment of metal loads in watersheds affected by acid mine drainage by using tracer injection and synoptic sampling: Cement Creek, Colorado, USA. *Applied Geochemistry* **17**: 1183 – 1207.

Macalady, D.L, Smith, K.S., and Ranville, J.F., 1990. Acid mine drainage: Streambed sorption of copper, cadmium, and zinc. Colorado Water Resources Research Institute Completion Report No. 154, 16 pp.

Macalady, D.L., Ranville, J.F., Smith, K.S., and Daniel, S.R., 1991. Adsorption of copper, cadmium, and zinc on suspended sediments in a stream contaminated by acid mine drainage: The effect of seasonal changes in dissolved organic carbon. Colorado Water Resources Research Institute Completion Report No. 159, Colorado State University, Fort Collins, Colorado. 14 pp.

McKnight, D.M., Bencala, K.E., Zellweger, G.W., Aiken, G.R., Feder, G.L., and Thorn, K.A., 1992. Sorption of dissolved organic carbon by hydrous aluminum and iron oxides occurring at the confluence of Deer Creek with the Snake River, Summit County, Colorado. *Environmental Science & Technology* **26**: 1338-1396.

Morrison, M.A., and Benoit, G., 2001. Filtration artifacts caused by overloading membrane filters. *Environmental Science & Technology* **35**(**18**): 3774-3779.

Mudroch, A., Zeman, A.J., and Sandilands, R., 1977. Identification of mineral particles in fine grained lacustrine sediments with transmission electron microscope and x-ray energy dispersive spectroscopy. *Journal of Sedimentary Petrology* **47**: 244-250.

Mudroch, A., Azcue, J.M., and Mudroch, P., 1997. *Physico-Chemical Analysis of Aquatic Sediments*. Lewis Publishers, Boca Raton, Florida.

Paschke, S., Kimball, B., and Runkel, R., 2005. Quantification and simulation of metal loading to the upper Animas River, Eureka to Silverton, San Juan County, Colorado, September 1997 and August 1998. Scientific Investigations Report 2005-5054, U.S. Geological Survey, Reston, Virginia, 4-8.

Pham, M.K., and Garnier, J.M., 1998. Distribution of trace elements associated with dissolved compounds (0.45 μm – 1 nm) in freshwater using coupled (frontal cascade) ultrafiltrations and chromatographic separations. *Environmental Science & Technology* **32**(**4**): 440-449.

Schemel, L.E., Kimball, B.A., and Bencala, K.E., 2000. Colloid formation and metal transport through two mixing zones affected by acid mine drainage near Silverton, Colorado. *Applied Geochemistry* **15**:1003-1018.

Smith, K.S., Macalady, D.L., and Briggs, P.H., 1990. Partitioning of metals between water and flocculated bed material in a stream contaminated by acid mine drainage near Leadville, Colorado. Colorado Water Resources Research Institute Completion Report No. 154, 101-109.

Soule, J.M., 1976. Geologic hazards in the Crested Butte-Gunnison area, Gunnison County, Colorado. Publication No. GS-VDSD 34-45, Colorado Geological Survey, Department of Natural Resources, Denver, Colorado, 4-6.

Streufert, R.K., 1999. Geology and mineral resources of Gunnison County, Colorado. Resource Series 37, Colorado Geological Survey, Department of Natural Resources, Denver, Colorado. 76.

Sullivan, A.B., and Drever, J.I., 2001. Geochemistry of suspended particles in a mine-affected mountain stream. *Applied Geochemistry* **16**: 1663-1676.

Tate, C.M., Broshears, R.E., and McKnight, D.M., 1995. Phosphate dynamics in an acidic mountain stream: interactions involving algal uptake, sorption by iron oxide, and photoreduction. *Limnology and Oceanography* **40**(**5**): 938-946.

U.S. Energy, 2006. History of Mt. Emmons molybdenum project known as the "Luck Jack Project," U.S. Energy Corporation. Retrieved May 17, 2006 from http://www.usnrg.com/MolybdenumProjects.php.

USFS, 1981. Mount Emmons mining project environmental impact statement, Gunnison County, Colorado. U.S. Forest Service, Department of Agriculture, Report 02-04-81-03, Gunnison Colorado.

USGS, 2006. USGS 09111000 Coal Creek near Crested Butte, Colorado, U.S. Geological Survey. Retrieved May 31, 2006 from http://waterdata.usgs.gov/co/nwis/inventory/?site_no=09111000.

Wentz, D.A., 1974. Effect of mine drainage on the quality of streams in Colorado, Colorado Water Resources Research Institute, Circular No. 21.

Wood, A.R, Cholas, R., Harrington, L., Isenhart, L., Turner, N., and Ryan, J.N., 2004. Characterization and prioritization of mining-related metal sources in the streams and streambed sediments of the Lefthand Creek watershed, northwestern Boulder County, Colorado, 2002-2003, Report No. 04-01, Department of Civil, Environmental, and Architectural Engineering, University of Colorado, Boulder, Colorado.

WRCC, 2006. Crested Butte, Colorado, Monthly Climate Summary, Period of Record 6/1/1909 – 12/31/2005. Western Regional Climate Center. Retrieved May 29, 2006 from http://www.wrcc.dri.edu/cgi-bin/climMAIN.pl?cocres.

Zanker, H., Moll, H., Wolfgang, R., Brendler, V., Hennig, C., Reich, T., Kluge, A., and Huttig, G., 2002. The colloid chemistry of acid rock drainage solution from an abandoned Zn-Pb-Ag mine. *Applied Geochemistry* **17**: 633-648.

Zanker, H., Richter, W., and Huttig, G., 2003. Scavenging and immobilization of trace contaminants by colloids in the waters of abandoned ore mines. *Colloids and Surfaces A: Physicochemical and Engineering Aspects* **217**: 21-31.

Zellweger, G. W., Avanzino, R.J., and Bencala, K.E., 1989. Comparison of tracer dilution and current-meter discharge measurements in a small gravel-bed stream, Little Lost Man Creek, California. U.S. Geological Survey Water-Resources Investigations Report 89-4150.